

**Investigations on the photochemistry and
photophysics of a few enone appended
dibenzobarrelenes**

*Thesis submitted to the
Cochin University of Science and Technology
in partial fulfilment of the requirements for the degree of*

*Doctor of Philosophy
in
Chemistry*

*In the Faculty of Science
By*

Saumya T. S.

(Reg. No: 3991)

Under the supervision of

Dr. P. A. Unnikrishnan



**DEPARTMENT OF APPLIED CHEMISTRY
COCHIN UNIVERSITY OF SCIENCE AND TECHNOLOGY
KOCHI- 682 022, KERALA, INDIA**

August 2017

Dedicated

To my dearest Amma.....



DEPARTMENT OF APPLIED CHEMISTRY
COCHIN UNIVERSITY OF SCIENCE AND TECHNOLOGY
KOCHI – 682 022, KERALA, INDIA

Dr. P. A. Unnikrishnan
Assistant Professor
E-mail: paunni@cusat.ac.in
Ph: 0484 2575804

CERTIFICATE

This is to certify that the thesis entitled “**Investigations on the photochemistry and photophysics of a few enone appended dibenzo-barrelenes**” is a genuine record of research work carried out by **Ms. Saumya T. S.**, under my supervision, in partial fulfilment of the requirements for the degree of Doctor of Philosophy of Cochin University of Science and Technology, and further that no part thereof has been presented before for the award of any other degree. All the relevant corrections and modifications suggested by the audience and recommended by the doctoral committee of the candidate during the pre-synopsis seminar have been incorporated in the thesis.

Kochi-22
August, 2017

P. A. Unnikrishnan
(Thesis Supervisor)

DECLARATION

I hereby declare that the work presented in the thesis entitled “**Investigations on the photochemistry and photophysics of a few enone appended dibenzobarrelenes**” is the result of genuine research carried out by me under the supervision of **Dr. P. A. Unnikrishnan**, Assistant Professor of Organic Chemistry, Department of Applied Chemistry, Cochin University of Science and Technology, Kochi-22, and the same has not been submitted elsewhere for the award of any other degree.

Kochi-22

August, 2017

Saumya T. S.

Acknowledgements

*Words are inadequate to express my thanks to all those who helped me, supported me and stood by my side in this venture to accomplish my dreams. First and foremost, I express my sincere gratitude and obligation to my thesis supervisor **Dr. P. A. Unnikrishnan**, Assistant Professor, Department of Applied Chemistry, Cochin University of Science and Technology, for his valuable suggestions and boundless support throughout my research work. His guidance helped me at all times of research and writing of this thesis.*

I express my sincere thanks to Dr. S. Prathapan, Associate Professor, Department of Applied Chemistry, CUSAT for being my doctoral committee member and for his wholehearted support and guidance during the tough times of my research. His valuable suggestions and fruitful discussions throughout the research, has helped me a lot for the successful completion of this work.

I wish to thank Dr. K. Girishkumar present Head and also the former Heads, Dr. K. Sreekumar, Dr. N. Manoj and Dr. M. R. Prathapachandra Kurup for providing me with all the necessary facilities of the department for carrying out my research work. I would like to extend my sincere thanks to all the former and present members of the Faculty of the Department of Applied Chemistry. I also thank the administrative staff of the Department and University office, CUSAT.

I express my heartfelt gratitude to Dr. P. R. Rajmohan, NCL Pune for doing the variable temperature NMR studies. I also thank, Dr. C. Selvaraj, Assistant Professor, NCUIFP (National Centre for Ultrafast Processes), Chennai, for providing me the facilities for doing the Laser Flash photolysis studies. My special thanks to P. Karunakaran, and K. Ramamurthy, Research Scholars, NCUIFP, Chennai for the valuable help they rendered for our studies at Chennai.

I remember the Cheerful days I have spent in the lab with my colleagues., I thank Ms. Kala K., Ms. Nithya C., Ms. Ligi M. L., Mr. Shandev P.

P., Mr. Tomson D., Ms. Nishad K. M., Mr. Jith C. J., Ms. Amrutha U., Ms. Rani M., Ms. Jesna A., Ms. Vineetha P. K., Ms Parvathy O. C., Ms Aswathy Ajaykumar, Mr. Midhun, Mr. Kiran James and all other M.phil and M. Sc. project students who worked in our lab, for the love and endless support they rendered me. It will not be good if I don't remember my seniors who supported me, encouraged me and shared their experiences in research with me which helped me a lot in my work. I also thank friends of other groups in the Department of Applied Chemistry for their support. My special thanks to my Junieur Ms. Aswathy. C. S. for all the support and help she gave me for conducting the studies at Chennai and althrough out my thesis writing.

I remember with respect and prayers all my teachers who encouraged me to go ahead with my career goals.

I thank SAIF, CUSAT for the analytical and spectral data. I thank CSIR, New Delhi for the financial support in the form of research fellowship.

My Amma was my constant inspiration to overcome all the hurdles I have faced, during the period of research. She was the one who prayed for me and more tensed than me when I go for my exams during my school and college days. She always asked for professional advices to show me the right path in my career. But today, when I am nearing to her dreams for me she is not with me to share my happiness. I dedicate my thesis to my beloved amma who is my great strength and guide throughout my life.and career. I also thank my achan and my sisters Swathy and Surya for the support they gave me to complete my research. I earnestly express my gratitude and thanks to my in laws, who are more like my parents. Without their support I could not have completed my work .They took care of my kid with utmost love and care when I was busy with my research. They gave me extreme support and encouragement to accomplish my dreams.

My husband Arun was always there encouraging me to go ahead with my research. He stood by my side with immense patience love and care during my busy schedules and helped me in every possible way he could. I thank him for supporting me to overcome all difficulties. Above all, I thank the super power I believe in for giving me the strength and for all the blessings.

Saumya, T. S.

Abstract

The thesis entitled “**Investigations on the photochemistry and photophysics of a few enone appended dibenzobarrelenes**” is divided into five chapters. **Chapter 1** gives an overview of the photochemistry of dibenzobarrelenes. **Chapter 2** describes the synthesis of the enone appended anthracenes which served as the precursors for the targeted dibenzobarrelenes. In **Chapter 3** the synthesis of the dibenzobarrelenes is described. **Chapter 4** deals with the photochemical and photophysical studies on enone appended dibenzobarrelenes synthesized by us. **Chapter 5** explains the variable temperature NMR studies and Frontier Orbital analysis using Density Functional theory which provides additional support for the findings we have made.

Chapter 1: Photochemistry of dibenzobarrelenes - An overview

This is the introduction chapter for the thesis. In this chapter we have discussed the progresses made in exploring the photochemistry of dibenzobarrelenes. A detailed description of the basic photo-transformations so far observed for dibenzobarrelenes and the effect of various substituents on the regioselectivity and reactivity of dibenzobarrelenes are included.

Chapter 2: Synthesis of some enone appended anthracenes

This chapter describes the synthesis of enone appended anthracenes. We utilized the Claisen–Schmidt condensation reaction of various ketones with anthracene-9-carbaldehyde for the synthesis of these anthracenes. Ketones were selected in such a way that geometry effects of enone components on the photochemistry can also be studied. Various enone appended anthracenes synthesized by us are collected in Chart 1.

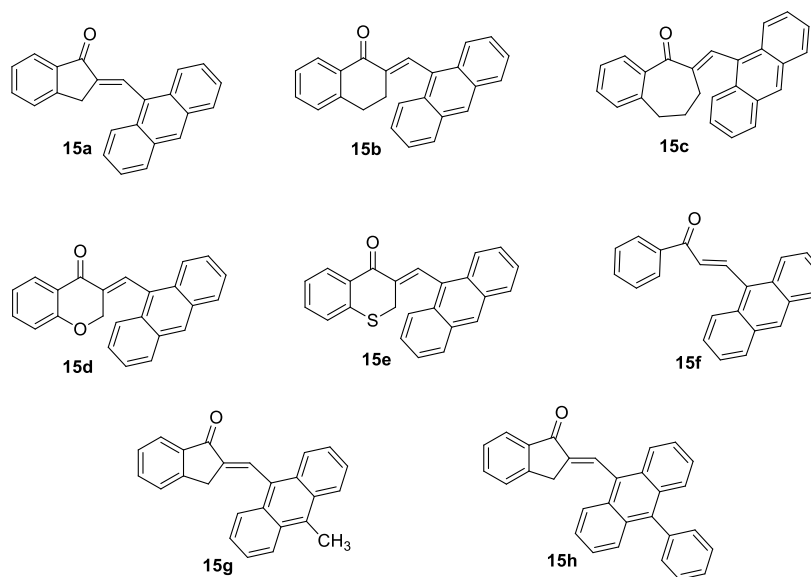
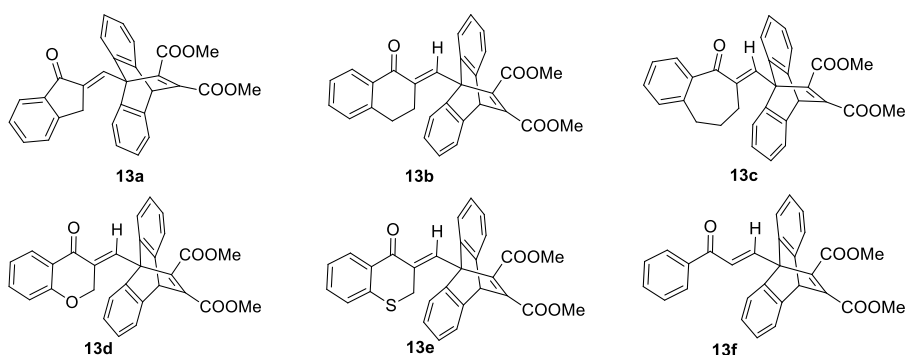


Chart 1

Chapter 3: Synthesis of enone appended dibenzobarrelenes

This chapter describes the synthesis and characterization of enone appended dibenzobarrelenes by Diels–Alder reaction of the corresponding enone appended anthracenes and dienophiles such as dimethyl acetylenedicarboxylate (DMAD), dibenzoylacetylene (DBA) and *in situ* generated benzyne intermediate. Various barrelenes synthesized by us are collected in Chart 2.



Steady state photolysis of the compounds were carried out in a Rayonet photochemical reactor employing 300 nm lamps in deaerated benzene. Irradiation of the compounds with the carbomethoxy substituents at the vinylic positions underwent *E-Z* isomerization to give the corresponding *Z*-isomers as evidenced by SCXRD data. Irradiation of the compounds with benzoyl substituents at 11,12 positions resulted in extensive decomposition. To get more information on transient intermediates formed, nanosecond laser flash photolysis was carried out. The third harmonic (355 nm) of a Q-switched Nd:YAG laser (Quanta-Ray, LAB 150, Spectra Physics, USA) with 8 ns pulse width and 150 mJ pulse energy was used to excite the samples. Laser flash photolysis of degassed benzene solution of the compounds resulted in the formation of a transient species characterized by two absorption maxima at around 390 and 600 nm. We attributed the absorption around 390 to barrelene triplet and the one around 600 nm species to the diradical intermediate formed by H-abstraction.

Chapter 5: Variable temperature NMR studies and Frontier Orbital analysis using DFT for selected compounds

NMR spectra of several of the *E* and *Z*-isomers of enone appended barrelenes exhibited broad, characterless peaks. We attributed this anomalous behavior to the presence of fast interconverting rotamers. In order to resolve their spectra, we attempted variable temperature NMR studies on a representative sample and the ¹H NMR spectrum (700 MHz) recorded at 248 K clearly indicated the presence of two rotamers in nearly 1:1 ratio.

To account for the difference in reactivity of the compounds with carbomethoxy and benzoyl groups at 11,12-positions, we did the Frontier

Orbital Analysis using Density Functional Theory. Based on this we could establish that in case of dibenzobarrelenes with ester moiety LUMO is concentrated on the enone moiety and thus the reaction is only a *cis-trans* isomerization. In the dibenzobarrelene with benzoyl group at 11,12-positions, LUMO is spread over the entire molecule enabling multiple reaction pathways.

Note: The numbers given to various compounds herein correspond to those given in respective chapters and each chapter of the thesis is an independent unit. All new compounds were fully characterized on the basis of spectral and analytical data. Relevant references are included at the end of each chapter.

List of Abbreviations

CV	: cyclic voltammetry
d	: doublet
DBA	: dibenzoyl acetylene
DCM	: dichloromethane
DFT	: density functional theory
DMAD	: dimethyl acetylene dicarboxylate
DME	: dimethoxy ethane
DNA	: deoxy ribonucleic acid
DRS	: diffuse reflectance spectroscopy
EPR	: electron paramagnetic resonance
ESR	: electron spin resonance
FAB	: fast atom bombardment
FMO	: frontier molecular orbital
FT-IR	: fourier transform infrared
FT-NMR	: fourier transform nuclear magnetic resonance
g	: gram
GC-MS	: gas chromatography-mass spectrometry
h	: hour
HOMO	: highest occupied molecular orbital
HIV	: human immunodeficiency virus
ICT	: intramolecular charge transfer
IFV	: internal free volume
IMDA	: intramolecular Diels-alder reaction
IR	: infrared
KOH	: potassium hydroxide
LUMO	: lowest unoccupied molecular orbital
m	: multiplet
Me	: methyl
MeCN	: acetonitrile
MeOH	: methanol
mg	: milligram
MHz	: mega hertz
min	: minute
mL	: millilitre
mmol	: millimol

mp	: melting point
MS	: mass spectrometry
mT	: milli tesla
nm	: nanometre
ns	: nanosecond
NMR	: nuclear magnetic resonance
NaOH	: sodium hydroxide
OLED	: organic light emitting diode
ORTEP	: oak ridge thermal ellipsoid plot
PMT	: photomultiplier tube
ppm	: parts per million
RPR	: rayonet photochemical reactor
s	: singlet
SCXRD	: single crystal X-ray diffraction
<i>s</i> -Bu	: secondary butyl
t	: triplet
<i>t</i> -Bu	: tertiary butyl
TLC	: thin layer chromatography
TMS	: tetramethylsilane
UV	: ultraviolet
UV-DRS	: ultraviolet diffuse reflectance spectroscopy
VT-NMR	: variable temperature nuclear magnetic resonance
T _c	: coalescence temperature

CONTENTS

	<i>Page</i>
	<i>No.</i>
CHAPTER 1	
Photochemistry of dibenzobarrelenes - An overview	1-62
1.1 <i>Abstract</i>	1
1.2 <i>Introduction</i>	2
1.3 <i>Light absorption and fate of the excited state</i>	5
1.4 <i>History of Barrelenes</i>	8
1.5 <i>Phototransformations of Barrelenes</i>	8
1.5.1 <i>Di-π-methane rearrangement: general mechanism</i>	8
1.5.2 <i>Reaction multiplicity</i>	9
1.5.3 <i>Regioselectivity</i>	10
1.6 <i>Major phototransformations of Dibenzobarrelenes</i>	12
1.6.1 <i>Regioselectivity in the di-π-methane rearrangement of dibenzobarrelenes and the role of different substituents</i>	14
1.7 <i>Controlling the reaction multiplicity and product formation of Dibenzobarrelenes</i>	14
1.8 <i>Dibenzobarrelenes and related compounds: Applications</i>	16
1.9 <i>Photochemistry of enones</i>	20
1.10 <i>Defining the research problem</i>	20
1.11 <i>Objectives of the present study</i>	22
<i>References</i>	47
CHAPTER 2	
Synthesis of a few enone appended anthracenes	63-119
2.1 <i>Abstract</i>	63
2.2 <i>Introduction</i>	63
2.3 <i>Results and Discussion</i>	71
2.3.1 <i>Synthesis of 10-substituted anthraldehydes</i>	71
2.3.1.1 <i>Synthesis of 9-substituted anthracenes</i>	74
2.3.1.2 <i>Formylation of 9-substituted anthracenes</i>	74
2.3.2 <i>Synthesis of enone appended anthracenes</i>	77
2.4 <i>Experimental</i>	81
2.4.1 <i>Materials and methods</i>	97
2.4.2 <i>Synthesis of 9-substituted anthracenes</i>	99
2.4.2.1 <i>Synthesis of 9-methylantracene (10)</i>	103
2.4.2.2 <i>Synthesis of 9-phenylantracene (13)</i>	107
2.4.3 <i>Synthesis of 10-substituted anthraldehydes 8 and 9</i>	108
2.4.4 <i>Synthesis of (E)-2-(anthracen-9-ylmethylene)-2,3-dihydro-1H-inden-1-one (14a)</i>	117
2.4.5 <i>Synthesis of (E)-2-(anthracen-9-ylmethylene)-3,4-dihydronaphthalene-1(2H)-one (14b)</i>	117

2.4.6	Synthesis of (E)-6-(anthracen-9-ylmethylene)-6,7,8,9-tetrahydro-5H-benzo[7]annulen-5-one (14c)	
2.4.7	Synthesis of (E)-3-(anthracen-9-ylmethylene)chroman-4-one (14d)	
2.4.8	Synthesis of (E)-3-(anthracen-9-ylmethylenethiochroman-4-one (14e)	
2.4.9	Synthesis of (E)-3-(anthracen-9-yl)-1-phenylprop-2-en-1-one (14f)	
2.4.10	Synthesis of (E)-2-((10-methylantracen-9-yl)methylene)-2,3-dihydro-1H-inden-1-one (14g)	
2.4.11	Synthesis of (E)-2-((10-phenylantracen-9-yl)methylene)-2,3-dihydro-1H-inden-1-one (14h)	
	References	

CHAPTER 3

	Synthesis of enone appended dibenzobarrelenes	121-150
3.1	Abstract	121
3.2	Introduction	121
3.3	Results and Discussion	
3.3.1	Synthesis of enone appended dibenzobarrelenes with DMAD as dienophile	
3.3.2	Synthesis of enone appended dibenzobarrelenes with DBA as dienophile	125
3.3.3	Synthesis of enone appended dibenzobarrelenes with in situ generated benzyne as dienophile	125
3.4	Experimental	130
3.4.1	General procedures	137
3.4.2	Starting materials	138
3.4.3	General Procedure for the Synthesis of enone–appended dibenzobarrelenes 13a-h	141
3.4.4	Spectral and analytical data for the dibenzobarrelenes 13a-h	143
3.4.5	General Procedure for the Synthesis of enone–appended Dibenzobarrelenes 14a-f	
3.4.6	Spectral and analytical data for the dibenzobarrelenes 14a-f	
3.4.7	General Procedure for the Synthesis of enone–appended Dibenzobarrelene 15	
	References	

CHAPTER 4

	Photochemical and photophysical studies on enone appended dibenzobarrelenes	
4.1	Abstract	151
4.2	Introduction	151
4.2.1	Introduction to organic photochromic compounds	154
4.2.1.1	Mechanism of photochromism	154

4.2.2	<i>Laser flash photolysis</i>	156
4.3	<i>Results and discussion</i>	159
4.3.1	<i>Steady state irradiation of dibenzobarrelenes 12a-f & 13a-f</i>	162
4.3.2	<i>Photochromic properties of the dibenzobarrelenes in the solid state</i>	172
4.3.3	<i>Laser flash photolysis studies</i>	175
4.3.4	<i>Comparison of the photochromic behavior in different compounds</i>	178
4.3.5	<i>Solvent Polarity dependence studies</i>	180
4.4	<i>Experimental</i>	181
4.4.1	<i>Materials and method</i>	185
4.4.1.1	<i>Nanosecond Laser Flash Photolysis</i>	187
4.4.2	<i>General Procedure for the photochemical reaction of enone– appended dibenzobarrelenes</i>	191
4.4.3	<i>Spectral and analytical data of the photoproducts obtained</i>	193
	<i>References</i>	
CHAPTER 5		
Variable temperature NMR studies and frontier orbital analysis using DFT for selected compounds		
5.1	<i>Abstract</i>	201
5.2	<i>Introduction</i>	202
5.2.1	<i>Variable Temperature NMR–basics and applications</i>	
5.3	<i>Results and Discussion</i>	205
5.3.1	<i>Variable temperature NMR studies (VTNMR)</i>	213
5.3.2	<i>Cyclic voltammetric studies</i>	216
5.3.3	<i>Frontier orbital analysis using DFT</i>	218
5.4	<i>Experimental</i>	220
	<i>References</i>	
	<i>Summary and Conclusions</i>	241
	<i>List of Publications</i>	

Photochemistry of Dibenzobarrelenes - An Overview

1.1. Abstract

This chapter introduces various mechanistic aspects of barrene photochemistry. A detailed description of the basic photo-transformations so far observed for dibenzobarrelenes and the effect of various substituents on deciding regioselectivity and controlling reactivity of dibenzobarrelenes is included.

1.2. Introduction

Synthetic organic chemistry has developed fascinatingly during the past decades and many complex organic synthetic procedures have been simplified through the development of highly selective procedures.¹ Polycyclic compounds are the key structural intermediates in the synthesis of natural or biologically active products² but their total synthesis is a very tedious process. In this scenario photochemical reactions have emerged as a powerful tool for organic synthesis, since in many cases it can provide easy, more efficient and green route for the synthesis of complex organic compounds from simple substrate.^{3,4} The feasibility of these reactions in supramolecular assemblies which are more stable, with a constraint environment have been successfully utilized for many stereoselective reactions. Organic photochemistry and its applications in synthesis is now a dynamic research field.⁵

1.3. Light absorption and fate of the excited state

Light absorption by molecules follows two basic laws. The first law of photochemistry, also known as Grotthuss-Draper law, states that light

must be absorbed by a compound in order for a photochemical reaction to take place. The second law of photochemistry, the Stark-Einstein law, states that for each photon of light absorbed by a chemical system, only one molecule is activated for subsequent reaction. This "photoequivalence law" was derived by Albert Einstein during his development of the quantum theory of light and forms the basis for calculation of quantum yields (Φ). Absorption of a single photon of appropriate energy by a single molecule results in the promotion of an electron from a lower lying orbital to a higher orbital. Usually, an electron from either a bonding or nonbonding orbital is promoted to an antibonding orbital. In other words, light absorption leads to the formation of electronically excited states of molecules. Excited states have electronic configurations different from that of the corresponding ground states.⁶ In the ground state, organic compounds in general are closed shell species with a net spin = 0. Promotion of a single electron from either a bonding or nonbonding orbital to an antibonding orbital can result in an excited state species with net spin = 0 (singlet excited state), or ± 1 (triplet excited state). The fate of an excited molecule determines the photoreactivity of that molecule. If the molecule returns to the original ground state then it is only a physical change and the processes involved are called photophysical processes, and if it is accompanied by the formation of a new chemical species then it is a photochemical process. Interestingly, singlet and triplet excited states can exhibit different photochemical and photophysical behavior. Unimolecular excited state photophysical processes can be schematically explained with the help of a Jablonski diagram (Fig. 1.1). Photophysical processes

are the transitions which interconvert the singlet and triplet states with each other or with the ground state. This involves radiationless processes such as internal conversion, intersystem crossing and radiative processes such as phosphorescence and fluorescence. These are all intramolecular processes. Relaxation via energy transfer or electron transfer process can also happen and it can be intramolecular or intermolecular in nature.⁷

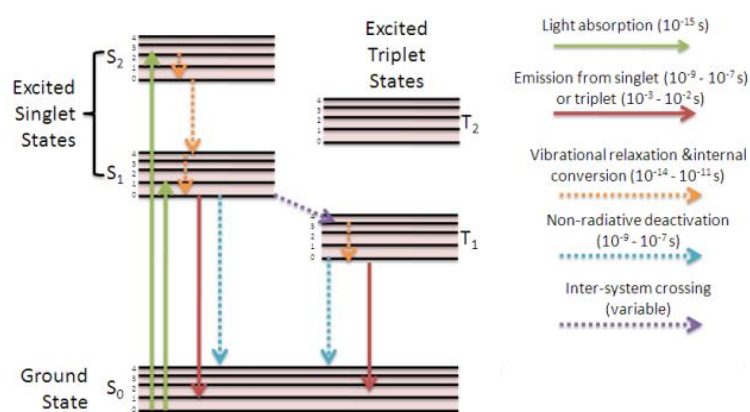
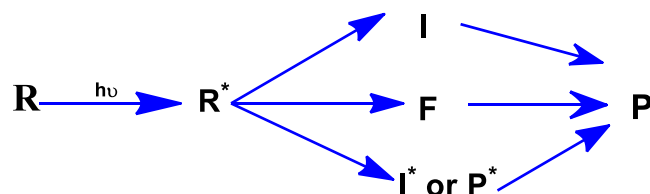


Fig. 1.1: Jablonski diagram illustrating various excited state photophysical processes (reproduced from photochemistry.wordpress.com).

In comparison with photophysical events, photochemical transformations are slower in nature as they involve bond reorganization processes. A molecule in the excited state possess different energy (E), electronic structure (ψ) and lifetime (τ) with respect to the same in the ground state and can, therefore, undergo chemical reactions which do not occur in the ground state. Compared with ground state reactions, unravelling the mechanism of photochemical reactions is more challenging due to the multitude of variables involved here. Product formation arises through either the singlet or triplet excited state. Photochemical reactions originating from a specific electronically excited state give primary

products in either electronically excited (adiabatic processes) or in ground state (diabatic processes). Adiabatic processes which occur on excited state potential energy surfaces are reversible. Proton transfer, electron transfer, H-atom transfer and exciplex formation are typical examples for adiabatic processes while *cis-trans* isomerization and photodimerization are typically diabatic processes.⁸ Schematic representation of reaction possibilities available to a molecule in the excited state is given in Fig. 1.2.



F= Funnel from excited to ground state surface

I= Ground state reactive intermediates

I*/P*= Excited state reactive intermediates/products

Fig. 1.2: Global paradigm for the plausible overall pathways from ground state reactants (**R**) to isolable products (**P**).⁷

Fig. 1.2 shows that there are three fundamental pathways that **R*** follow on the way to **P**.⁷ The first pathway (diabatic) involves the formation of ground state intermediates **I** that can be a biradical, radical pair or a zwitter ion. The second pathway (also diabatic) does not involve reactive intermediates but proceeds through a funnel (**F**) which can be described in terms of energy surface as conical surface intersection or a minimum produced by surface avoided intersections. Typical example for funneling is *cis-trans* isomerization of olefins where the twisted ground and excited state geometries are isoenergetic. The third pathway (adiabatic) involves

the formation of electronically excited intermediates or products. Of the three possibilities, $\mathbf{R}^* \rightarrow \mathbf{I}$ is the most commonly observed pathway for organic photochemical reactions. Common organic photochemical reactions include *cis-trans* isomerization, cycloadditions, cyclization, rearrangements etc.

For compounds, depending on irradiation conditions, there exists a plethora of photoreactions (Fig. 1.3). Since electronically excited states are high energy species, photoinduced dissociation may be expected as an immediate outcome. Indeed, dissociative processes are important. Gas-phase photochemistry and photodissociation of small molecules driven by the UV radiation is of profound importance for atmospheric photochemistry. On the other hand, photodissociation is not so common for large molecules in solution. For large molecules, electronic excitation is usually not localized and in solution, primary products of the dissociation have a high probability to recombine, because of cage effects. In addition, solvents as well as adventitious oxygen and water present in solvent can also participate in reactions carried out in solution.

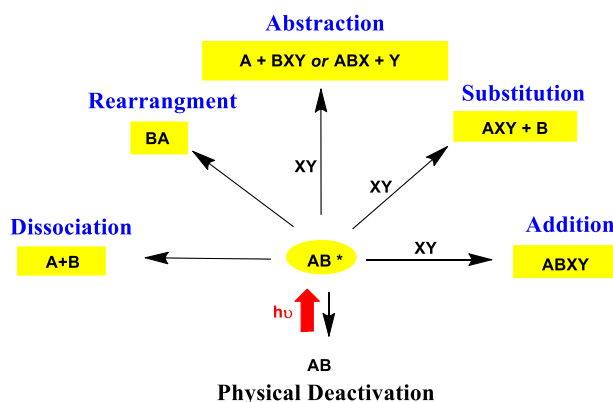


Fig. 1.3: Multiple reaction pathways for electronically excited species

Unravelling the mechanism of photochemical transformations is gruesomely challenging on one hand while immensely satisfying on the other. Once the mechanism of photochemical reactions is established, it is possible to design molecules that can undergo competing reactions in a controllable fashion. In the present work we explored the possibility of controlling the photochemistry of enone appended dibenzobarrelenes that can undergo a multitude of phototransformations. So, a brief description of the major phototransformations of the dibenzobarrelenes is given in the following sections.

1.4. History of Barrelenes

Barrelenes are bicyclic compounds with a three dimensional carbon framework. It was first noted by Hine⁹ in 1955, with the presence of a cyclic system with 6 π electrons in a nonplanar arrangement. The parent compound of this group is bicyclo[2.2.2]octa-2,5,7-triene (**1**), with the trivial name barrelene attributed to its barrel-shaped array of π -molecular orbitals consisting of the 6 π electron system.

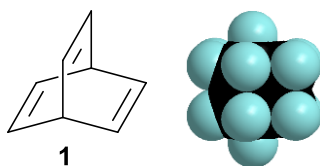


Fig. 1.4: Barrel shaped electron cloud of barrelenes

The first synthetic procedure for the simplest barrelene (**1**) was reported by Zimmerman and Paufler in 1960 using α -pyrone and methyl vinyl ketone as basic starting materials.¹⁰ Benzoannulation of **1** leads to

monobenzobarrelene **2** then to dibenzobarrelene **3** and finally to triptycene **4**.

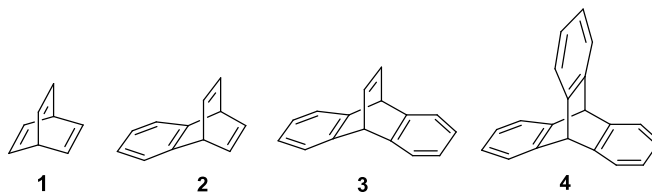
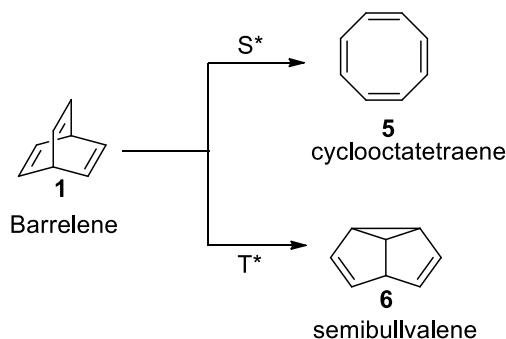


Fig. 1.5: Structural analogues of barrelenes

The barrelenes **1-3** are capable of undergoing interesting photo-transformations and several research groups including ours have contributed towards unravelling the mechanistic intricacies of their photochemistry. In the present work we have concentrated on the photochemistry of dibenzobarrelenes decorated with enone appendages.

1.5. Phototransformations of Barrelenes

The phototransformation reactions of barrelenes was hotly pursued ever since it was first reported by Zimmerman and Grunewald in 1966.^{11,12} They reported that barrelene undergo photoisomerization to give a mixture of cyclooctatetraene (**5**) and semibullvalene (**6**).



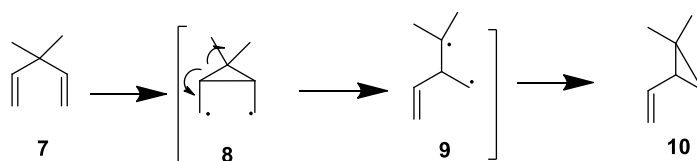
Scheme 1.1

Later detailed mechanistic investigation on this reaction revealed that product formation is multiplicity dependent. Semibullvalene is formed via triplet mediated pathway and cyclooctatetraene formation proceeds via singlet mediated pathway. The rearrangement involved in the formation of semibullvalene is recognized as di- π -methane rearrangement since it involves two π systems, connected through a methane unit.¹³ In honor of Zimmerman and coworkers who contributed much to the generalization of this reaction in many 1,4-dienes di- π -methane rearrangement is also called as Zimmerman rearrangement. It is one of the most thoroughly investigated organic photoreactions. In the literature we can find many reactions which at first glance seem unrelated, but on closer scrutiny of mechanism proves to be proceeding via a di- π -methane rearrangement.¹⁴ This shows the generality of this reaction and its relevance in synthetic organic chemistry. Extensive studies were carried out to explore the scope of this reaction in many acyclic, cyclic and bicyclic systems. Thus it is one of the most versatile and best understood photochemical transformations.

1.5.1. Di- π -methane rearrangement: general mechanism

The prerequisite for a substrate to undergo di- π -methane rearrangement is the presence of two double bonds connected through a sp^3 hybridized carbon atom.¹³⁻¹⁶ The basic skeletal rearrangement involved in all types of di- π -methane rearrangement is illustrated in Scheme 1.2. Initially, a three-step mechanism involving the generation of two biradical intermediates was proposed. Upon excitation of 1,4-pentadienes, a 1,4-biradical is initially formed which then rearranges to another biradical. In

the final step, radical combination leads to the formation of a cyclopropane derivative. The mechanism involved is still under investigation to establish the involvement of the two biradical intermediates and their possible reaction pathways. A concerted mechanism is also proposed recently.¹⁷⁻²⁰ In the case of benzonorbornadiene derivatives, the electronically excited 1,4-diene is transformed to a 1,3-biradical via a 1,2-aryl shift.²¹



Scheme 1.2

The core 1,4-diene component can be part of an acyclic or cyclic system or even an allyl substituted arene derivative. Representative examples for compounds which undergo di- π -methane rearrangement are shown in Fig 1.6.

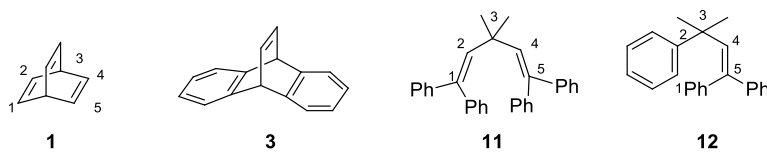
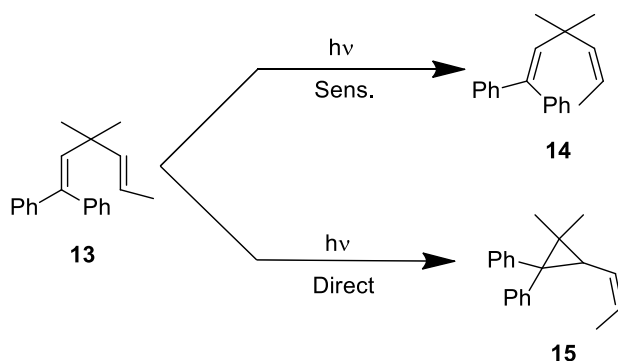


Fig. 1.6: Examples for different types of 1,4-pentadienes capable of undergoing di- π -methane rearrangement

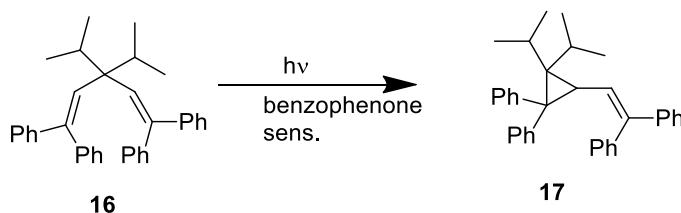
The course of this reaction is controlled by various factors such as multiplicity of the excited state involved, the nature and stability of diradical intermediates, substituents involved and also their position. Several research groups have carried out detailed investigations on the state selectivity, regioselectivity and stereoselectivity of this reaction.¹⁴

1.5.2. Reaction multiplicity

There is a structure-multiplicity relationship observed for di- π -methane rearrangement. Depending on the nature of the substrate selected, di- π -methane rearrangement can take place through either a singlet or triplet excited state. In the case of acyclic compounds, *cis-trans* isomerization is a competing reaction. In acyclic compounds where free rotation about unconstrained bonds is possible it can bring about efficient deactivation of their triplet excited states.²² In such systems di- π -methane rearrangement proceeds mainly through the singlet excited state. An example for an acyclic diene with unconstrained double bond is shown in Scheme 1.3. If there is any hindrance to free rotor group, triplet deactivation is not possible and we can observe a reactive triplet. Illustrative example for such a compound is given in Scheme 1.4.²³ Here the presence of two bulky isopropyl groups prevents free rotation around the σ -bond.



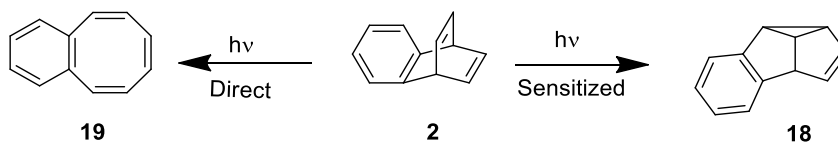
Scheme 1.3



Scheme 1.4

In the case of cyclic and bicyclic systems like barrelene and its derivatives, the reaction proceeds only through triplet states. The common sensitizers used are ketones like acetone, benzophenone and xanthone. The role of the sensitizer is to produce the triplet state with certainty. Without a sensitizer the reaction generally proceeds through singlet state, but there are instances where the initially formed singlet excited state may convert to a triplet state through intersystem crossing and it is this triplet which undergoes further rearrangement.

The direct irradiation (without sensitizer) of cyclic compounds does not give the di- π -methane rearrangement does not mean that their singlet states are incapable of undergoing di- π -methane rearrangement. Rather it is due to alternative pericyclic pathways available for singlet states which are more facile.¹⁴ Sensitized and direct reaction products for benzobarrelene are shown in Scheme 1.5.²⁴



Scheme 1.5

The structure-multiplicity relation observed for di- π -methane

rearrangement is summarized in Table 1.1.

Structural feature for the substrate	Singlet excited state	Triplet excited state
Presence of free π moiety	efficient	inefficient
Absence of free π moiety	inefficient	efficient

Table 1.1

Zimmerman and co-workers have also studied the behaviour of the independently generated cyclopropyldicarbonyl diradical species, which are considered as the biradical intermediates involved in the di- π -methane rearrangement of barrelenes and related compounds.²⁵ They have taken three azo- compounds which are the formal homo Diels-Alder adducts of nitrogen to barrene (20), benzobarrene (21) and 2,3-naphthobarrene (22). When they were subjected to thermal reactions, the products formed were exclusively the corresponding barrelenes via nitrogen exclusion whereas the photo irradiation gave a mixture of corresponding barrene, semibullvalene and cyclooctatetraene. Studies revealed that the cyclopropyldicarbonyl species in the S_0 state can undergo a Grob fragmentation²⁶ leading to the starting reactant and in the S_1 state it can proceed along the excited hypersurface to the di- π -methane product. This experiment provide a clear cut evidence for the involvement of the biradical species²⁷ and their reactivity in the ground and excited states.

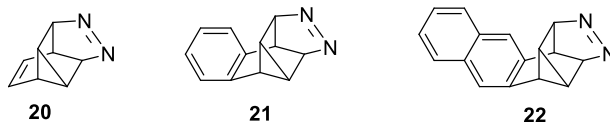
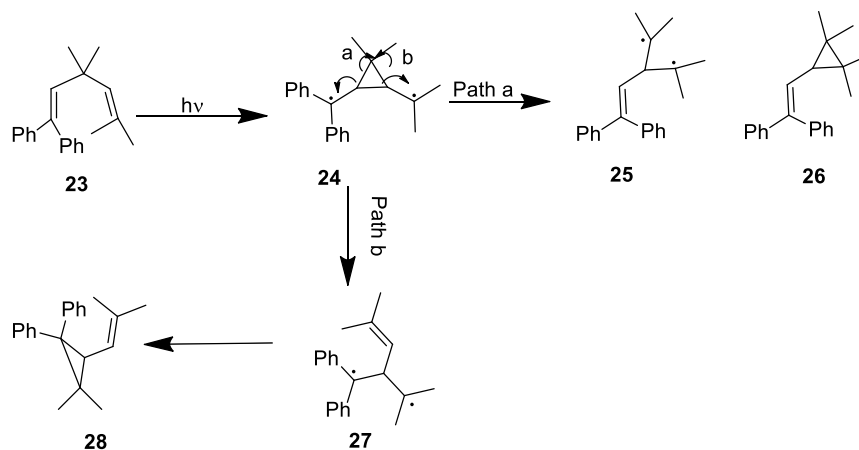


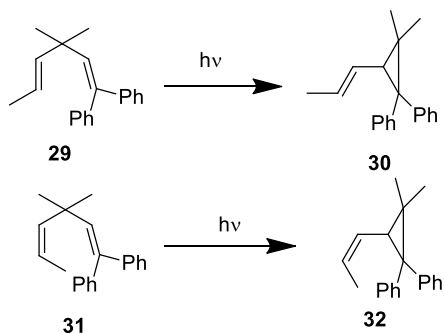
Fig. 1.7: Azo precursors for the synthesis of cyclopropyldicarbonyl diradical species

1.5.3. Regioselectivity

In symmetrically substituted di- π -methane substrates a single product is formed, since the two π systems are identical. But this is not the case with unsymmetrically substituted systems. Zimmerman and Pratt were the first to report regioselectivity in di- π -methane reactions. They observed a preference for the migratory aptitude of the two π moieties attached to the methane carbon. There is a preferred direction for the ring opening of the cyclopropyl dicarbinyl species. This is well illustrated by the examples of 3,3,5-trimethyl-1,1-diphenyl-1,4-hexadiene (Scheme 1.6) and the *E,Z*-isomers of 1,1-diphenyl-3,3-dimethyl-1,4-hexadiene (Scheme 1.7). Here there are two possible pathways available for the ring opening of the biradical. The ring opening occurs to afford the more stable 1,3-biradical. In such cases the product formed is the regioisomer with the less delocalizing group on the residual bond.²²

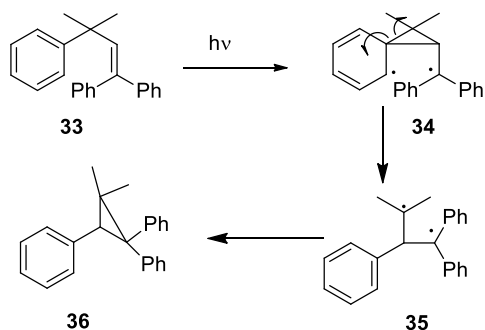


Scheme 1.6



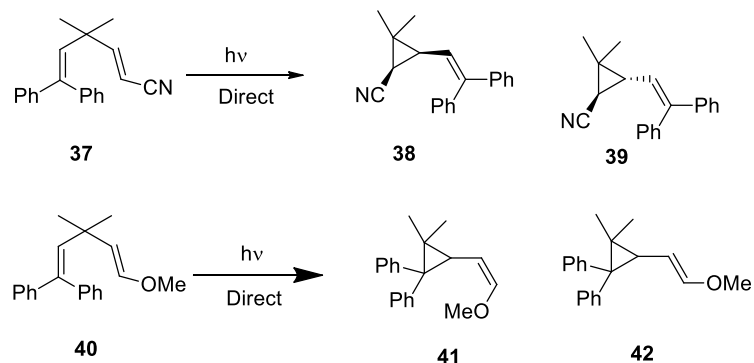
Scheme 1.7

The regioselectivity determination in aryl-vinyl systems is easier and predictable. Here the ring opening is favored through the pathway which regains the aromaticity of the system (Scheme 1.8).²⁸

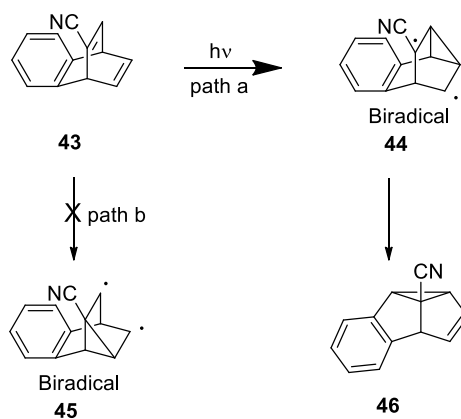


Scheme 1.8

In cases where electron donating or withdrawing groups are present on the π moieties, a general rule has been formulated based on several investigations to predict the regioselectivity of the rearrangement. The residual π bond will hold electron donating groups while electron withdrawing groups will be retained on the cyclopropane ring of the photoproduct (Scheme 1.9).²⁹

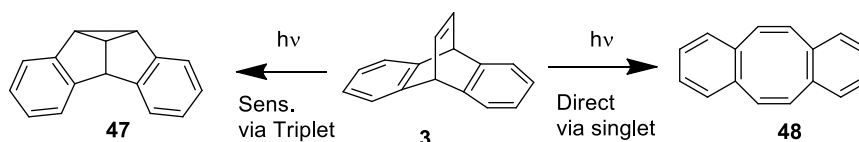


Bender *et al.* have studied the effect of substituents in bicyclic systems like benzobarrelenes and benzonorbornadienes. In the rearrangement of 2-cyanobarrelene (**43**) studied by Bender the regioselectivity depends on the formation of the most stable biradical **44** *i.e.* the one in conjugation with cyano group (Scheme 1.10).³⁰ Here the bridging occurs between two vinyl groups in such a way that the cyano group is retained at an odd electron center (path a).



1.6. Major Phototransformations of Dibenzobarrelenes

Dibenzobarrelenes, depending on the reaction conditions, undergo photorearrangement to give primarily two photoproducts: triplet mediated dibenzosemibullvalene (**47**) and singlet mediated dibenzocyclooctatetraene (**48**) (Scheme 1.11).¹² Ciganek³¹ in 1966 reported acetone sensitized irradiation of dibenzobarrelene to give dibenzosemibullvalene. Friedman³² and coworkers in 1968 showed that direct irradiation gave dibenzocyclooctatetraene. There are also cases in which both singlet mediated dibenzocyclooctatetraene and triplet mediated dibenzosemibullvalene are formed concurrently under both direct and sensitized irradiation conditions. This is due to the intersystem crossings occurring under direct irradiation condition and partial absorption of light by barrelenes under sensitized irradiation condition.³³

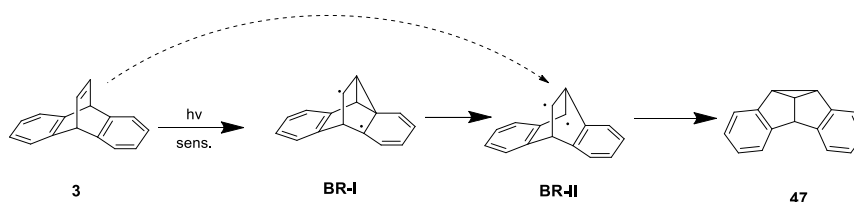


Scheme 1.11

As in the case of other cyclic systems and simple barrelenes the triplet state mediated di- π -methane rearrangement of dibenzobarrelenes also proceeds through a biradical mechanism. There are two biradical intermediates involved BR-I and BR-II in the triplet excited state as shown in Scheme 1.12. In the case of unsubstituted dibenzobarrelenes there is unique product formation but this is not the case with substituted dibenzobarrelenes the regioselectivity of the rearrangement depends on the stability of the two possible biradical intermediates. Major

regioisomer is formed via the more stable biradical intermediate. The regioisomers formed in di- π -methane rearrangement of bridgehead substituted dibenzobarrelenes will hold the bridgehead substituent at either the 4b or 8b positions.³⁴ A detailed description on the regioselectivity depending on the electronic and steric factors observed for di- π -methane rearrangement of dibenzobarrelenes is given in the following sections.

Zimmerman *et al.* had studied the aryl-vinyl di- π -methane rearrangement of *m*-cyanodibenzobarrelene labeled with deuterium on the vinyl bridge and thus they established the presence of different biradical pathways and the importance of the stabilization of the biradical intermediate in determining the regioselectivity of the product.³⁵ They showed that major product is derived from the most stable biradical intermediate **BR-I** arising through aryl-vinyl bridging instead of the more demanding aryl-aryl bridging (not shown). This is consistent with a mechanism in which the transition states leading to isomeric triplet biradicals of **BR-I** determine the regioselectivity of the reaction. However, a mechanism skipping the **BR-I** intermediate has been also suggested by Paquette invoking a direct 1,2-aryl shift^{36,18} as shown by dotted lines in the Scheme 1.12.



Scheme 1.12

Recently theoretical studies were carried out by different groups to establish the relevance of the two biradical intermediates and the possibilities for the one step and two step pathways. Houk and coworkers have done computational studies to establish the mechanism involved in the di- π -methane rearrangement.^{37,38} The electronic energies of different species involved were calculated using DFT (Density Functional Theory) (Fig. 1.8).³⁹ They concluded that the reaction can occur by competing one step or two step mechanisms on the triplet surface. Their studies showed that the minimum energy pathway for the reaction involves two barriers and after overcoming the first barrier the triplet excited state can proceed directly to the second biradical intermediate **BR-II** avoiding discrete formation of first biradical intermediate **BR-I**.

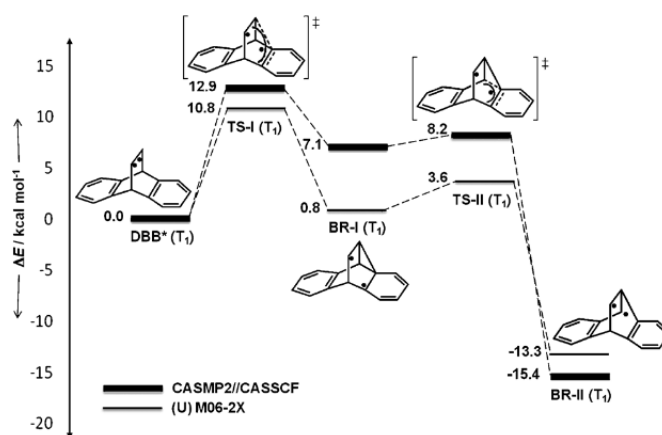
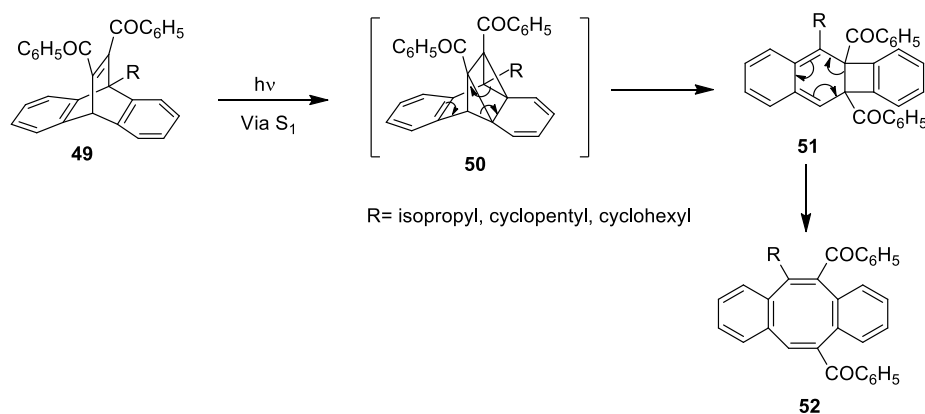


Fig. 1.8: Energy profile diagram showing the biradical intermediates and the energy of the transition states involved in di- π -methane rearrangement of dibenzobarrelenes.

Under direct irradiation condition dibenzocyclooctatetraene is the expected product but in certain cases an efficient intersystem crossing occurs to generate the triplet state and finally leads to the formation of

dibenzosemibullvalene along with dibenzocyclooctatetraene.⁴⁰ Dibenzobarrelenes with ester or benzoyl groups at vinylic position prefer the triplet mediated pathway because these substituents facilitate rapid intersystem crossing. George *et al.* have reported that when the bridgehead positions of 11,12 dibenzoyl substituted dibenzobarrelene derivatives are substituted by isopropyl, cyclopentyl or cyclohexyl groups substantial amounts of dibenzocyclooctatetraenes are formed.⁴¹ The proposed mechanism in the case of dibenzocyclooctatetraenes involve an initial intramolecular [2+2] cycloaddition through the singlet excited states followed by thermal reorganization of the resulting cage compound **50** (Scheme 1.13).⁴² In this mechanism the cyclooctatetraene formed possess a C_s symmetry.



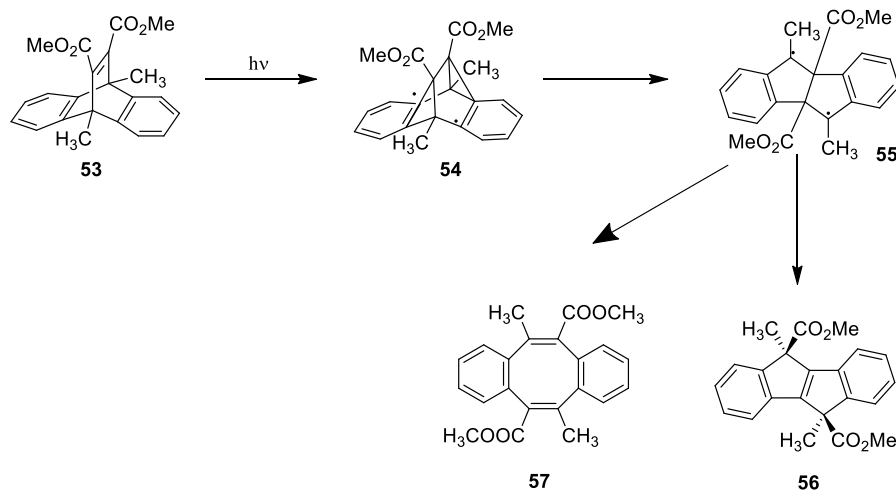
Scheme 1.13

Scheffer and coworkers later reported a tri- π -methane route⁴³ for the formation of dibenzocyclooctatetraene. They observed that in the irradiation of certain bridgehead-substituted dibenzobarrelenes, dibenzocyclooctatetraenes were formed with a different labeling pattern

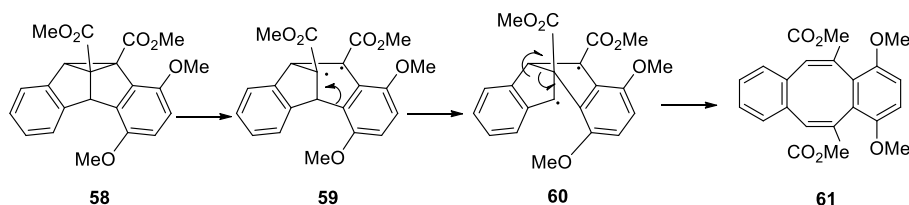
from that expected.⁴⁴ They were having a C_2 symmetry rather than a C_s symmetry as in the case of reactions which proceeds through [2+2] cycloaddition followed by rearrangement. So they proposed a different mechanism which involves all the three π bonds present in dibenzobarrelenes later named as the tri- π -methane pathway for photoisomerization of dibenzobarrelenes.

Photorearrangement through tri- π -methane pathway is observed in the direct irradiation of 11,12-dicarbomethoxy-9-10-dimethyl substituted dibenzobarrelenes to give a mixture of dibenzocyclooctatetraene and dibenzopentalene derivatives (Scheme 1.14).⁴⁵ The mechanism proposed for the formation of dibenzocyclooctatetraene involves the formation of a diradical intermediate **54** through a tri- π -methane route. Further transformations lead to the formation of a benzylic 1,4-diradical **55** which undergoes either a Grob type fragmentation resulting in dibenzocyclooctatetraene **57** or sequential carbomethoxy group migration to give dibenzopentalene derivative **56**.

Ihmels *et al.* reported the secondary transformation of initially formed dibenzosemibullvalene resulting in the formation of dibenzocyclooctatetraene.⁴⁶ They suggested that the reaction proceeds through a π -bond cleavage to give a 1,3-diradical **59**, which subsequently undergoes 1,2-aryl shift to give the 1,4-diradical **60**. Further transformation of 1,4-diradical will give the dibenzocyclooctatetraene **61** (Scheme 1.15).



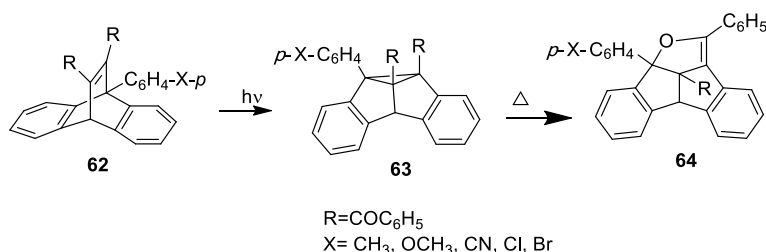
Scheme 1.14



Scheme 1.15

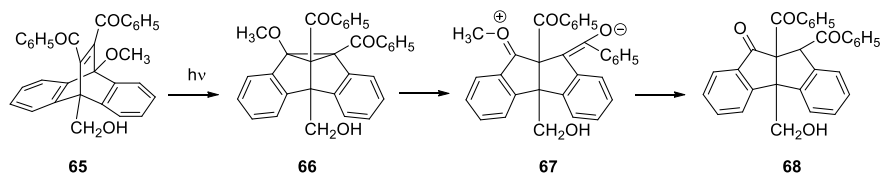
George *et al.* have carried out extensive studies on secondary product formation in several 11,12-dibenzoyl substituted dibenzobarrelenes and related systems. Apart from the formation of dibenzosemibullvalene and dibenzocyclooctatetraene they have observed the formation of some interesting and synthetically important polycyclic compounds as a result of primary photoreactions of the dibenzobarrelenes as well as from the secondary reactions of the initially formed photoproducts. They have reported the formation of dibenzopentalenodihydrofurans, dibenzopentalenes, oxygen containing heterocycles and other polycyclic compounds.

When dibenzobarrelenes with substituents such as hydroxyl, cyano and aryl groups were photoirradiated they give photoproducts which are formed from the transformation of the initially formed dibenzosemibullvalenes.^{47,48} In the irradiation of 9-aryl substituted barrelenes **62**, dibenzopentalenodihydrofurans **64** were exclusively formed at ambient reaction conditions.⁴⁷ The corresponding dibenzosemibullvalenes **63** could be detected only in irradiations carried out at low temperatures. At room temperature itself, **63** underwent thermal isomerization to dibenzopentalenodihydrofurans **64** (Scheme 1.16).



Scheme 1.16

Dibenzopentalenes can be obtained by the hydrogenation of the dibenzosemibullvalenes using 5% Pd on charcoal.³⁴ Formation of dibenzopentalenones were reported in the photolysis of the 11,12-dibenzoyl dibenzobarrelene with hydroxyl⁵⁰ and methoxy⁵¹ substituents at the bridge head positions. Here the mechanism suggested involves the ionic ring opening of the cyclopropyl functionality of the initially formed dibenzosemibullvalene to give a dipolar intermediate followed by hydrolysis to give the corresponding dibenzopentalenones. A representative example is shown in Scheme 1.17.



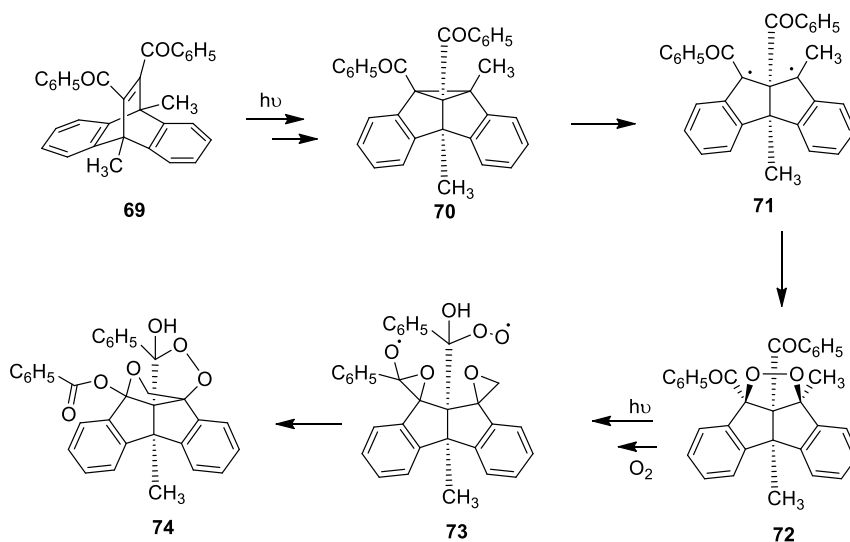
Scheme 1.17

In the photolysis of the 11,12-dibenzoyl-9,10-dimethyl substituted dibenzobarrelenes in benzene, along with the major products dibenzocyclooctatetraene and dibenzopentalenes, small amount of hexacyclic peroxy carbinol⁴⁵ was also formed. Formation of the hexacyclic peroxy carbinol is supposed to be from the initially formed dibenzosemibullvalene which undergoes cleavage of the cyclopropane ring to give a new 1,3-diradical which combines with oxygen to give an endo-peroxide and further transformations result in the formation of the hexacyclic peroxy carbinol as shown in Scheme 1.18. Besides these products lactone formation was also observed through dibenzoylalkene type rearrangement in certain cases.⁵²

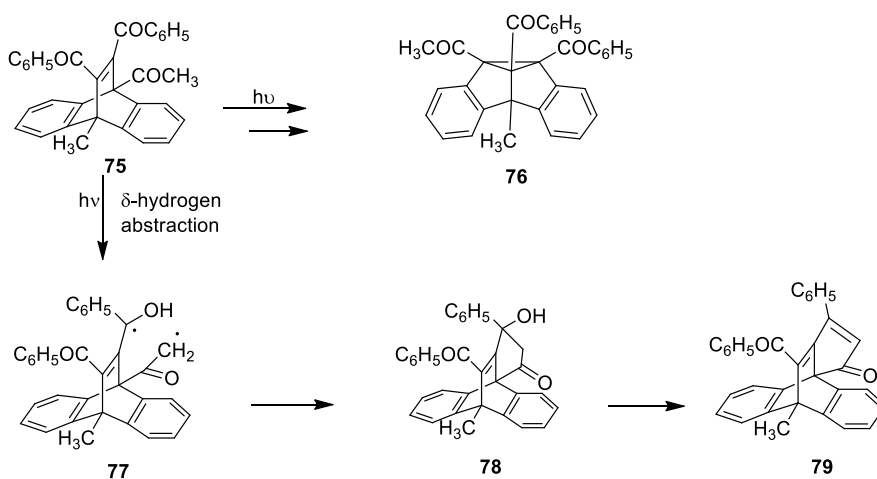
Scheffer and coworkers have isolated a peroxide similar to that of **72** during the photolysis of dimethyl 9,10-dichlorodibenzobarrelene-11,12-dicarboxylate.⁵³ This is a supporting evidence for this type of reaction pathways. Similarly a heptacyclic peroxide formation was observed in the case of 11,12-dibenzoyl-9-ethyldibenzobarrelene.⁵⁴

A novel polycyclic ketone was isolated by Sajimon *et al.* in the photolysis of 11,12-dibenzoyl-9-acetyl-10-methyl substituted dibenzobarrelene along with the major product dibenzosemibullvalene.⁵⁵ Dibenzosemibullvalene is formed through the expected di- π -methane

rearrangement whereas the formation of **79** involves a δ -hydrogen abstraction by the excited state of **75** to give a 1,5-biradical intermediate **77** which then cyclizes to give an alcohol derivative **78** followed by elimination of water to give the final product (Scheme 1.19).



Scheme 1.18

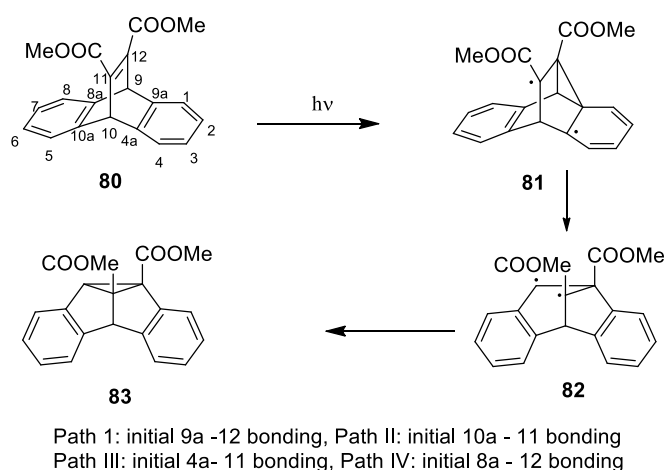


Scheme 1.19

Formation of several other heterocyclic compounds from the photolysis of appropriately substituted dibenzobarrelenes is also reported. All these reports highlight the synthetic potential of the dibenzobarrelenes for the generation of different synthons which can be used for the synthesis of other complex molecules.³³

1.6.1. Regioselectivity in the di- π -methane rearrangement of dibenzobarrelenes and the role of different substituents.

It is established beyond reasonable doubt that di- π -methane rearrangement of dibenzobarrelenes involves initial benzo-vinyl bridging to give diradical intermediates. In the case of dibenzobarrelenes having C_2 molecular symmetry, *ie.* when vinylic positions or the bridge head positions are symmetrically substituted, all the four possible pathways for benzo vinyl bridging as shown in scheme 1.20 will lead to the same product.⁵⁶ On the other hand, in unsymmetrically substituted dibenzobarrelenes regioisomeric photoproducts can be formed.



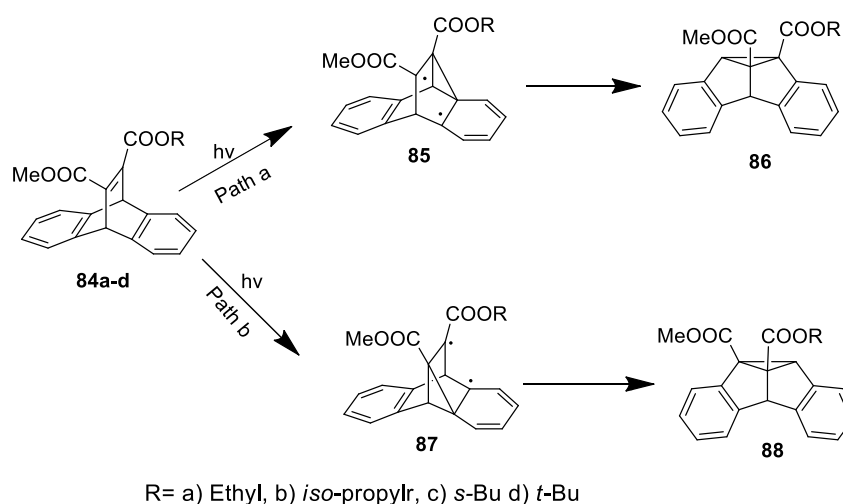
Scheme 1.20

When dibenzobarrelenes have different substituents on the vinylic bond they give two regioisomeric di- π -methane photoproducts. Path 1 and III lead to two regioisomers and path II and IV lead to their enantiomers.⁵⁷ Effect of the vinylic substituents is also reflected on the reactivity of dibenzobarrelenes. In literature we find that when ester substituents are attached to the vinylic positions, even under direct irradiation, dibenzobarrelenes show triplet reactivity presumably due to the rapid intersystem crossing of the initially formed singlet excited states.⁵⁸

Scheffer and coworkers have carried out detailed investigations on the regioselectivity of the reactions of dibenzobarrelenes having different substituents at the vinylic positions in solid as well as solution state and observed greater regioselectivity in solid state than in solution state. The diesters with different alkyl groups attached were subjected to investigation to study the odd electron stabilization and steric effects involved. They found that steric packing effects were playing the major role in the solid state reactivity of these compounds. Even though the photochemical reactions of dibenzobarrelene are feasible in solution state as well as in crystalline state there is remarkable difference in the reactivity and this provides an insight into the geometric requirements for a specific reaction to occur.⁵⁸

Solid state reactions of dibenzobarrelenes showed greater regio-stereo and enantioselectivity. They have studied the solid state reactivity of dibenzobarrelenes with different substituents at the vinylic positions as shown in Scheme 1.21.⁵⁷ Here the methyl ester group was held constant and second ester varied from ethyl to tertiary butyl. As in the case of

solution state, solid state reactions also gave two different regioisomers but the substituent effects were not regular as they tend in solution. In solution state there was a preference for the regioisomer in which the smaller ester group occupying the less hindered apical position of the dibenzosemibullvalene ring but in solid state the proportion of the regioisomers formed did not show any uniform trend. On the basis of X-ray crystallographic⁵⁸ studies they have proposed that there is a crystal packing effect on the observed regioselectivity. Even though the regioselectivity in solid state is unpredictable, from the results tabulated in Table 1.2 we can see that one of the two regioisomers is formed in considerably larger amounts in solid state. In solution state the regioselectivity is controlled by the differential biradical stabilization brought about by the initial benzo-vinyl bridging whereas in the solid state crystal packing effects control regioselectivity.^{59,60}

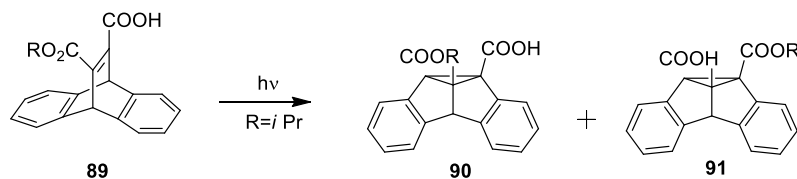
**Scheme 1.21**

Diester	Product ratio (86:88)	
	In solution	In solid state
84a	53:47	45:55
84b	55:45	93:7
84c	60:40	99:1
84d	60:40	15:85

Table 1.2: Regioselectivity shown by dibenzobarrelenes **78a-d** in solution and solid phase

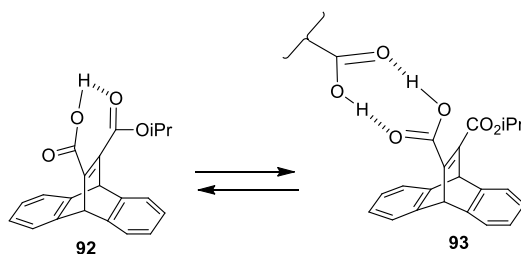
Scheffer also studied the enantioselectivity by irradiating enantiomorphically pure crystals of dibenzobarrelene derivatives and they could isolate the corresponding dibenzosemibullvalene in nearly quantitative enantiomeric excess.⁶¹ The steric course of the rearrangement was followed from the absolute configuration of the reactants and products with the aid of X-ray crystallographic studies, and this helped them to identify the topochemical factors responsible for the high enantioselectivity.⁶²

Hydrogen bonding effects depending on the reaction medium were observed in the photochemical reactivity of isopropyl monoester of dibenzobarrelene dicarboxylic acid.⁶³ In dilute benzene solutions photolysis of **89** resulted in the regioisomer **90** as the major product, whereas in solid state and in concentrated solutions isomer **91** predominated. This difference in reactivity was explained on the basis of different hydrogen bonded structures formed in different medium.



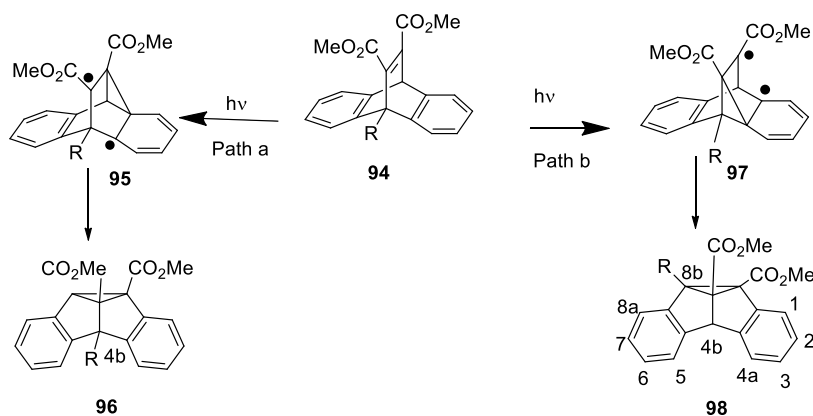
Scheme 1.22

Intramolecular and dimeric hydrogen bonded structures were detected spectroscopically for compound **86** in different reaction conditions.⁶⁴ Monomeric intramolecularly hydrogen bonded structure **92** was predominant in dilute solutions of nonpolar solvents and in concentrated solutions as well as in solid state the dimeric hydrogen bonded structure **93** dominated. Ratio of the regioisomeric semibullvalenes formed was in correlation with ratio of the intramolecular and dimeric hydrogen bonded structures. The intermolecular hydrogen bonding anchors the carboxylic acid group and hinders the formation of the initial benzo vinyl bonding at this carbon and the bond formation takes place at the other vinyl carbon atom leading to the formation of **91** as major product. In dilute solutions of benzene intramolecular hydrogen bonding is prevalent and as a result a partial positive charge on the carboxylic acid bearing vinyl carbon atom due to the internal proton transfer to the carbonyl oxygen of the ester group favors the formation of product **90**.



Scheme 1.23

The effect of one or two substituents on the bridge head position on the regioselectivity of di- π -methane rearrangement has been studied extensively by Bender *et al.*,⁶⁵ Paquette *et al.*,⁶⁶ Hemmetsberger *et al.*⁶⁷ and George *et al.*⁶⁸ The electronic as well as the steric effects of the substituents play a major role on the outcome of the phototransformations. In the case of bridgehead monosubstituted dibenzobarrelenes the di- π -methane pathway leads to two regioisomeric 4b substituted and 8b substituted dibenzosemi-bullvalenes (Scheme 1.24) depending on the initial benzo-vinyl bridging in the triplet excited states. It has been observed that dibenzobarrelenes bearing π -electron acceptors such as CN, CHO and CO₂CH₃ at the bridgehead position predominantly give the 8b substituted dibenzosemibullvalene and those with π -electron donors such as OCH₃, 4b substituted dibenzosemibullvalene is formed as major product. The regioselectivity exhibited by the different bridgehead substituted dibenzobarrelenes can be attributed to the radical stabilizing effects of the substituents.⁶⁹

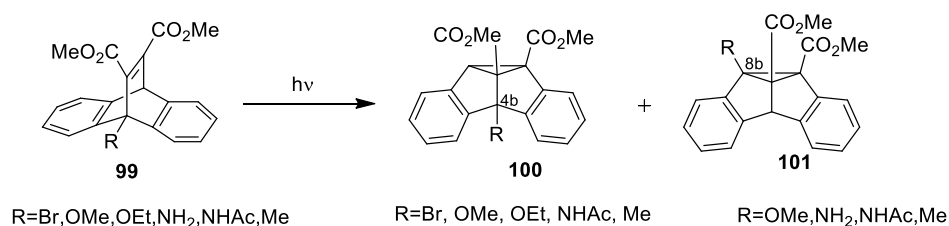


Scheme 1.24

Steric effects operating in the regioselectivity of bridgehead substituted 11,12-dibenzoyldibenzobarrelene derivatives were studied in detail by Prathapan *et al.* The photolysis of 9-methyl substituted⁴¹ dibenzobarrelenes gave 4b-substituted dibenzosemibullvalene whereas 9-ethyl and 9-benzyl substituted compounds gave partially or exclusively 8b substituted dibenzosemibullvalenes. Since the electronic effects are not relevant here, this can be attributed to the steric effects of the bulky substituents. For 9-aryl substituted dibenzobarrelenes^{34,50} they could isolate dibenzopentalenofurans which are formed as a result of the thermal isomerization of the corresponding dibenzosemibullvalenes.

Hydrogen bonding and electronegativity effects of the bridgehead substituents were studied in detail by Paddick *et al.*^{70,71} A series of 9-substituted 11,12-dicarbomethoxydibenzobarrelenes were synthesized and their photoisomerization was investigated. The bromo compound gave the 4b-regiosomer whereas the amine formed the 8b-isomer which then rearranged via an imine to give a keto diester. Acetamido compound gives a mixture of 4b and 8b where the 8b undergoes further rearrangement to a keto diester. Methoxy, ethoxy and methyl substituents gave mixture of 4b and 8b isomers, among which methyl giving more 8b-products. The regioselectivity in these compounds can be explained in terms of hydrogen bonding and electronegativity of the bridgehead substituents, more electronegative substituent favors the formation of 4b-isomer whereas hydrogen bonding favors 8b-isomer. Hydrogen bonding diminishes the stabilizing effect of the methoxy carbonyl group on the adjacent radical site and this favors the path b resulting in the formation of 8b-isomer. In the absence of any hydrogen bonding effect the

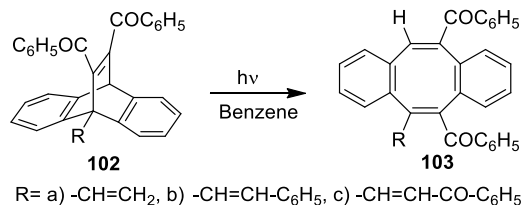
electronegativity plays the role and more electronegative substituents favor path a. This is evident from examining the product distribution in bromo, methoxy, ethoxy and methyl substituted compounds, bromo gives exclusively the 4b-isomer, methoxy and ethoxy give mixtures and methyl give predominantly 8b-isomer (Scheme 1.25).



Scheme 1.25

The influence of two alkoxy groups in the α positions of one benzene ring on the di- π -methane rearrangement of dibenzobarrelenes was studied by Ihmels *et al.*⁴⁶ In the case of methoxy substituted compounds dibenzocyclooctatetraene was formed as the secondary photoproduct of dibenzosemibullvalene and the synergic effect of the ester group and the alkoxy benzene moiety plays a significant role in stabilizing the radical intermediates leading to the formation of dibenzocyclooctatetraene (Scheme 1.15).

Bridge head olefin substituted 11,12-dibenzoyldibenzobarrelenes⁷² were synthesized and their photochemical reactions were reported earlier from our group. In those systems the olefin appendages acted as triplet quenchers and exclusive formation of the singlet mediated products were observed. The mechanism involved was the trivial [2+2]cycloaddition followed by rearrangement.



Scheme 1.26

With a view of studying the effect of orientation of the bridge head substituents on the di- π -methane regioselectivity of dibenzobarrelene a few tethered dibenzobarrelenes having fused ring system and also bridgehead substituents were synthesized and studied in our group earlier (Fig. 1.9). The presence of fused rings restricts the rotational freedom of the bridge head substituents. We have synthesized tethered ethers, esters, sulfides and sulfones and upon sensitized irradiation they were found to give the corresponding 4b- or 8b- substituted tethered dibenzosemibullvalenes. Regioselectivity observed was explained on the basis of structural features, energy minimization and Single crystal X-ray studies. The study revealed drastic variations in the distribution ratio of the 4b and 8b substituted products for the different tethered systems. This was explained on the basis of the steric effects and the ring strains in different systems.⁷³

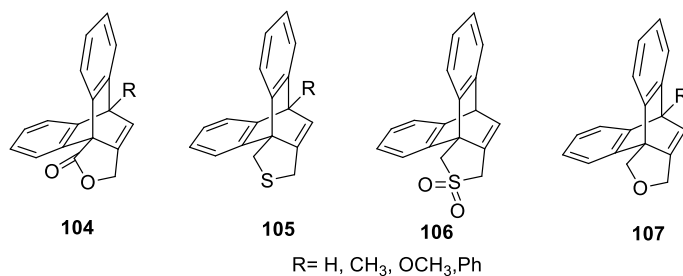
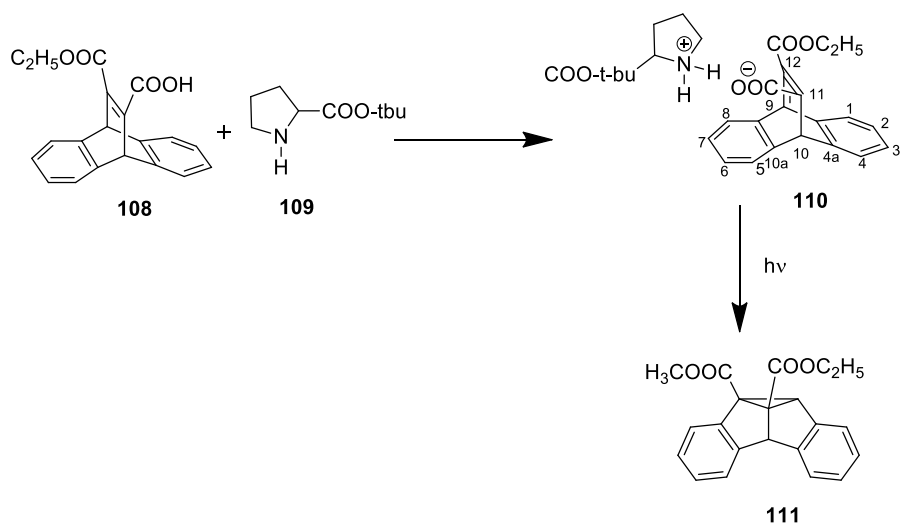


Fig. 1.9

1.7. Controlling the reaction multiplicity and product formation of Dibenzobarrelenes

We know that the photochemical reactions of dibenzobarrelene are multiplicity dependent reactions and to control the reaction, multiplicity is a difficult task. In solution state photochemistry a sensitizer or quencher is added to the reaction medium to achieve this but for solid state photochemistry, it requires the co-crystallization of the components and it is not an easy process. Scheffer and coworkers succeeded in overcoming this problem by introducing the ionic auxiliary concept.⁷⁴ They linked the chromophore to a sensitizer or heavy atom and subsequent solid state irradiation resulted in an increase in the triplet photoproduct. The presence of the ionic auxiliary group also improved the enantioselectivity of the reaction. A representative example for this type of reaction is given in scheme 1.27.



Scheme 1.27

In this reaction, first a salt is formed between the dibenzobarrelene ester-acid and the *tert*-butyl ester of (*S*)-proline. Irradiation of crystals of this, followed by acidic work-up to remove the ionic chiral auxiliary and the esterification of the resulting carboxylic acid with diazomethane gave exclusively the regioisomer **111**.⁷⁵ It was concluded that the initial “benzo–vinyl” bridging occurs between C (11) and C (4a) to give the observed enantiomer **111**. The authors have suggested that one of the contributing factors for the preferential enantioselectivity is an intramolecular steric effect in which the substituents on the vinyl group would like to remain far apart during the “benzo–vinyl” bridging. The steric interference is less in the case of C(11) – C(4a) bridging as compared to C(11) – C(10a) bridging.

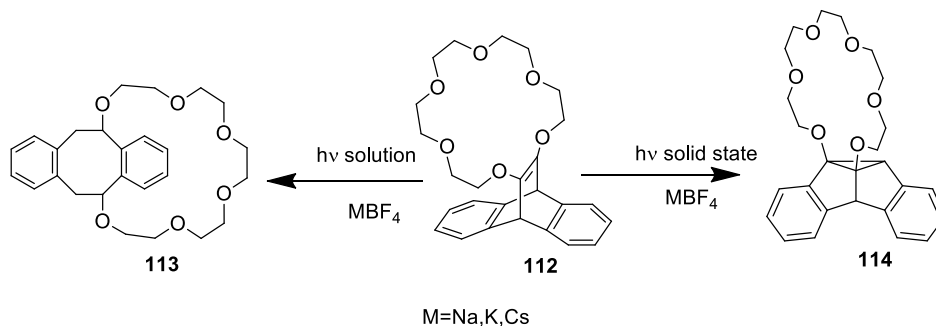
Kasha⁷⁶ in 1952 reported the possibilities of singlet-triplet transitions by the use of external heavy atoms. Here the spin orbit coupling induced by the heavy atoms enhances the rate of intersystem crossing and thus control the product distribution in photochemical reactions which are multiplicity dependent. Later it has become a common practice to use this heavy atom effect to facilitate the rate of intersystem crossing. Molecules that are commonly employed for this purpose includes oxygen, alkyl halides, organometallic compound and rare gases such as Xenon.⁷⁷ This heavy atom effect have also been utilized to control the photochemical reactions of dibenzobarrelenes. Pitchumani *et al.* employed this technique to control the photoproduct distribution in the case of dibenzobarrelenes. Stronger heavy atom effects were observed when dibenzobarrelene and the heavy atom perturber were enclosed in a constrained environment such as that of Zeolite.⁷⁸ When dibenzo-

barrelenes are incorporated in zeolite with a heavy cation such as Tl^+ , it accelerates the $S^1 \rightarrow T^1$ intersystem crossing and thereby triplet mediated photoproduct dibenzosemibullvalene is formed selectively.

We achieved moderate success in controlling state selectivity of barrene photochemistry by incorporating singlet and triplet quenchers on to barrene chromophores through appropriate spacers. Tertiary amine components were used as singlet quenchers (by electron transfer) and olefin components were used as triplet quenchers (by energy transfer). Though preliminary results appear promising, more detailed investigation is required to validate our approach.^{79,80}

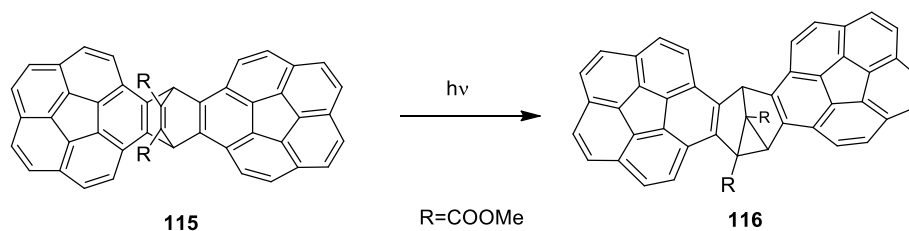
A recent report on the modification of photochemical properties of dibenzobarrene by association of alkali metal ion through crown ether complexation is seen in literature.⁴² Through crown ether complexation they have achieved medium dependent type selectivity in the photoreactions of dibenzobarrene. The dibenzobarrene **106**, which is annulated with crown ether, complexes with alkali metals such as sodium, potassium and cesium, on treatment with $NaBF_4$, KBF_4 and $CsBF_4$, respectively. Irradiation of this alone or its alkali metal complexes in acetonitrile or benzene, led preferentially to the dibenzocyclooctatetraene **113** as the photoproduct. In contrast, the solid state irradiation of the alkali metal complexes of **112** leads exclusively to the dibenzosemibullvalene **114**. Here in the solid state photoreaction of the dibenzobarrene crown ether complex, a cation effect operates which induces the di- π -methane rearrangement and such an effect is absent in solution. Thus they have achieved a successful combination of

supramolecular assembly and solid state photochemistry which leads to a type selectivity.



Scheme 1.28

Visible light induced phototransformation of biscorrannulenobarrelene dicarboxylate to the respective semibullvalene was reported by Sygula *et al.*⁸¹ Barrelene-semibullvalene rearrangement was generally observed only upon UV irradiation and so this was the first reported example of such a rearrangement induced by visible light.



Scheme 1.29

They observed that when solutions of the biscorrannulenobarrelene dicarboxylate **112** were irradiated with a sunlamp they undergo facile photochemical conversion to the respective semibullvalenes. In further studies carried out by them based on the comparison of the reactivity of **112** with other model barrelenes, they found that corannulene moiety

plays a crucial role in stabilization of the biradical intermediates in the di- π -methane rearrangement.

Another report showing the use of chiral mesoporous organicsilica as a host for the stereoselective di- π -methane rearrangement is seen in literature.⁸² Here a 1,2-bis-(ureido)-cyclohexyl linker is attached to the walls of the chiral mesoporous organic silica and then a host guest complex with 11-formyl-12-methyl dibenzobarrelene is formed (Fig. 1.10). When the stereoselectivity of the di- π -methane rearrangement is studied they have got an enantiomeric excess of 24 % at 11 % conversion to the corresponding dibenzosemibullvalene. Greater enantioselectivity was observed with chiral mesoporous organic silica when compared to the use of zeolites.

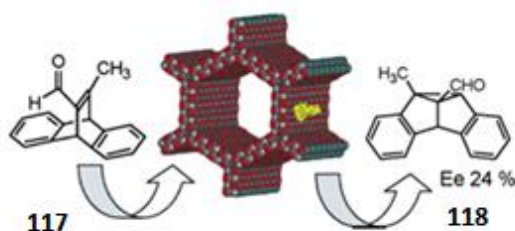


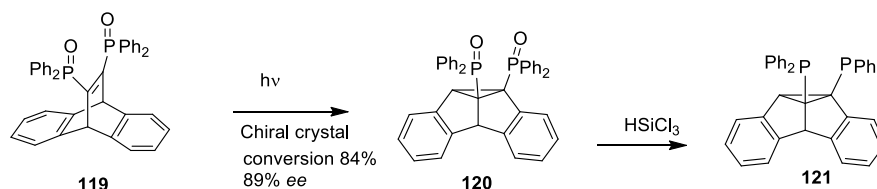
Fig. 1.10: Chiral mesoporous silica in the stereoselective di- π -methane rearrangement of 11-formyl-12-methyl dibenzobarrelene

1.8. Dibenzobarrelenes and related compounds:

Applications

Di- π -methane rearrangement of dibenzobarrelenes have been studied intensively and applied to the synthesis of many functional products. The

feasibility of this reaction in solid state have made it possible to use this for chiral induction in photochemical reactions. In solid state for absolute asymmetric synthesis, crystallization of the achiral compounds in chiral space groups leading to enantiomorphous crystals is the most common technique employed.⁸³ Scheffer and coworker have carried out detailed study of the asymmetric photorearrangement in dibenzobarrelene derivatives. They have synthesized a dibenzobarrelene with bis diphenylphosphine oxide⁸⁴ at the vinylic doublebonds which crystallizes in a chiral space group. This chiral crystal undergoes absolute asymmetric di- π -methane rearrangement in solid state with high enantiomeric excess. The reduction of the dibenzosemibullvalene formed results in a chiral ligand for transition metal catalyzed asymmetric hydrogenation (Scheme 1.30).



Scheme 1.30

There are several reports regarding the use of dibenzobarrelene frameworks in artificial receptors. Presence of both polar and nonpolar interactions in a geometrically well-defined manner is the criteria for the development of artificial receptors.⁸⁵ Dibenzobarrelenes possess a rigid molecular backbone in which a nonpolar area is surrounded by polar groups and C-9 and C-10 sites can be modified suitably. Thus it is an ideally suited molecule for amphiphilic scaffolds. Dougherty and coworkers have used 2,6-disubstituted dibenzobarrelenes in the synthesis

of macrocycles which are synthetic receptors in water.⁸⁶ They have synthesized several cyclophane hosts incorporating dibenzobarrelenes and other aromatic residues and they possess well defined hydrophobic binding sites that can bind a wide range guests. Some representative examples of the cyclophane host synthesized by them are shown in Fig. 1.11. Guest molecules that can effectively bind with these hosts include cationic and neutral organic compounds through a variety of non-covalent interactions such as cationic- π interactions, hydrophobic binding forces and weak electrostatic interactions.

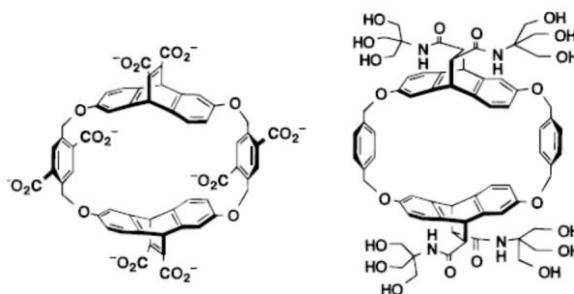
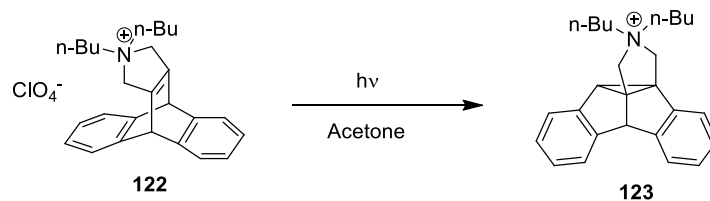


Fig. 1.11: Cyclophane hosts incorporating dibenzobarrelenes used as synthetic receptors in water

A recent report illustrates the phase transfer catalytic activity of cationic pyrrolinium-annelated dibenzosemibullvalene derivatives which in turn are synthesized by the photoinduced di- π -methane rearrangement of appropriately substituted dibenzobarrelene substrates (Scheme 1.31).⁸⁷ They act as phase-transfer catalysts in alkylation reactions with comparable or even better performance than the commonly employed tetrabutylammonium salts. This report throws light to the possibilities of using this class of chiral compounds as a promising platform for the development of versatile phase-transfer catalysts.



Scheme 1.31

Dibenzobarrelene fused azacenes⁸⁸ were found suitable for application in organic light emitting diodes. Dibenzobarrelene diones were condensed with a variety of diamines in a solution of acetic acid and dichloromethane in refluxing condition for the synthesis of these dibenzobarrelene fused azacenes (Fig. 1.12). They showed improved solubility and optical properties than other azacene derivatives which makes them suitable for fabricating light emitting diodes.

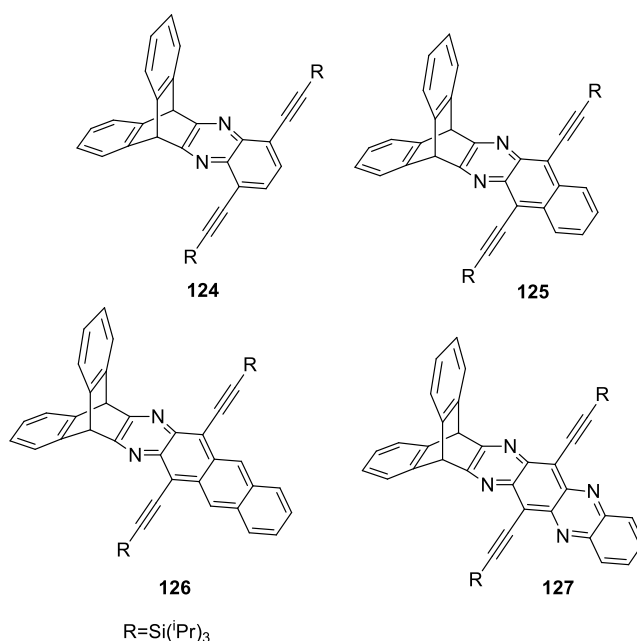
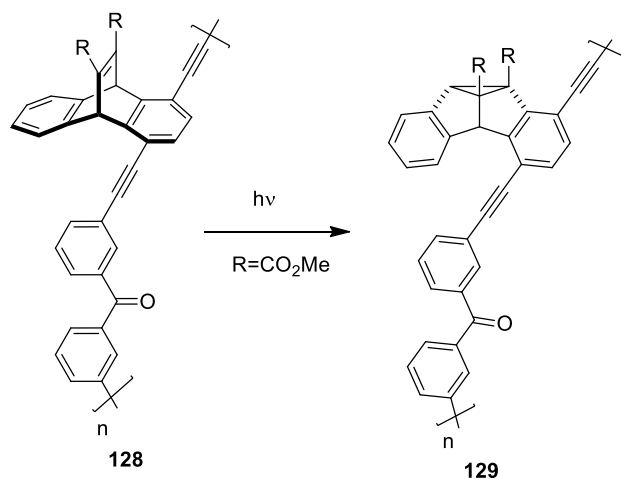


Fig. 1.12: Dibenzobarrelene fused azacene derivatives having improved OLED properties

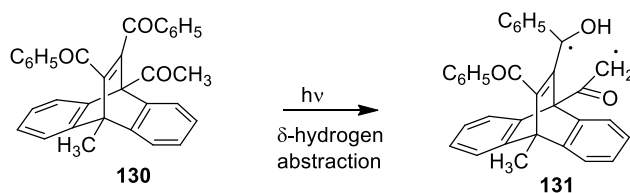
A recent report on the photoalignment of nematic liquid crystal via di- π -methane rearrangement of the dibenzobarrelene moieties incorporated in the polymer backbone have added new horizons in this field of research.^{89,90} The polymer is designed in such a manner that a triplet sensitizer such as benzophenone unit is attached near to the dibenzobarrelene substrates. First step is the selective excitation of the benzophenone units by polarized light with transition dipole moments oriented parallel to the electric vector of the exciting light. Triplet excited states of the dibenzobarrelenes were formed and di- π -methane rearrangement takes place and fast energy transfer to the adjacent di- π -methane units resulting in subsequent rearrangements (Scheme 1.32). Since the di- π -methane rearrangement is accompanied by large structural changes and it is effectively passivated to the remaining polymer segments by the liquid crystal director to achieve a uniform alignment in the liquid crystal phases. The dibenzosemibullvalene formed possess diminished internal free volume (IFV) and lacks strong interactions with the liquid crystal directors and allowing the remaining dibenzobarrelenes groups to dictate the direction of liquid crystal alignment.

Photochromic properties were observed for some dibenzobarrelene derivatives by Ramaiah *et al.*⁹¹ In the case of 11,12-dibenzoyl-9-acetyl-10-methyl-substituted dibenzobarrelenes, they observed that upon UV exposure the compound showed a green colour which disappeared within several hours in dark. The photochromic species proposed are long lived triplet biradical intermediates formed by a reversible hydrogen abstraction (Scheme 1.33). The photochromic properties of these organic compounds can be utilized for the fabrication of photochromic organic

materials having wide variety of applications.⁹²



Scheme 1.32



Scheme 1.33

1.9. Photochemistry of enones

In the present work we have synthesized a few enone appended dibenzobarrelenes. In these compounds, apart from the presence of a dibenzobarrelene chromophore we are also having an enone chromophore which is also a photochemically active group. So a brief outlook on the general photochemistry of enones is also included in this section.

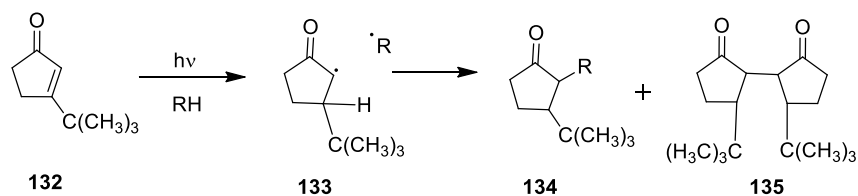
Enones as the name implies are class of compounds having both a

carbonyl (C=O) and an alkene (C=C) group in same molecule either in conjugation or not. Here we have an α,β -enone. Since enones have both n,π^* and π,π^* excited states, reactions are likely to occur depending on the nature of the lowest excited state based on the chemistry of olefins and carbonyls. Lowest excited singlet state of α,β -enones is typically $S_1(n,\pi^*)$; triplet (n,π^*), and (π,π^*) are very close in energy so the lowest triplet can be either a $T_1(n,\pi^*)$, or a $T_1(\pi,\pi^*)$ and also a mixing of orbitals also can occur depending on polarity of solvent and substituents attached.⁹³ The exact nature of the lowest reactive state depends on the substituents, solvent and molecular framework in which the enone chromophore is situated.

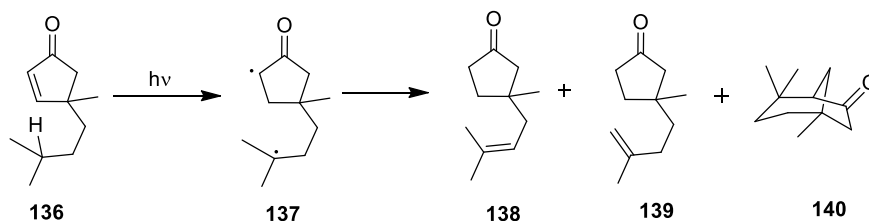
In analogy to the photochemistry of the n,π^* of carbonyls and π,π^* of alkenes, the n,π^* and π,π^* of α,β -enones are expected to undergo reactions involving intermolecular or intramolecular hydrogen abstraction, electron transfer processes, α -cleavage, β -cleavage, addition to π bonds and also *cis-trans* isomerization of the triplet π,π^* states in a competing reaction unless there is some steric hindrance to C=C rotation.⁹⁴

Hydrogen abstraction, both inter and intramolecular, is a commonly observed reaction for α,β -enones.⁹⁵ If the hydrogen abstraction is prompted by the triplet π,π^* state then it occurs by the initial hydrogen abstraction by the β -carbon of the α,β -enone. If this is intermolecular (Scheme 1.34) then the radical pair produced undergo a series of radical-radical reactions that leads to final products.⁹⁶ Intramolecular hydrogen abstraction results in the formation of a biradical which undergoes

disproportionation or coupling reaction (Scheme 1.35).⁹⁷



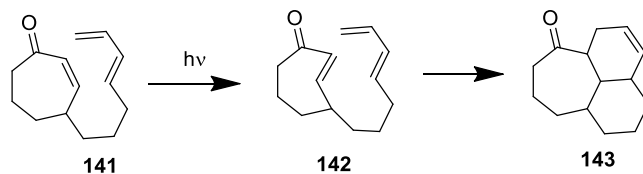
Scheme 1.34



Scheme 1.35

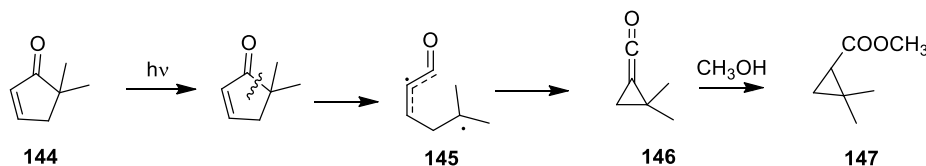
If the hydrogen abstraction is prompted by the n,π^* state hydrogen is abstracted by the carbonyl oxygen leading to the formation of biradicals which leads to products. There are also cases in which the hydrogen abstraction from both n,π^* and π,π^* states⁹⁸ takes place and forming different products. This happens mainly when these states are close in energy.

cis-trans Isomerization is a competing reaction from the triplet π,π^* state. The C=C double bond in an acyclic enone readily undergoes *cis-trans* isomerization. If it is situated in a small ring the isomerization is inhibited but in medium and large rings *cis-trans* isomerization to a transient strained *trans*-cycloalkene results which can be trapped by Diels-Alder reaction with suitable 1,3 dienes (Scheme 1.36).⁹⁹



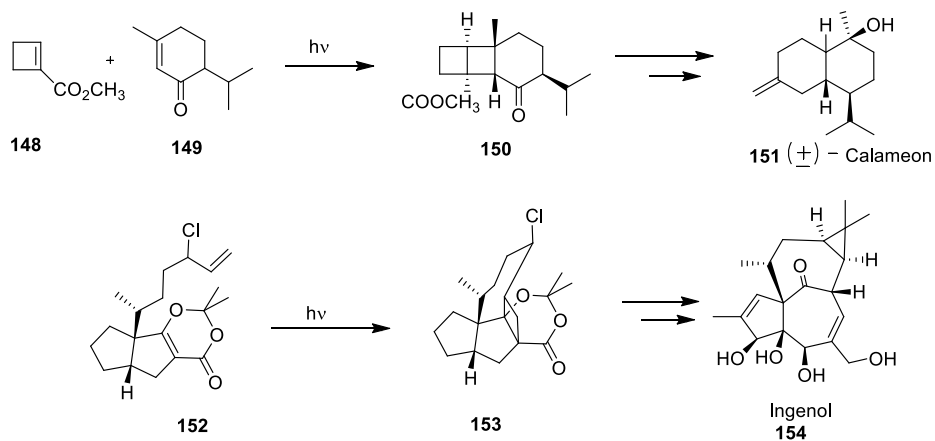
Scheme 1.36

α -Cleavage, β -cleavage, electron transfer reactions and photocycloaddition are the other major photoreactions shown by α,β -enones.⁹⁴ α -Cleavage and β -cleavage reactions results mainly in fragmentation and disproportionation. Here also the reaction can be from the n,π^* or π,π^* state. A representative example showing α -cleavage from the n,π^* state is shown in Scheme 1.37.



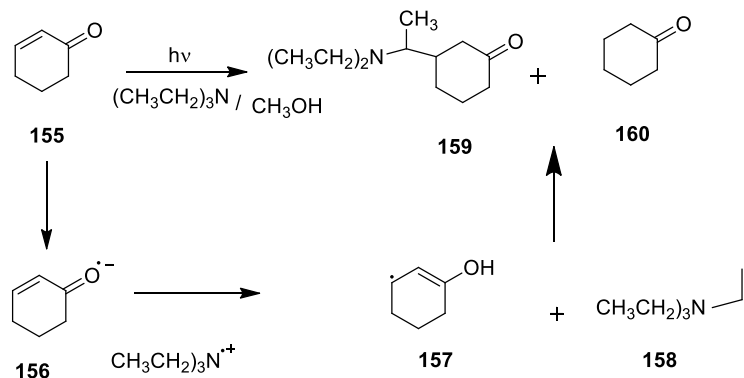
Scheme 1.37

Photocycloaddition of α,β -enones to olefins is a major synthetic tool for the synthesis of many complex organic molecules.^{100,101} Intramolecular as well as intermolecular photocycloaddition reactions involving α,β -enones are reported for the synthesis of many polycyclic Compounds.¹⁰² Scheme 1.38 shows the synthetic application of intermolecular and intramolecular photocycloaddition reaction of α,β -enones for the total synthesis of various natural products.^{103,104} These reactions are via the π,π^* state. If the reaction proceeds through the n,π^* state it leads to the formation of oxetane.



Scheme 1.38

Photo induced electron transfer reactions can occur in α,β -enones in the presence of an effective electron donor such as tertiary amines.¹⁰⁵ An illustrative example is given in Scheme 1.39.



Scheme 1.39

1.10. Defining the research problem

Literature review reveals the rich photochemistry of dibenzobarrelenes and its derivatives. Several attempts have been made to unravel new reaction pathways for dibenzobarrelenes by varying the substituents in

the dibenzobarrelenes. Great deal of effort has gone in to explain the regioselectivity shown by these compounds. Even though dibenzobarrelene reactions can potentially exhibit multiplicity dependence, there is no clear demarcation between the singlet and triplet reactivity. In some cases we can see the simultaneous formation of the singlet mediated and triplet mediated products, mainly due to the presence of substituents promoting intersystem crossing. In triplet mediated reactions the major product is dibenzosemibullvalene whereas in the singlet mediated route there are possibilities for alternative pericyclic reactions which competes with the cyclooctatetraene formation. So if we can synthesize dibenzobarrelene with suitable substituents favoring the singlet mediated pericyclic reaction pathways it can lead to the synthesis of some potentially useful compounds

Herein we have made such an attempt through the synthesis of a few dibenzobarrelenes with enone appendages. The presence of these enone the component quenches the triplet excited state of the barrelene chromophore and as a result, rather than the expected triplet photochemistry we can expect the reaction proceeding through singlet pathways leading to other reaction possibilities.

1.11. Objectives of the present study

- Synthesis of a few enone appended anthracenes.
 - Synthesis of the corresponding dibenzobarrelenes via the Diels-Alder reaction of the enone appended anthracenes with suitable dienophiles.
 - Photochemical studies of these dibenzobarrelenes in solid state
-

and solution state.

- Photophysical studies especially laser flash photolysis to study the nature of intermediates formed in the photochemical reaction.
- Single crystal X-ray crystallographic studies to reveal the structural features of the synthesized dibenzobarrelenes and their photochemical products.
- Cyclic voltammetric study of the redox properties of the system.

References

1. a) Kishi, Y. *Pure Appl. Chem.* **1993**, *65*, 771. b) Suh, E. M.; Kishi, Y. *J. Am. Chem. Soc.* **1994**, *116*, 11205.
2. Tietze, L. F.; Beifuss, U. *Angew. Chem., Int. Ed. Engl.* **1993**, *32*, 131.
3. Bach, T.; Hehn, J. P. *Angew. Chem. Int. Ed.* **2011**, *50*, 1000.
4. Nicolaou, K. C.; Vourloumis, D.; Winssinger, N.; Baran, P. S. *Angew. Chem.* **2000**, *112*, 46.
5. Hoffmann, N. *Chem. Rev.* **2008**, *108*, 1052.
6. Turro, N. J. *Angew. Chem., Int. Ed. Engl.* **1986**, *25*, 882.
7. Turro, N. J.; Ramamurthy, V.; Scaiano, J. C. *Modern Molecular Photochemistry of Organic Molecules*, University Science Books, Sausalito, CA, **2010**.
8. Turro, N. J.; Mc Vey, J.; Ramamurthy, V.; Lechtken, P. *Angew. Chem., Int. Ed. Engl.* **1979**, *18*, 572.
9. Hine, J.; Brown, J. A.; Zaldow, L. H.; Gardner, W. R.; Hine, M. *J. Am. Chem. Soc.* **1955**, *77*, 594.
10. Zimmerman, H. E.; Paufler, R. M. *J. Am. Chem. Soc.* **1960**, *82*, 1514.
11. Zimmerman, H. E.; Grunewald, G. L. *J. Am. Chem. Soc.* **1966**, *88*, 183.
12. Zimmerman, H. E.; Binkley, R. W.; Givens, R. S.; Sherwin, M. A. *J. Am. Chem. Soc.* **1967**, *89*, 3932.
13. a) Zimmerman, H. E. In *Rearrangements in Ground and Excited States*; Vol. 3, DeMayo, P., Ed.; Academic Press: New York, **1980**, Vol. 3. b) Zimmerman, H. E. *Org. Photochem.* **1991**, *11*, 1.
14. Zimmerman, H. E.; Armesto, D. *Chem. Rev.* **1996**, *96*, 3065.

15. Zimmerman, H. E.; Mariano, P. S. *J. Am. Chem. Soc.* **1969**, *91*, 1718.
16. Zimmerman, H. E. *The Di-pi-methane Rearrangement in CRC Handbook of Organic Photochemistry and Photobiology*; Horspool, W.; Song, P. S.: Eds. C R C Press: BocaRaton, **1995**, 184.
17. Hixson, S. S.; Mariano, P. S.; Zimmerman, H. E. *Chem. Rev.* **1973**, *73*, 531.
18. a) Reguero, M.; Bernardi, F.; Jones, H. *J. Am. Chem. Soc.* **1993**, *115*, 2073. b) Robb, M. A.; Bernardi, F.; Olivucci, M. *Pure Appl. Chem.* **1995**, *67*, 783.
19. Furtos, L. M.; Sancho, U.; Castan˜o, O. *Org. Lett.* **2004**, *6*, 1229.
20. a) Mori, Y.; Takano, K. *J. Photochem. Photobiol. A Chem.* **2011**, *219*, 278. b) Su, M. D. *Chem. Phys. Lett.* **1995**, *237*, 317.
21. Paquette, L. A.; Varadarajan, A.; Burke, L. D. *J. Am. Chem. Soc.* **1986**, *108*, 8032.
22. Zimmerman, H. E.; Pratt, A. C. *J. Am. Chem. Soc.* **1970**, *92*, 6259.
23. Zimmerman, H. E.; Schissel, D. N. *J. Org. Chem.* **1986**, *51*, 196.
24. a) Zimmerman, H. E.; Givens, R. S.; Pagni, R. M. *J. Am. Chem. Soc.* **1968**, *90*, 6096-6108. b) Zimmerman, H. E.; Givens, R. S.; Pagni, R. M. *J. Am. Chem. Soc.* **1968**, *90*, 4191.
25. Zimmerman, H. E.; Boettcher, R. J.; Buehler, N. E.; Keck, G. B.; Steinmetz, M. G. *J. Am. Chem. Soc.* **1976**, *98*, 7680 .
26. Grob, C. A. *Angew. Chem.* 1969, *81*, 543.
27. a) Adam, W.; DeLucchi, O.; Dorr, M. *J. Am. Chem. Soc.* **1989**, *111*, 5209. b) Adam, W.; Dorr, M.; Kron, J.; Rosenthal, R. J. *J. Am. Chem. Soc.* **1987**, *109*, 7074.
28. Zimmerman, H. E.; Klun, R. T. *Tetrahedron.* **1978**, *43*, 1775.
29. Zimmerman, H. E.; Steinmetz, M. G.; Kreil, C. L. *J. Am. Chem. Soc.* **1978**, *100*, 4146.
30. Bender, C. O.; Brooks, D. W.; Cheng, W.; Dolman, D.; O'Shea, S. F.; Shugarman, S. *Can. J. Chem.* **1979**, *56*, 3027.
31. Ciganek, E. *J. Am. Chem. Soc.* **1966**, *88*, 2882.
32. Rabideau, P. W.; Hamilton, J. B.; Friedman, L. *J. Am. Chem. Soc.* **1968**, *90*, 4465.
33. Ramaiah, D.; Sajimon, M. C.; Joseph, J.; George, M. V. *Chem. Soc. Rev.* **2005**, *34*, 48.
34. Kumar, C. V.; Murty, B. A. R. C.; Lahiri, S.; Chackachery, E. Scaiano, J. C.; George, M. V. *J. Org. Chem.* **1984**, *49*, 4923.
35. Zimmerman, H. E.; Sulzbach, H. M.; Tollefson, M. B. *J. Am. Chem. Soc.* **1993**, *115*, 6548.

36. Paquette, L. A.; Bay, E. *J. Am. Chem.* **1982**, *47*, 4597.
37. Matute, R.A.; Houk, K. N. *Angew. Chem.* **2012**, *124*, 13274.
38. Matute, R.A.; Miguel, A.; Garcia-Garibay, M.; Houk, K. N. *Org. Lett.* **2014**, *16*, 5232.
39. Matute, R.A.; Houk, K. N. *Angew. Chem. Int. Ed.* **2012**, *51*, 13097.
40. Scheffer, J. R.; Yang, J. *CRC Handbook of Organic Photochemistry and Photobiology*, ed. W. M. Horspool and P. S. Sean, CRC Press, Boca Raton, FL, USA, **1995**, ch. 16, pp. 204.
41. Prathapan, S.; Ashok, K.; Cyr, D. R.; Das, P. K.; George, M. V. *J. Org. Chem.* **1987**, *52*, 5512.
42. Ihmels, H.; Schneider, M.; Waidelich, M. *Org. Lett.* **2002**, *4*, 3247.
43. Pokkuluri, P. R.; M.; Scheffer, J. R.; Trotter, J. *J. Am. Chem. Soc.* **1990**, *112*, 3676.
44. Pokkuluri, P. R.; M.; Scheffer, J. R.; Trotter, J. *Acta Crystallogr. Sect. B: Cryst. Struct. Commun.* **1993**, *B49*, 1049.
45. Asokan, C. V.; Kumar, S. A.; Das, S.; Rath, N. P.; George, M. V. *J. Org. Chem.* **1991**, *56*, 5890.
46. Ihmels, H.; Mohrschladt, C. J.; Grimme, J. W.; Quast, H. *Synthesis* **2001**, *8*, 1175.
47. Sajimon, M. C.; Ramaiah, D.; Muneer, M.; Ajithkumar, E. S.; Rath, N. P.; George, M. V. *J. Org. Chem.* **1999**, *64*, 6347.
48. Muneer, M.; Ramaiah, D.; Ajithkumar, E. S.; Sajimon, M. C.; Rath, N. P.; George, M. V. *Acta Crystallogr. Sect. C: Cryst. Struct. Commun.* **1999**, *C55*, 996.
49. Prathapan, S.; Ashok, K.; Gopidas, K. R.; Rath, N. P.; Das, P. K.; George, M. V. *J. Org. Chem.* **1990**, *55*, 1304.
50. Murty, B. A. R. C.; Prathapan, S.; Kumar, C. V.; Das, P. K.; George, M. V. *J. Org. Chem.* **1985**, *50*, 2533.
51. a) Ramaiah, D.; Kumar, S.A.; Asokan, C. V.; Mathew, T.; Das, S.; Rath N. P.; George, M. V. *J. Org. Chem.* **1996**, *61*, 5468. b) Kumar, S. A.; Mathew, T.; Das, S.; Rath, N. P.; George, M. V. *Acta Crystallogr. Sect. C: Cryst. Struct. Commun.* **1996**, *C52*, 2797.
52. Zimmerman, H. E.; Durr, H. G. C.; Givens, R. S.; Lewis, R. G. *J. Am. Chem. Soc.* **1967**, *89*, 1863.
53. Pokkuluri, P. R.; Scheffer, J. R.; Trotter, J. *Acta Crystallogr. Sect. C: Cryst. Struct. Commun.*, **1993**, *C49*, 2014.
54. Mathew, T.; Kumar, S. A.; Das, S.; Rath, N. P.; George, M. V. *J. Photochem. Photobiol., A*, **1996**, *95*, 137.

55. Sajimon, M. C.; Ramaiah, D.; Muneer, M.; Rath, N. P.; George, M. V. *J. Photochem. Photobiol. A* **2000**, *136*, 209.
56. Chen, J.; Scheffer, J. R.; Trotter, J. *Tetrahedron*, **1992**, *48*, 3251.
57. Garcia-Garibay, M.; Scheffer, J.R.; Trotter, J.; Wireko, F. *Tetrahedron Lett.* **1988**, *29*, 2041.
58. Garcia-Garibay, M.; Scheffer, J.R.; Trotter, J.; Wireko, F. *Acta Cryst.* **1990**, *B46*, *79*, 431.
59. Garcia-Garibay, M.; Scheffer, J.R.; Trotter, J.; Wireko, F. *Tetrahedron Lett.* **1987**, *28*, 1741.
60. Scheffer, J.R.; Trotter, J.; Garcia Garibay, M.; Wireko, F. *Mol. Cryst. Liq. Cryst. Inc.Nonlin. Opt.* **1988**, *156*, 63.
61. Evans, S. V.; Garcia-Garibay, M.; Onkaram, N.; Scheffer, J. R.; Trotter, J.; Wireko, F. *J. Am. Chem. Soc.* **1986**, *108*, 5648.
62. Garcia-Garibay, M.; Scheffer, J. R.; Trotter, J.; Wireko, F. *J. Am. Chem. Soc.* **1989**, *111*, 4985.
63. Garcia-Garibay, M.; Scheffer, J. R.; Watson, D. G. *J. Chem. Soc., Chem. Commun.* **1989**, 600.
64. Garcia-Garibay, M.; Scheffer, J. R.; Watson, D. G. *J. Org. Chem.* **1992**, *57*, 241.
65. a) Bender, C. O.; Brooks, D. W.; Cheng, W.; Dolman, D.; O'Shea, S. F.; Shugarman, S. S. *Can. J. Chem.* **1978**, *56*, 3027. b) Bender, C. O.; King-Brown, E. H. *J. Chem. Soc., Chem. Commun.* **1976**, 878. c) Bender, C. O.; Wilson, J. *Helv. Chim. Acta* **1976**, *59*, 1469.
66. Paquette, L. A.; Bay, E. *J. Am. Chem. Soc.*, **1984**, *106*, 6693.
67. Hemmetsberger, H.; Nobbe, M. *Tetrahedron* **1988**, *44*, 6728.
68. Sajimon, M. C.; Ramaiah, D.; Kumar, S. A.; Rath, N. P.; George, M. V. *Tetrahedron* **2000**, *56*, 5421.
69. Iwamura, M.; Tukada, H.; Iwamura, H. *Tetrahedron Lett.* **1980**, *21*, 4865.
70. Richards, K. E.; Tillman, R.W.; Wright, G. J. *Aust. J. Chem.* **1975**, *28*, 1289.
71. Paddick, R. G.; Richards, K. E.; Wright, G. J. *Aust. J. Chem.* **1976**, *29*, 1005.
72. Jacob, A. M.; George, G.; Mathew, E. M. *J. Chem. Res.* **2015**, *39*, 202
73. Mathew, E. M. *Ph. D. Thesis*, Cochin University of Science and Technology, **2013**.
74. Gamlin, J. N.; Jones, R.; Leibovitch, M.; Patrick, B.; Scheffer, J.R.; Trotter, J. *Acc. Chem. Res.* **1996**, *29*, 203.
75. Gudmundsdottir, D.; Scheffer, J. R. *Tetrahedron Lett.* **1990**, *31*, 6807

76. Kasha, M. *J. Chem. Phys.* **1952**, *20*, 7.
77. a) Evans, D. J. *J. Chem. Soc.* **1957**, 1351. b) Evans, D. J. *J. Chem. Soc.* **1959**, 2753. c) Evans, D. J. *J. Chem. Soc.* **1960**, 1735. d) Tsubomura, H.; Mulliken, R. S. *J. Am. Chem. Soc.* **1960**, *82*, 5966. e) Evans, D. J. *J. Chem. Soc.* **1987**, 1961.
78. Pitchumani, K.; Warriar, M.; Lakshmi, S. K.; Ramamurthy, V. *Tetrahedron* **2003**, *59*, 5763.
79. Jomon, P. J. *Ph. D. Thesis*, Cochin University of Science and Technology, **2013**.
80. Reshma, G. *Ph. D. Thesis*, Cochin University of Science and Technology, **2014**.
81. Sygula, A.; Sygula, R.; Rabideau, P.W. *Tetrahedron Lett.* **2005**, *46*, 1189.
82. Benitez, M.; Bringmann, G.; Dreyer, M.; Garcia, H.; Ihmels, H.; Waidelich, M.; Wissel, K. *J. Org. Chem.* **2005**, *70*, 2315.
83. Sakamoto, M. *J. Photochem. Photobiol. C Photochem. Rev.* **2006**, *7*, 183.
84. Fu, T. Y.; Liu, Z.; Scheffer, J. R.; Trotter, J. *J. Am. Chem. Soc.* **1993**, *115*, 12202.
85. Davis, A. M.; Teague, S. *J. Angew. Chem., Int. Ed. Eng.* **1999**, *38*, 736
86. a) Petti, M. A.; Shepodd, T. J.; Barrans, R. E.; Dougherty, D. A. *J. Am. Chem. Soc.* **1988**, *110*, 6825. b) Stauffer, D. A.; Barrans, R. E., Jr.; Dougherty, D. A. *J. Org. Chem.* **1990**, *55*, 2762. c) Forman, J. E.; Barrans, R. E., Jr.; Dougherty, D. A. *J. Am. Chem. Soc.* **1995**, *117*, 9213. d) Ngola, S. M.; Kearney, P. C.; Mecozzi, S.; Russell, K.; Dougherty, D. A. *J. Am. Chem. Soc.* **1999**, *121*, 1192.
87. Ihmels, H.; Luo, J. *Beilstein. J. Org. Chem.* **2011**, *7*, 119.
88. Ganschow, M.; Koser, S.; Hahn, S.; Rominger, F.; Freudenberg, J.; Brunz, U. *H. F. Chem. Eur. J.* **2017**, *23*.
89. Cox, J. R.; Simpson, J.H.; Swager, T. M. *J. Am. Chem. Soc.* **2013**, *135*, 640.
90. a) Long, T. M.; Swager, T. M. *J. Am. Chem. Soc.* **2002**, *124*, 3826. b) Zhu, Z.; Swager, T. M. *J. Am. Chem. Soc.* **2002**, *124*, 9670.
91. Sajimon, M. C.; Ramaiah, D.; Suresh, C. H.; Adam, W.; Lewis, F. D.; George, M. V. *J. Am. Chem. Soc.* **2007**, *129*, 9439.
92. Irie, M.; Yokoyama, Y.; Seki, T. *New Frontiers in Photochromism*; Springer: Tokyo, **2013**.
93. Jones, C.R.; Kearns D. R. *J. Am. Chem. Soc.* **1977**, *99*, 344.
94. Schuster, D.I. *Photochemical rearrangements of enones. In rearrangements in ground and excited states*, Vol.3, Academic press, Newyork, **1980**.
95. Jeger, O.; Schaffner, K. *Pure Appl.Chem.* **1970**, *21*, 247.

96. Schaffner, K.; Jeger, O. *Tetrahedron*. **1974**, *30*, 1891.
97. Wolff, S.; Schreiber, W. L.; Smith, A. B. I.; Agosta C. *J. Am. Chem. Soc.* **1972**, *94*, 7797.
98. Chan, A. C.; Schuster, D.I. *J. Am. Chem. Soc.* **1986**, *108*, 4561.
99. a) Dorr, H.; Rawal, V. H. *J. Am. Chem. Soc.* **1999**, *121*, 10229. b) Noyori, R.; Kato, M. *Bull. Chem. Soc. Jpn.* **1947**, *47*, 1460.
100. a) Bauslaugh, P.G. *Synthesis*, **1970**, *6*, 287. b) Eaton, P. E. *Acc. Chem. Res.*, **1968**, *1*, 50. c) Demuth, M.; Mikhail, G. *Synthesis* **1989**, *3*, 145.
101. Bach, T. *Synthesis*, 1998, 683.
102. Crimmins, M. T. *Chem. Rev.* **1988**, *88*, 1453.
103. Winkler, J. D.; Bowen, C.M.; Liotta, F. *Chem. Rev.* **1995**, *95*, 2003.
104. Oppolzer, W. *Acc. Chem. Res.* **1982**, *15*, 135.
105. Schuster, D.I.; Patai, S.; Rappoport, Z. *The chemistry of enones*, John Wiley & Sons, Ltd., New York, **1989**.

Synthesis of a few enone appended anthracenes

2.1. Abstract

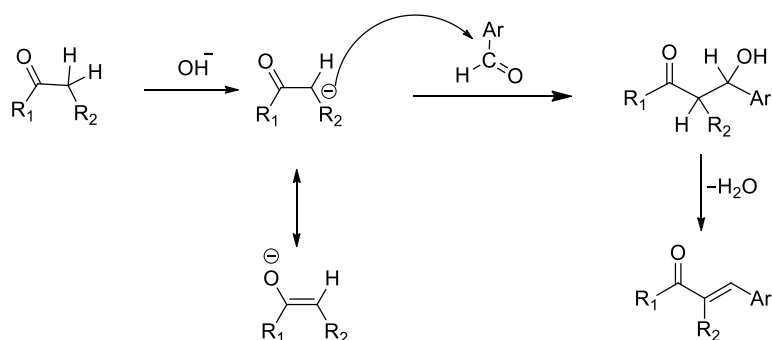
This chapter deals with the synthesis of enone appended anthracene precursors for the synthesis of dibenzobarrelenes. We utilized Claisen-Schmidt condensation reaction of various ketones with anthracene-9-carbaldehyde and its derivatives for the synthesis of the required enone appended anthracenes. The ketones were selected in such a way that the geometry of enone components with respect to anthracene moiety is subtly changed. Such changes will be translated to incipient dibenzobarrelenes affecting their overall photochemistry and photophysics.

2.2. Introduction

Carbon-carbon bond forming reactions play a significant role in synthetic organic chemistry.¹ Aldol condensation reaction is one among the major synthetic strategies used for carbon-carbon bond formation.² α,β -Unsaturated ketones which are the major products of this reaction are very important intermediates in natural product synthesis and also many of them exhibit pharmacological and biological activities. In literature there are many reports on Claisen-Schmidt condensation reaction, which is a crossed-aldol³ reaction. Condensation of aromatic aldehydes with cyclic ketones is utilized for the synthesis of many α,α' -bis (substituted benzylidene) cycloalkanones. These compounds have gained much attention owing to their broad spectrum of biological activities such as HIV-1 integrase inhibitory, cytotoxicity, antiangiogenicity, cholesterol lowering activity, and antioxidant properties.⁴ Kamath and co-workers have reported that these are also suitable for nonlinear optical materials

because of their optical limiting properties and third order linearity.⁵ These also find application in liquid crystalline polymers⁶ and are also the precursors for the synthesis of many pyrimidine derivatives⁷ and intermediates in the total synthesis of many natural products.⁸

In the present work, we have employed Claisen-Schmidt condensation reaction^{9,10} for the synthesis of a few enone appended anthracenes. Claisen-Schmidt condensation is catalyzed by both acids and bases.¹¹ In the present investigation, we employed base catalyzed reaction in which the first step is the formation of an enolate ion from the ketone which then undergoes nucleophilic addition to the carbonyl carbon of the aldehyde to form a β -hydroxy ketone which then undergoes dehydration to give the corresponding α,β -unsaturated ketones (Scheme 2.1). In general, Claisen-Schmidt condensation reaction shows a preference for forming *trans* double bonds.¹²



Scheme 2.1

Synthesis of several anthracene and bisanthracene derived compounds by Claisen-Schmidt condensation has already been reported from our group.¹³ Presence of these anthracene component makes them good dienes for Diels-Alder reaction with suitable dienophiles.¹⁴

2.3. Results and discussion

We have synthesized a series of enone appended anthracenes by Claisen-Schmidt condensation reaction of various ketones (**1-6**) with anthracene-9-carbaldehyde (**7**) and its derivatives such as 10-methylanthracene-9-carbaldehyde (**8**) and 10-phenylanthracene-9-carbaldehyde (**9**). The ketones were selected in such a way that geometrical effects can also be accounted in the compounds synthesized. Ketones having different structural features, such as acyclic ketone, cyclic ketones with varying ring size and also heteroatom incorporated cyclic ketones were selected. Structure of ketones and aldehydes employed in this investigation are listed in Chart 2.1.

2.3.1. Synthesis of 10-substituted anthraldehydes

2.3.1.1. Synthesis of 9-substituted anthracenes

9-Methylanthracene (**10**) was synthesized by a modified Wolff-Kishner reduction of anthracene-9-carbaldehyde (**7**) with hydrazine hydrate and sodium hydroxide in diethylene glycol (Scheme 2.2).¹⁵⁻¹⁷

9-Phenylanthracene (**13**) was synthesized by the Grignard reaction of anthrone (**11**) with *in situ* generated phenyl magnesium bromide (**12**) in tetrahydrofuran followed by acid mediated dehydration.¹⁸⁻²¹

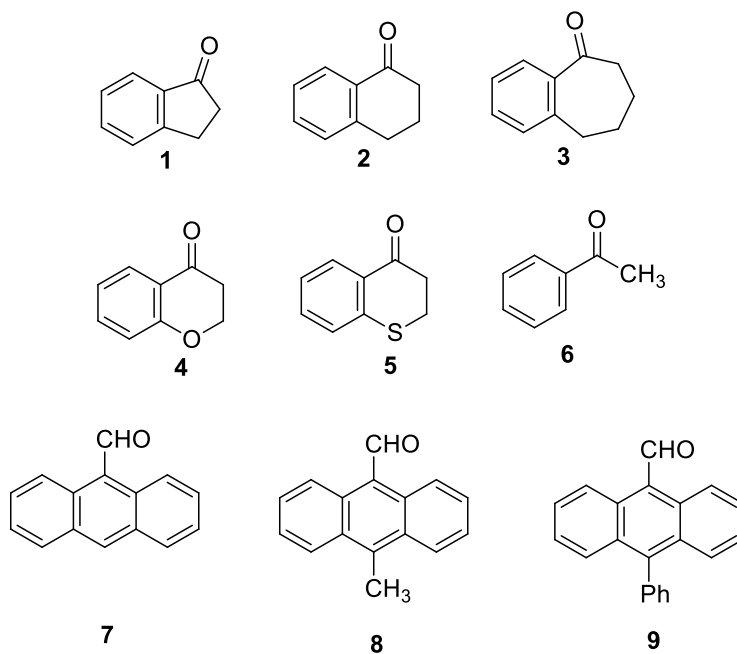
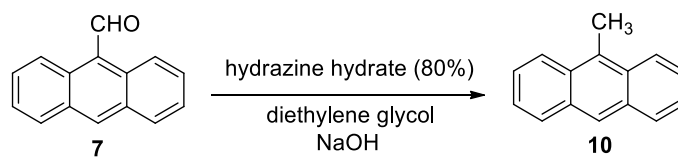
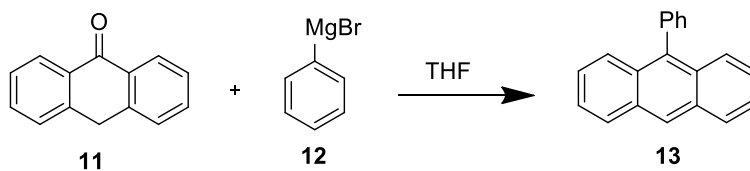


Chart 2.1



Scheme 2.2

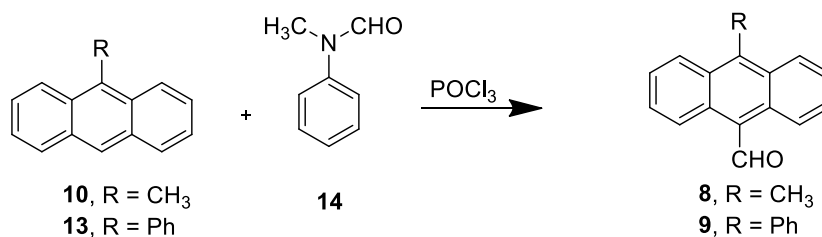


Scheme 2.3

2.3.1.2. Formylation of 9-substituted anthracenes

10-Substituted anthraldehydes were synthesized by formylation of the corresponding anthracene compounds using Vilsmeier-Haack reaction.²²

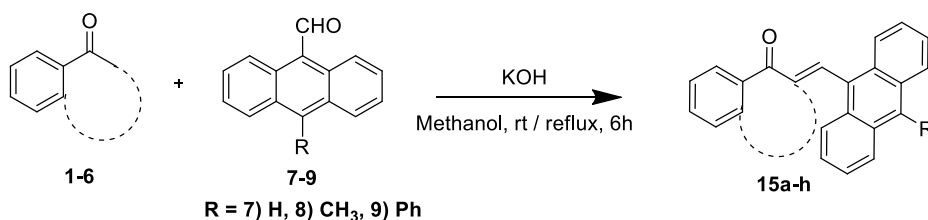
9-Substituted anthracenes were treated with formylating mixture of *N*-methylformanilide (**14**) and phosphorous oxychloride in *o*-dichlorobenzene. The reaction mixture was then treated with sodium-acetate water mixture.



Scheme 2.4

2.3.2. Synthesis of enone appended anthracenes

Syntheses of the enone appended anthracenes were carried out by employing base catalysed Claisen-Schmidt condensation reaction. Condensation of anthraldehyde or its derivatives with various ketones listed in Chart 2.1 in the presence of KOH afforded enone appended anthracenes **15a-h** (Chart 2.2) in good yields (Scheme 2.5).



Scheme 2.5

Structure of enone appended anthracenes **15a-h** synthesized by this method is given in Chart 2.2.

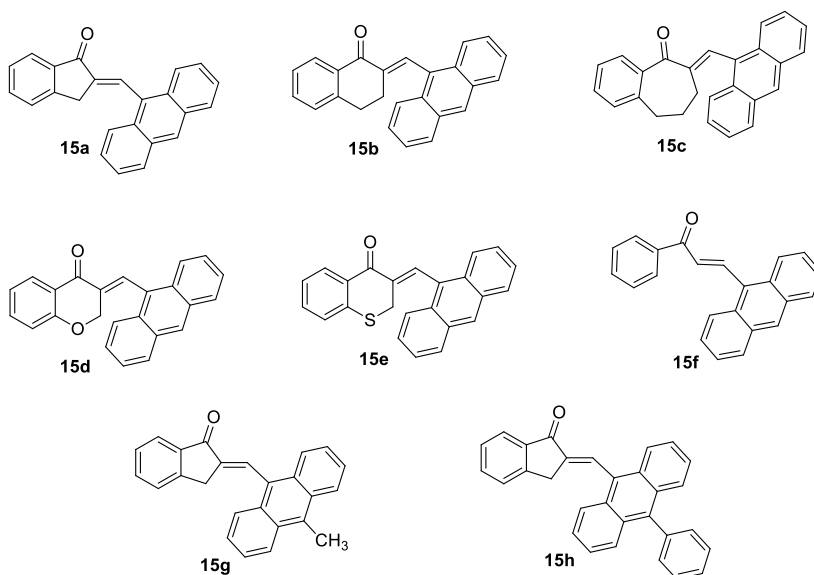


Chart 2.2

The enone appended anthracenes **15a-h** were characterized on the basis of analytical and spectral data. Pure samples were obtained upon recrystallization from chloroform-methanol mixture. Absorption spectra of all compounds were similar and absorption due to the anthracene part was prominent. Presence of α,β -unsaturated keto group is well characterized by the presence of a strong peak around 1660 cm^{-1} in the IR spectrum for all the compounds. The ^1H NMR spectrum of **15a** showed a singlet at δ 3.40 denoting the aliphatic protons of the indanone moiety, similarly in **15b** there were two triplets, one at δ 2.42 (2 H) and other at δ 2.73 (2 H) corresponding to the aliphatic protons of the tetralone moiety. In **15c** there were three peaks for the aliphatic protons of the benzosuberone component, two triplets at δ 2.89 (2 H) and δ 2.08 (2 H)

and a multiplet at δ 1.43 (2 H). Protons corresponding to the aromatic region and vinylic proton for **15a**, **15b** and **15c** were found as multiplets in the region from δ 7.1 to 8.5 (14 H). For **15d** and **15e** there were singlets corresponding to the aliphatic protons of the chromanone and thiochromanone residue at δ 4.70 (2 H) and δ 3.56 (2 H) respectively. Aromatic and vinylic protons were found as multiplets ranging from δ 6.75 to 8.60 (14 H). In the case of **15f** the doublets at δ 7.25 and δ 8.83 with $J_{AX} = 16.1$ Hz indicates the *E*-geometry of the double bond. The multiplets from δ 7.50 to δ 8.50 (14 H) corresponds to the aromatic region. The ^1H NMR spectrum of **15g** and **15h** were similar to **15a** except that in **15g**, the aliphatic region also showed the presence of the methyl protons at δ 3.15 (3 H) as a singlet and in the case of **15h** the aromatic region also showed the peaks corresponding to phenyl group attached to the anthracene.

2.4. Experimental

2.4.1. Materials and methods

All reactions were carried out using oven dried glassware. All experiments were done with distilled solvents by using standard protocols. All starting materials were purchased from either *Sigma-Aldrich* or *Spectrochem Chemicals* and were used without further purification. The products obtained were further recrystallized from suitable solvents. Melting points are uncorrected and were determined on a Neolab melting point apparatus. Infra-red spectra were recorded using *Jasco 4100* and *ABB Bomem (MB Series) FT-IR* spectrometers. The ^1H

spectra were recorded at 400 MHz on *Bruker Avance III* FT-NMR spectrometer with tetramethylsilane (TMS) as internal standard. Chemical shifts (δ) are reported in parts per million (ppm) downfield of TMS. Elemental analysis was performed using an Elementar systeme (Vario EL III). Molecular mass was determined by direct injection to a Waters 3100 mass detector with an electron spray ionization unit.

2.4.2. Synthesis of 9-substituted anthracenes

2.4.2.1. Synthesis of 9-methylanthracene (10)

9-Methylanthracene (**10**) was synthesized using a reported procedure in 90% yield, mp 77 °C.¹⁷

2.4.2.2. Synthesis of 9-phenylanthracene (13)

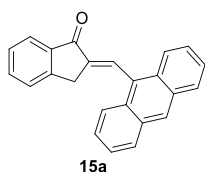
9-Phenylanthracene (**13**) was synthesized using a known procedure in 60% yield, mp 151 °C.¹⁸

2.4.3. Synthesis of 10-substituted anthraldehydes 8 and 9

10-Substituted anthraldehydes **8**, **9** were synthesized from the corresponding 9-substituted anthracenes using reported procedures.²² 10-Methylanthracene-9-carbaldehyde (**8**) was obtained in 80% yield, mp 169 °C.²³ 10-Phenylanthracene-9-carbaldehyde (**9**) was obtained in 85% yield, mp 165 °C.¹⁸

2.4.4. Synthesis of (*E*)-2-(anthracen-9-ylmethylene)-2,3-dihydro-1*H*-inden-1-one (15a)²⁴

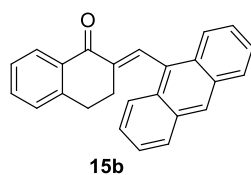
A solution of anthracene-9-carbaldehyde (**7**, 2.0 g, 9.6 mmol), 1-indanone (**1**, 1.28 g, 9.6 mmol), and potassium hydroxide (0.60 g, 9.6 mmol) in methanol (20 mL) was refluxed for 6 h with stirring. The reaction mixture was cooled in an ice bath for one hour. The yellow colored solid product precipitated out was filtered and washed several times with ice cold methanol and dried under reduced pressure to obtain the product as a yellow powder.



Yield 73 %; mp 136 °C; IR (KBr) ν_{\max} : 1668 cm^{-1} (C=O); ^1H NMR (CDCl_3): δ 8.56-8.50 (m, 2H), 8.07-7.98 (m, 4H), 7.56-7.44 (m, 4H), 7.28-7.25 (m, 4H), 3.40 (s, 2H); MS (FAB, $[\text{M}^++1]$): Calcd for $\text{C}_{24}\text{H}_{16}\text{O}$: 320.12, Found: 321.32; Anal. Calcd for $\text{C}_{24}\text{H}_{16}\text{O}$: C: 89.97, H: 5.03, Found: C: 89.82, H: 5.01

2.4.5. Synthesis of (*E*)-2-(anthracen-9-ylmethylene)-3,4-dihydro-naphthalen-1(2*H*)-one (15b)²⁵

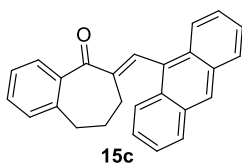
To a solution of anthracene-9-carbaldehyde (**7**, 2.0 g, 9.6 mmol) dissolved in methanol, α -tetralone (**2**, 1.42 g, 9.6 mmol) and NaOH (0.60 g, 9.6 mmol) dissolved in methanol were added and the mixture was allowed to stir at room temperature for 6 h and then was kept in refrigerator for 12 h. The precipitate formed was then filtered and washed with methanol and dried under reduced pressure in a vacuum oven.



Yield 67%; mp 128 °C; IR (KBr) ν_{\max} : 1670 cm^{-1} (C=O); ^1H NMR, (CDCl_3): δ 8.46 (s, 1H), 8.38 (s, 1H), 8.21-8.19 (m, 1H), 7.96-7.92 (m, 4H), 7.44-7.31 (m, 6H), 7.29 (s, 1H), 2.73 (t, 2H), 2.42 (t, 2H); MS (FAB, $[\text{M}^++1]$): Calcd for $\text{C}_{25}\text{H}_{18}\text{O}$: 334.13, Found: 335.15; Anal. Calcd for $\text{C}_{25}\text{H}_{18}\text{O}$: C: 89.79, H: 5.43, Found: C: 89.74, H: 5.42

2.4.6. Synthesis of (*E*)-6-(anthracen-9-ylmethylene)-6,7,8,9-tetrahydro-5*H*-benzo[7]annulen-5-one (15c).

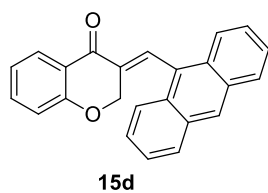
In a 150 mL round bottom flask, a mixture of anthracene-9-carbaldehyde (**7**, 2.0 g, 9.6 mmol), benzosuberone (**3**, 1.54 g, 9.6 mmol), and potassium hydroxide (0.60 g, 9.6 mmol) in methanol was taken and refluxed for 6 h with continuous stirring and later kept in a refrigerator overnight. The yellow colored solid product formed was filtered out and washed with methanol and dried under reduced pressure in a vacuum oven.



Yield 75%; mp 132 °C; IR (KBr) ν_{max} : 1667 cm^{-1} (C=O); ^1H NMR (CDCl_3): δ 8.45 (s, 1H), 8.21-7.95 (m, 4H), 7.52-7.42 (m, 4H), 7.28- 7.25 (m, 4H), 7.24 (s, 1H), 2.89 (t, 2H), 2.08 (t, 2H), 1.43 (m, 2H); MS (FAB, $[\text{M}^++1]$): Calcd for $\text{C}_{26}\text{H}_{20}\text{O}$: 348.15, Found: 349.16; Anal. Calcd for $\text{C}_{26}\text{H}_{20}\text{O}$: C: 89.62, H: 5.79, Found: C: 89.60, H: 5.68

2.4.7. Synthesis of (*E*)-3-(anthracen-9-ylmethylene)chroman-4-one (15d)

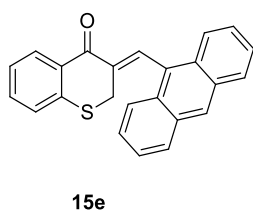
In a 150 mL round bottom flask a mixture of anthracene-9-carbaldehyde (**7**, 1.0 g, 4.8 mmol), 4-chromanone (**4**, 0.70 g, 4.8 mmol), and potassium hydroxide (0.30 g, 4.8 mmol) in methanol was taken and refluxed for 6 h with stirring and later kept in refrigerator overnight. The yellow colored solid product formed was filtered out and washed with methanol and dried under reduced pressure using vacuum oven.



Yield 76% ; mp 138 °C; IR (KBr) ν_{\max} : 1671 cm^{-1} (C=O); $^1\text{H NMR}$ (CDCl_3) δ 8.60 (s, 1H), 7.25 (s, 1H), 8.03-8.17 (m, 4H), 7.92-7.97 (m, 4H), 7.46 (m, 4H), 4.70 (s, 2H); MS (FAB, $[\text{M}^++1]$): Calcd for $\text{C}_{24}\text{H}_{16}\text{O}_2$: 336.11, Found: 337.12; Anal Calcd for $\text{C}_{24}\text{H}_{16}\text{O}_2$: C: 85.69, H: 4.79, Found: C: 85.70, H: 4.64

2.4.8. Synthesis of (*E*)-3-(anthracen-9-ylmethylene)thiochroman-4-one (15e)

In a 150 mL round bottom flask a mixture of anthracene-9-carbaldehyde (**7**, 1.00 g, 4.8 mmol), thiochromanone (**5**, 0.70 g, 4.8 mmol), and potassium hydroxide (0.30 g, 4.8 mmol) in methanol was taken and refluxed for 6 h with stirring and later kept in a refrigerator overnight. The yellow colored solid product formed was filtered out and washed with methanol and dried under reduced pressure using a vacuum oven.

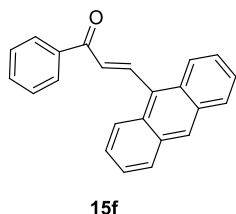


Yield 69%; mp 123 °C; IR (KBr) ν_{\max} : 1672 cm^{-1} (C=O); $^1\text{H NMR}$ (CDCl_3): δ 8.49 (s, 1H), 7.67 (s, 1H), 8.25-7.95 (m, 4H), 7.52-7.36 (m, 4H), 7.28-7.25 (m, 4H), 3.56 (s, 2H); MS (FAB, $[\text{M}^++1]$): Calcd for $\text{C}_{24}\text{H}_{16}\text{OS}$: 352.09, Found: 353.10; Anal. Calcd for $\text{C}_{24}\text{H}_{16}\text{OS}$: C: 81.79, H: 4.58, Found: C: 81.70, H: 4.45

2.4.9. Synthesis of (*E*)-3-(anthracen-9-yl)-1-phenylprop-2-en-1-one (15f)²⁶

To a solution of anthracene-9-carbaldehyde (**7**, 2.0 g, 9.6 mmol) dissolved in methanol, acetophenone (**6**, 1.16 g, 9.6 mmol) and KOH (0.60 g, 9.6 mmol) dissolved in methanol were added and the mixture was stirred at room temperature for 6 h and then kept in a refrigerator for 12 h. The precipitate formed is then filtered and washed out with

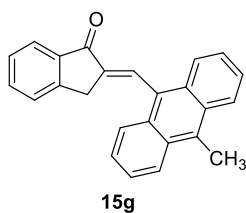
methanol and dried under reduced pressure using vacuum oven to get an yellow colored powder.



Yield 65%; mp 120 °C; IR (KBr) ν_{\max} : 1664 cm^{-1} (C=O); $^1\text{H NMR}$ (CDCl_3): δ 7.21 (1H, d, J_{AX} = 16.16 Hz, vinylic), 7.50-8.50 (m, 14H aromatic), 8.81 (1H, d, J_{AX} = 16.08 Hz, vinylic); MS (FAB, $[\text{M}^+ + 1]$): Calcd for $\text{C}_{23}\text{H}_{16}\text{O}$: 308.12, Found: 309.12; Anal. Calcd for $\text{C}_{23}\text{H}_{16}\text{O}$: C: 89.58, H: 5.23, Found: C: 89.78, H: 5.20

2.4.10. Synthesis of (*E*)-2-((10-methylanthracen-9-yl)methylene)-2,3-dihydro-1*H*-inden-1-one (15g)

In a 150 mL round bottom flask a mixture of 10-methylanthracene-9-carbaldehyde (**8**, 2.0 g, 9.1 mmol), 1-indanone (**1**, 1.20 g, 9.1 mmol), and potassium hydroxide (0.51 g, 9.1 mmol) in methanol was taken and refluxed for 6 h with stirring. After the reaction was completed, the mixture was cooled in an ice bath for about half an hour. The yellow colored solid product precipitated out was filtered and washed several times with ice cold methanol and dried under reduced pressure.

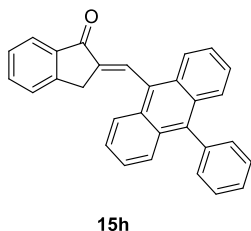


Yield 75%; mp 120 °C; IR (KBr) ν_{\max} : 1693 cm^{-1} (C=O); $^1\text{H NMR}$ (CDCl_3): δ 8.57 (s, 1H), 8.38-8.34 (m, 2H), 7.97-8.10 (m, 2H), 7.58-7.43 (m, 4H), 7.30-7.25 (m, 4H), 3.37 (s, 2H), 3.15 (s, 2H); MS (FAB, $[\text{M}^+ + 1]$): Calcd for $\text{C}_{25}\text{H}_{18}\text{O}$: 334.13, Found: 335.13; Anal. Calcd for $\text{C}_{25}\text{H}_{18}\text{O}$: C: 89.97, H: 5.43, Found: C: 89.84, H: 5.00

2.4.11. Synthesis of (*E*)-2-((10-phenylanthracen-9-yl)methylene)-2,3-dihydro-1*H*-inden-1-one (15h)

A solution of 10-phenylanthracene-9-carbaldehyde (**9**, 2.0 g, 7.1 mmol), 1-indanone (**1**, 0.94 g, 7.1 mmol), and potassium hydroxide (0.40g, 7.1

mmol) in methanol were taken and refluxed for 6 h with stirring. When the mixture was cooled in an ice bath, the light orange colored solid product precipitated out. It was filtered and was washed several times with ice cold methanol and dried under reduced pressure.



Yield 77%; mp 146 °C; IR (KBr) ν_{\max} : 1698 cm^{-1} (C=O); $^1\text{H NMR}$ (CDCl_3): δ 8.56-8.50 (m, 2H), 8.07-7.98 (m, 4H), 7.59-7.54 (m, 4H), 7.52-7.46 (m, 4H), 7.47-7.39 (m, 4H), 3.47 (s, 2H); MS (FAB, $[\text{M}^++1]$): Calcd for $\text{C}_{30}\text{H}_{20}\text{O}$: 396.15, Found: 397.15; Anal. Calcd for $\text{C}_{30}\text{H}_{20}\text{O}$: C: 90.88, H: 5.08, Found: C: 90.82, H: 5.03

References

1. Li, C. J. *Chem. Rev.* **1993**, 93, 2025.
2. Norcross, R. D.; Paterson, I. *Chem. Rev.* **1995**, 95, 2041.
3. Rahman, A. F. M.; Ali, R.; Jahng, Y.; Kadi, A. A. *Molecules* **2012**, 17, 571.
4. a) Piantadosi, C.; Hall, I. H.; Irvine, J. L.; Carlson G. L. *J. Med. Chem.* **1973**, 16, 771. b) Modzelewska, A.; Pettit, C.; Achanta, G.; Davidson, N. E.; Huang, P.; Khan, S. R. *Bioorg. Med. Chem.* **2006**, 14, 3491. c) Robinson, T. P.; Hubbard, R. B.; Ehlers, T. J.; Arbiser, J. L.; Goldsmith, D. J.; Bowen, J. P. *Bioorg. Med. Chem.* **2005**, 13, 4007.
5. Kamath, L.; Manjunatha, K. B.; Shettigar, S.; Umesh, G.; Narayana, B.; Samshuddin, S.; Sarojini, B. K. *Opt. Laser Technol.* **2014**, 56, 425.
6. Gangadharan, K.; Kaushal, K. *Polymer* **1995**, 36, 1903.
7. Deli, J.; Lorand, T.; Szabo, D.; Foldesi, A.; *Pharmazie*. **1984**, 39, 539.
8. a) Woodward, R. B. *Pure Appl. Chem.* **1968**, 17, 519. b) Han, Y.K.; Paquette, L. A. *J. Org. Chem.* **1979**, 44, 3731. c) Burke, S. D.; Murtiashaw, C. W.; Saunders, J. O.; Oplinger, J. A.; Dike, M. S. *J. Am. Chem. Soc.* **1984**, 106, 4558. d) Crimmins, M. T.; Gould, L. D. *J. Am. Chem. Soc.* **1987**, 109, 6199. e) Eschenmoser, A.; Wintner, C. *Science* **1977**, 196, 1410. f) Banwell, M. G. *Pure Appl. Chem.* **1996**, 68, 539.
9. Claisen, L.; Claparede, A. *Ber.* **1881**, 14, 2460.
10. Schmidt, J. G. *Ber.* **1881**, 14, 1459.

11. Nielsen, A. T.; Houlihan, W. J. *Org. React.* **1968**, *16*, 1.
12. House, H. O. *Modern Synthetic Reactions*, 2nd ed.; Benjamin, W. A.: New York, **1972**.
13. George, G. *Ph. D Thesis*. CUSAT, **2010**.
14. Becker, H. D. *Chem. Rev.* **1993**, *93*, 145.
15. Soffer, M. D.; Soffer, M. B.; Sherk, K. W. *J. Am. Chem. Soc.* **1945**, *67*, 1435.
16. Herr, C. H.; Whitmore, F. C.; Schiessler, R. W. *J. Am. Chem. Soc.* **1945**, *67*, 2061.
17. Minlon, H. *J. Am. Chem. Soc.* **1946**, *68*, 2487, b) Norman, R. O. C.; Waters, W. A. *J. Chem. Soc.* **1958**, 167.
18. Julian, P. L.; Cole, W.; Diemer, G.; Schafer, J. G. *J. Am. Chem. Soc.* **1949**, *71*, 2058.
19. Barnett, E. D. B.; Cook, J. W. *J. Chem. Soc.* **1923**, *123*, 2631.
20. Cook, J. W. *J. Chem. Soc.* **1926**, 2170.
21. Bradsher, C. K. *J. Am. Chem. Soc.* **1940**, *62*, 486.
22. Fieser, L. F.; Hartwell, J. L. *J. Am. Chem. Soc.* **1938**, *60*, 2555.
23. Ranganathan, S.; Ranganathan, D.; Ramachandran, P.V. *Tetrahedron*, **1984**, *40*, 3145.
24. Harada, J.; Harakawa, M.; Sugiyama, S.; Ogawa, K. *Cryst. Eng. Comm.* **2009**, *11*, 1235.
25. Mori, Y.; Maeda, K. *Acta Crystallographica Section B* **1994**, *50*, 106.
26. Dong, B.; Wang, M.; Xu, C. *Luminescence* **2013**, *28*, 628.

Synthesis of enone appended dibenzobarrelenes

3.1. Abstract:

This chapter describes the synthesis and characterization of enone appended dibenzobarrelenes by Diels–Alder reaction of the corresponding enone appended anthracenes with dienophiles such as dimethyl acetylenedicarboxylate (DMAD), dibenzoylacetylene (DBA) and in situ generated benzyne intermediate.

3.2. Introduction

Initial methods for dibenzobarrelene synthesis involved very high pressure and temperature in very low yields. An easy route for the synthesis of dibenzobarrelene was developed by Cristol *et al.* via the Diels–Alder reaction of the *cis* or (*E*)-1,2-dichloroethene with anthracene followed by dechlorination with zinc-copper couple.¹ Since then, Diels–Alder reaction of appropriate anthracenes with suitable dienophiles has emerged as the favored method for the synthesis of dibenzobarrelenes with required substituents at the bridgehead and vinyl positions.

Diels–Alder reaction offers a highly versatile method for the synthesis of cyclic structures.² This reaction was discovered by Otto Diels and his student Kurt Alder in 1928.³ In 1950 they were awarded Nobel Prize for this discovery and after that this reaction turned out to be the corner stone of organic synthesis. Since this reaction creates two C–C single bonds in a single step it is highly useful for the synthesis of complicated polycyclic compounds especially in natural product synthesis. This cycloaddition reaction takes place between a conjugated diene and a dienophile. The dienes can be cyclic or acyclic, the only necessary condition for the diene

is that it must be in the *cis* conformation for the reaction to take place⁴. 1,3-Butadiene with different substituents is a commonly used acyclic diene. Cyclic dienes such as cyclopentadiene, cyclohexadiene, cycloheptadiene, anthracene etc. are all active participants in Diels-Alder reaction. The dienophile can be ethylenic or acetylenic⁵ and the presence of electron withdrawing groups enhance their reactivity. The reaction proceeds through a concerted mechanism in which all bonds are broken and formed in a single step without the formation of any intermediate species. Since it involves the 4π electrons of the diene and 2π electrons of the dienophile it is also called as [4+2]cycloaddition reaction.

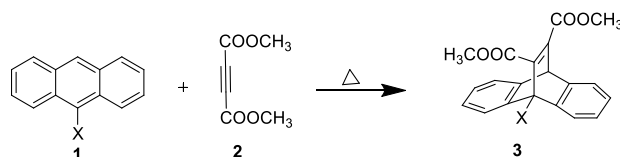
Diels-Alder reaction is a highly stereoselective reaction where the *cis* principle and Alder “endo rule” help us to predict the stereochemical outcome of the reaction.⁶ According to *cis* principle the stereochemistry of the reacting diene as well as the dienophile is retained in the product formed.⁷ According to Alder “endo rule”, of the two possible modes of approach of the diene to dienophile the one resulting in maximum orbital overlap leads to the major product and in most cases it is the *endo* adduct which is the major product.⁸

Diels-Alder reaction can be either intermolecular or intramolecular. If the dienophiles involved have any heteroatom it is called hetero Diels-Alder reaction,⁹ which is an important reaction for synthesis of heterocyclic systems which are the key intermediates in natural product synthesis.¹⁰ Diels alder reaction are usually insensitive to the polarity of solvents but in aqueous solution the reaction is accelerated.¹¹ It is believed that in water a hydrophobic effect operates which brings the diene and

dienophile in close proximity which accelerates the rate of the reaction. The reaction can also be accelerated by a Lewis-acid catalyst¹² and by pressure.¹³

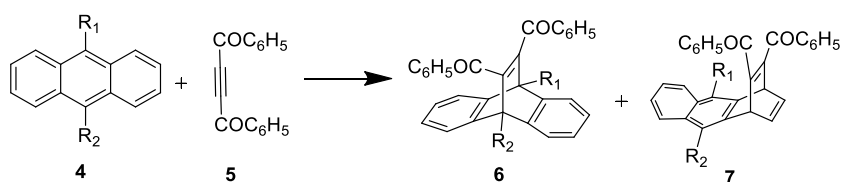
Diels-Alder reaction of anthracenes with a wide variety of dienophiles gives rise to synthetically important compounds.¹⁴ Anthracenes undergo thermal and photochemical Diels-Alder reactions with dienophiles across the 9,10 positions.¹⁵ Dibenzobarrelenes are synthesized mainly by the thermal Diels-Alder reaction. These reactions involve a *cis* addition of the dienophile to anthracene and *cis* or *trans* geometry of the dienophile is retained in the product. Reactivity of 9-substituted or 9,10-disubstituted anthracenes depend on the nature of the substituents with electron donating substituents facilitating the reaction.¹⁶ The dienophiles used for the dibenzobarrelene synthesis are mainly acetylenic compounds like dimethyl acetylenedicarboxylate (DMAD) and dibenzoylacetylene (DBA). When *in situ* generated benzyne intermediate is used as the dienophile, triptycenes are generated.¹⁷

In literature there are several reports on the synthesis of bridgehead substituted dibenzobarrelenes via the Diels-Alder reaction. Richard *et al.* synthesized a series of dibenzobarrelenes by refluxing a solution of the appropriate anthracene with DMAD in a suitable solvent.¹⁸



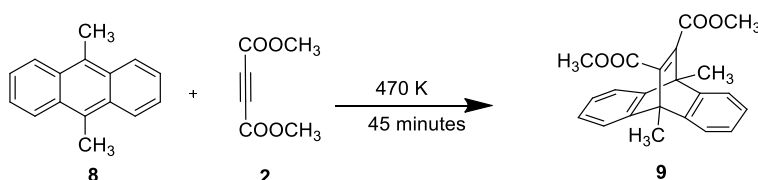
Scheme 3.1

George *et al.* have reported the synthesis of several 11,12-dibenzoyl substituted dibenzobarrelenes by the Diels-Alder reaction of 9-substituted or 9,10-disubstituted anthracene compounds with dibenzoylacetylene either thermally or in the presence of Lewis acid catalyst such as aluminium chloride.^{19,20} Apart from the formation of dibenzobarrelenes they have also observed the formation of dibenzoyl substituted naphthobarrelenes in some reactions depending on the substituents and reaction condition, as a result of addition across 1,4-positions of anthracenes.



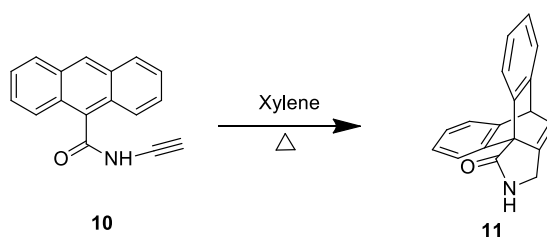
Scheme 3.2

Pyrolysis method was also used for the synthesis of dibenzobarrelenes.²¹ Scheffer and coworkers synthesized 9,10-dimethyl substituted dibenzobarrelenes-11,12-dicarboxylate by heating a mixture of 9,10-dimethylantracene and DMAD at about 470 K for 45 minutes and the brown mass obtained was subjected to column chromatography to obtain the product.



Scheme 3.3

Intramolecular Diels-Alder cycloaddition (IMDA) of tethered alkynes can be effectively utilized for the synthesis of tethered dibenzobarrelenes. Ciganek reported the synthesis of several tethered dibenzobarrelenes via IMDA.²² The major attractive feature of this reaction is that it occurs at mild conditions and helpful in the synthesis of heterocyclic rings. Our group has also synthesized several tethered dibenzobarrelenes through IMDA and they were subjected to photochemical studies.²³



Scheme 3.4

3.3. Results and discussion

In Chapter 2 we reported the synthesis of a series of enone appended anthracenes **12a-h** shown in Chart 3.1. This chapter describes the synthesis of several enone appended dibenzobarrelenes (**13a-h**, **14a-f**, **15**) using these anthracene compounds *via* Diels-Alder reaction with dienophiles such as dimethyl acetylenedicarboxylate (DMAD), dibenzoylacetylene (DBA) and *in situ* generated benzyne intermediate as shown in Chart 3.2. These dibenzobarrelenes were synthesized with an intention to study the effect of the enone appendage on the photoreactivity of these compounds. Ever since the discovery of di- π -methane rearrangement intensive studies were carried out on the effect of different substituent groups at bridgehead position of dibenzobarrelenes.

With the introduction of the enone component which is an effective triplet quencher, we expect that at the expense of triplet mediated pathway leading to the di- π -methane rearrangement there may occur some diversion in the reaction through singlet mediated pathways leading to some other products.

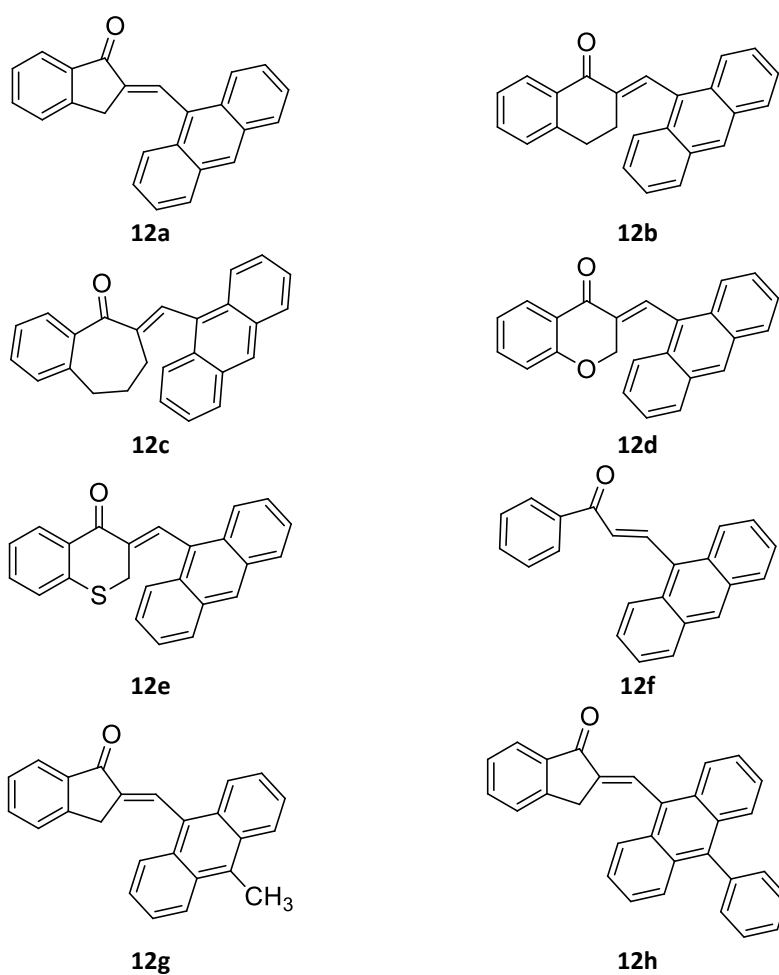


Chart 3.1

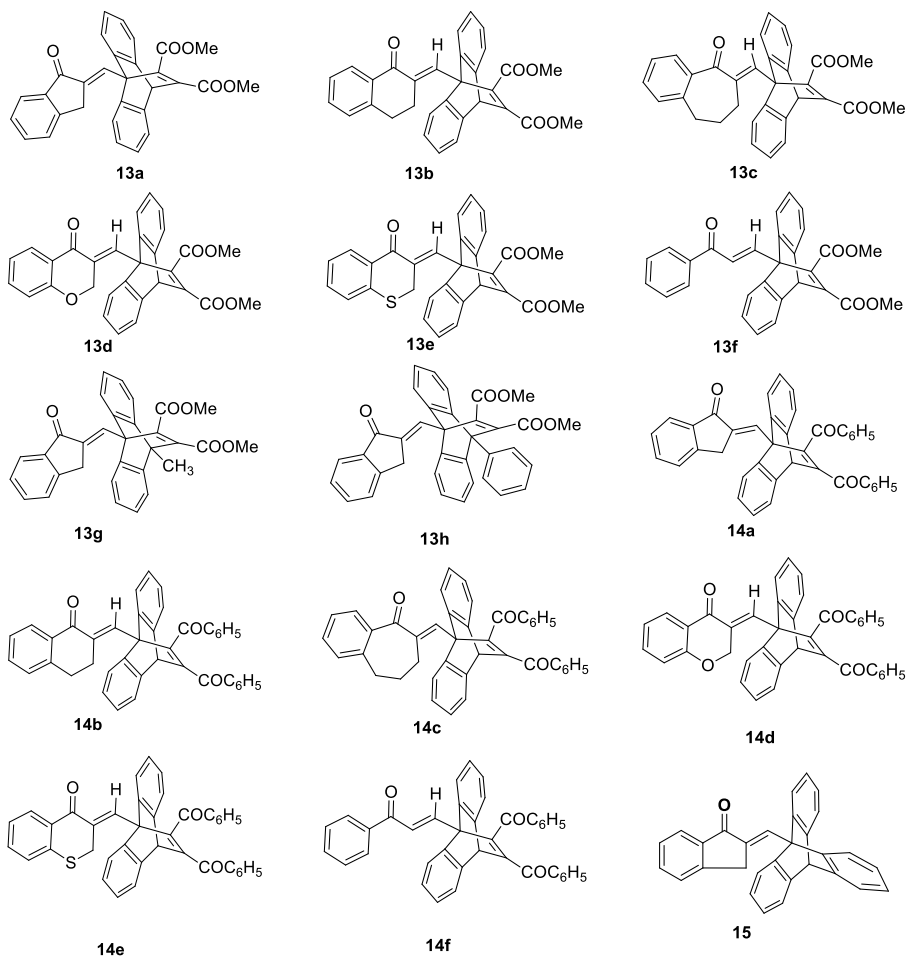
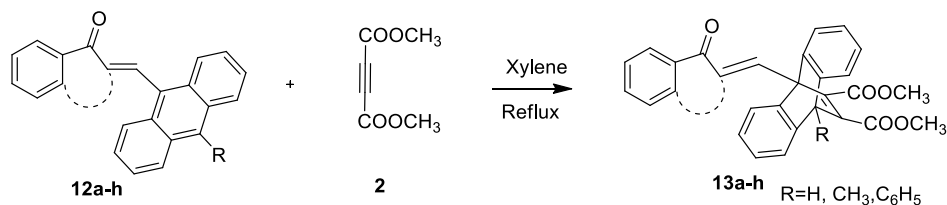


Chart 3.2

3.3.1. Synthesis of enone appended dibenzobarrelenes with DMAD as dienophile

When the anthracene compounds **12a-h** were refluxed in xylene for about 12 h with DMAD (**2**), they underwent Diels-Alder reaction to give the corresponding enone appended dibenzobarrelenes **13a-h** in good

yields (Scheme 3.5).*



Scheme 3.5

The structures of the dibenzobarrelenes **13a-h** were established on the basis of analytical and spectral data. For dibenzobarrelene **13a** the IR spectrum showed the ester carbonyl stretching peaks at 1711 and 1725 cm^{-1} and the absorption of α,β -unsaturated carbonyl group occurs at 1698 cm^{-1} . In the ^1H NMR spectrum, the two methoxy protons were found as two singlets at δ 3.79 (3 H) and 3.75 (3 H). The bridge head proton was observed as a singlet at δ 5.71 (1 H). The methylene protons of the indanone moiety was seen as a singlet at δ 3.63 (2 H). The aromatic protons and the vinylic protons were observed as multiplets in range from δ 7.07-7.99 (13 H). In the ^{13}C NMR spectrum the signals at δ 50.8, indicated the tertiary bridgehead carbon. The signals at δ 52.6 and δ 52.4 represented the methoxy carbons and that at δ 58.1 represented the quaternary bridgehead carbon. The two signals at 163.7 and 167.0 indicated the ester carbonyls and the signal at 193.1 indicated the α,β -unsaturated carbonyl group.

* A remarkable feature of several enone appended barrelenes was their unusual NMR spectra. Peak broadening and shift (from expected positions) was observed in several cases. Based on variable temperature NMR data described in Chapter 4 of this thesis, we identified the existence of discrete rotamers for the unusual NMR spectra obtained for these compounds.

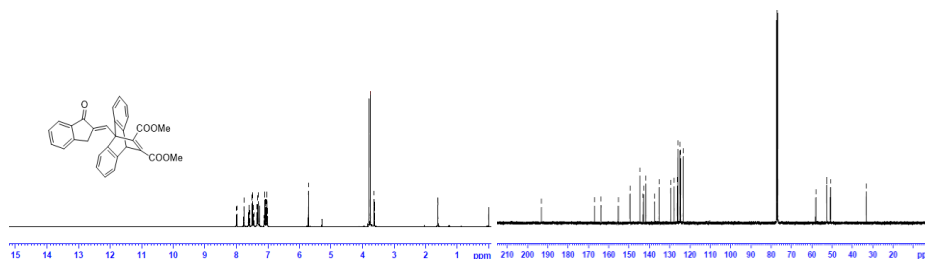


Fig 3.1: ^1H NMR and ^{13}C NMR spectrum for **13a**

The IR absorption peak of **13b** at 1715 cm^{-1} , 1720 cm^{-1} and 1663 cm^{-1} were due to the carbonyl stretching frequencies. For this compound the ^1H NMR showed some broad characterless peaks as shown in Fig 3.2 and ^{13}C NMR spectrum showed peak broadening. But in the FAB mass spectrum, the molecular ion peak at m/z 477 ($M^+ + 1$) is in accordance with the calculated mass.

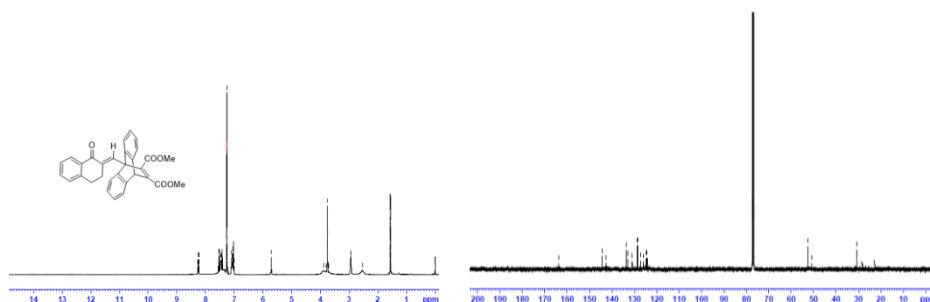


Fig 3.2: ^1H NMR and ^{13}C NMR spectrum for **13b**

For **13c** the ester carbonyl stretching frequencies were found at 1717 cm^{-1} and 1725 cm^{-1} and the α,β -unsaturated carbonyl stretching frequency at 1661 cm^{-1} . In the ^1H NMR spectrum the singlet at δ 5.71 (1 H) indicated the presence of bridgehead proton and the two methoxy protons were found as two singlets at δ 3.86 (3 H) and 3.73 (3 H). The aliphatic protons of the benzosuberone moiety appeared as two triplets at δ 3.00

(2 H) and 2.21 (2 H) and a multiplet at δ 1.86 (2 H). The vinylic and aromatic protons appeared as multiplets in the range from δ 7.01-7.99 (13 H). In the ^{13}C NMR spectrum carbonyl carbons corresponding to α,β -unsaturated and the ester carbonyl carbons appeared at δ 196.7, 167.1 and 163.9. The signals from δ 123.8-144.5 denoted the aromatic and vinylic carbons. The signals at δ 52.6 and δ 52.5 represented the methoxy carbons and the two bridge head carbons appeared at δ values 58.2 and 50.8. Signal due to the aliphatic carbons in the benzosuberone moiety were seen at δ values 31.6, 27.5 and 24.9.

Structure of **13c** was also confirmed by Single Crystal X-ray diffraction analysis and this helped us to confirm the *E*-geometry for the double bond connecting the dibenzobarrelene part and the benzosuberone moiety.

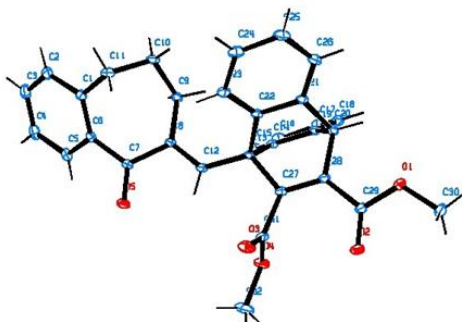


Fig 3.3: ORTEP diagram of **13c**

The IR spectrum of **13d** showed the ester carbonyl stretching frequencies at 1712 cm^{-1} and 1729 cm^{-1} and the α,β -unsaturated carbonyl stretching frequency at 1665 cm^{-1} . In the ^1H NMR spectrum the bridgehead proton

appeared as a singlet at δ 5.71 (1 H). The CH₂ protons adjacent to the oxygen of the chromanone moiety appeared as a broad peak at δ 4.68.

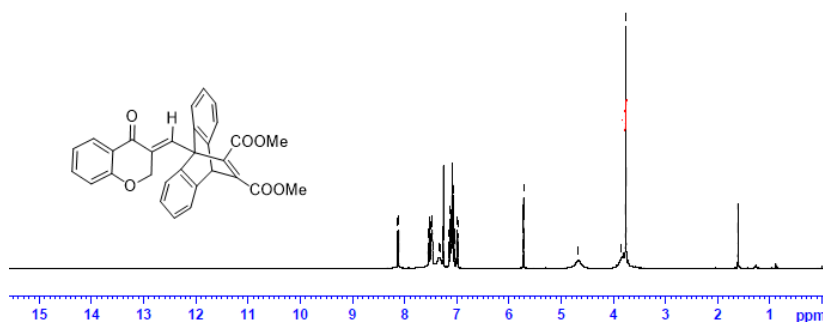


Fig. 3.4: ¹H NMR spectrum of **13d**

The signals due to the methoxy protons were seen at δ 3.76 and 3.85 but one of them was broadened and not a sharp peak as the other. The vinylic and aromatic protons appeared as multiplets in the range from δ 6.97-8.13 (13 H). ¹³C NMR spectrum of this compound missed several peaks.

For **13e** the ester carbonyl stretching frequencies were found at 1712 cm⁻¹ and 1729 cm⁻¹ and the α,β -unsaturated carbonyl stretching frequency at 1665 cm⁻¹. The singlet at δ 5.67 (1 H) represented the bridgehead proton. The CH₂ protons of the thiochromanone moiety was seen as singlet at δ 4.21 (2 H) and the methoxy protons appeared as two singlets at δ 3.75 (3 H) and δ 3.50 (3 H). The vinylic and aromatic protons appeared as multiplets in the range from δ 7.07- 8.7 (13 H). In the ¹³C NMR spectrum carbonyl carbons corresponding to α,β -unsaturated and the ester carbonyl carbons appeared at δ 179.4, 166.9 and 164.2 and the signals from δ 123.3-145.5 denoted the aromatic and vinylic carbons. The two bridgehead carbons appeared at δ values 54.1 and 51.1 and the two methoxy

carbons at δ 52.5 and 52.1. Signal due to the aliphatic carbon in the thiochromanone moiety was seen at δ 28.6.

For **13f**, the α,β -unsaturated carbonyl stretching peak appears at 1672 cm^{-1} and the ester carbonyls appear at 1724 and 1736 cm^{-1} . In the ^1H NMR spectrum, the methoxy protons appeared as two singlets at δ 3.71 (3 H) and δ 3.78 (3 H). The bridgehead methine proton appeared as a singlet at δ 5.71 (1 H). The multiplets from δ 7.05 to δ 8.12 (13 H) represented the aromatic protons. The doublets at δ 7.46 and at δ 7.56 represent the vinylic protons with coupling constants of 17.7 Hz and 19.5 Hz respectively, establishing the *E*-geometry of the olefinic bond. The signals at δ 50.4 in the ^{13}C NMR spectrum indicates the tertiary bridgehead carbon. The signals at δ 52.4 and δ 52.5 represent the methoxy carbons and that at δ 58.0 representing the quaternary bridgehead carbon. The two signals at δ 163.5 and δ 167.2 represent the ester carbonyls and the signal at δ 189.3 indicates the α,β -unsaturated carbonyl group.

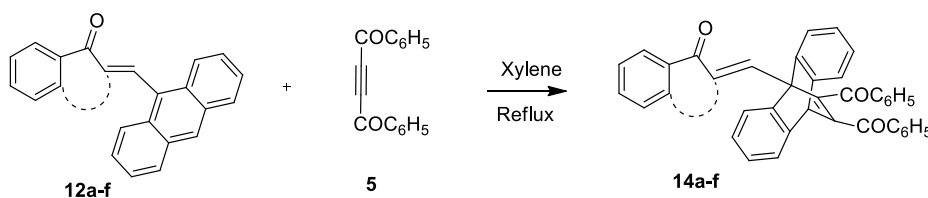
For dibenzobarrelene **13g**, the IR spectrum showed the ester carbonyl stretching peaks at 1700 and 1723 cm^{-1} and the absorption of α,β -unsaturated carbonyl group lied at 1648 cm^{-1} . In the ^1H NMR spectrum, the two methoxy protons were found as two singlets at δ 3.66 (3 H) and 3.54 (3 H). The methylene protons of the indanone moiety was seen as a singlet at δ 3.66 (2 H). The aromatic protons and the vinylic protons were observed as multiplets in range from δ 6.94-8.11. In the ^{13}C NMR spectrum the signals at δ 52.3 and δ 52.2 represented the methoxy carbons and that at δ 50.1 and δ 55.7 represented the bridgehead carbons.

The two signals at 166.6 and 166.1 indicated the ester carbonyls and the signal at 193.3 indicated the α,β -unsaturated carbonyl group

For dibenzobarrelene **13h** the IR spectrum showed the ester carbonyl stretching peaks at 1708 and 1735 cm^{-1} and the absorption of α,β -unsaturated carbonyl group lied at 1698 cm^{-1} In the ^1H NMR spectrum, the two methoxy protons were found as two singlets at δ 3.79 (3 H) and 3.75 (3 H). The methylene protons of the indanone moiety was seen as a singlet at δ 3.63 (2 H). The aromatic protons and the vinylic protons were observed as multiplets in range from δ 7.07-7.99 (18 H). In the ^{13}C NMR spectrum the signals at δ 50.8, indicated the tertiary bridgehead carbon. The signals at δ 52.6 and δ 52.4 represented the methoxy carbons and that at δ 58.1 and 51.1 represented the bridgehead carbon. The two signals at 165.7 and 167.2 indicated the ester carbonyls and the signal at 192.5 indicated the α,β -unsaturated carbonyl group.

3.3.2. Synthesis of enone appended dibenzobarrelenes with DBA as dienophile

Diels-Alder reaction of the anthracene compounds **12a-f** with dibenzoyl-acetylene (**5**) by refluxing in xylene overnight resulted in the formation of the dibenzobarrelenes **14a-f** in low yields (Scheme 3.6).



Scheme 3.6

The structures of the dibenzobarrelenes **14a-g** were confirmed on the basis of analytical results and spectral data. For **14a** the ester carbonyl stretching frequencies were found at 1656 cm^{-1} and 1699 cm^{-1} and the α,β -unsaturated carbonyl stretching frequency at 1643 cm^{-1} . The ^1H NMR spectrum showed the bridgehead proton as a singlet at δ 5.58 (1 H) and the methylene protons of the indanone moiety appeared as a singlet at δ 3.52 (2 H). The vinylic and aromatic protons as multiplets in the range from δ 7.10-7.90 (23 H). In the ^{13}C NMR spectrum, the α,β -unsaturated and the ester carbonyl carbons appeared at δ 194.5, 194.1, and 192.9 respectively, and the signals from δ 123.5-156.8 denoted the aromatic and vinylic carbons. The two bridgehead carbons appeared at δ values 58.4, 53.6. Signal due to the aliphatic carbon in the indanone moiety appeared at δ 32.9.

The IR absorption peak of **14b** at 1623 cm^{-1} , 1649 cm^{-1} and 1681 cm^{-1} corresponds to the carbonyl stretching frequencies. For this compound the ^1H NMR showed some broad characterless peaks as shown in Fig. 3.5 and in ^{13}C NMR spectrum many peaks were missing. But from the FAB mass spectrum the molecular ion peak at m/z 569.15 (M^++1) is in accordance with the calculated mass for the expected structure.

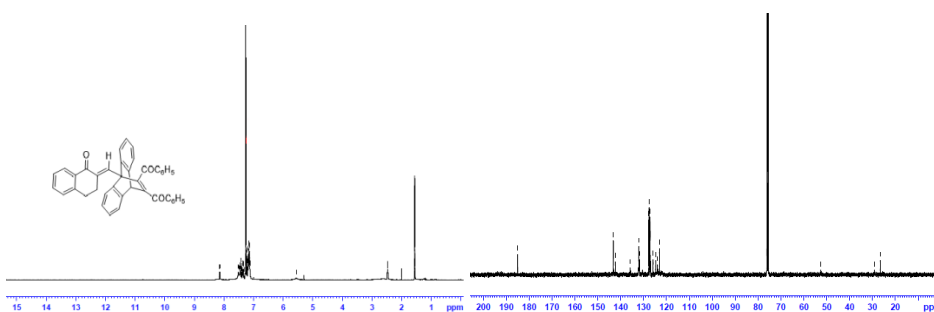


Fig 3.5: ^1H NMR and in ^{13}C NMR spectrum of **14b**

For **14c** the ester carbonyl stretching frequencies were found at 1655 cm^{-1} and 1671 cm^{-1} and the α,β -unsaturated carbonyl stretching frequency at 1643 cm^{-1} . The singlet at δ 5.54 (1 H) indicated the presence of bridge head proton. The aliphatic protons of the benzosuberone moiety appeared as two triplets at δ 2.87 (2 H) and 2.12 (2 H) and as a multiplet at δ 1.86 (2 H). The vinylic and aromatic protons appeared as multiplets in the range from δ 7.10-8.03 (23 H). In the ^{13}C NMR spectrum carbonyl carbons corresponding to α,β -unsaturated and the ester carbonyl carbons appeared at δ 196.5 and 194.1, and the signals from δ 123.7-144.3 denoted the aromatic and vinylic carbons. The two bridgehead carbons appeared at δ 58.3 and 53.7. Signal due to the aliphatic carbon in the benzosuberone moiety appeared at δ values 31.5, 27.3, and 24.8.

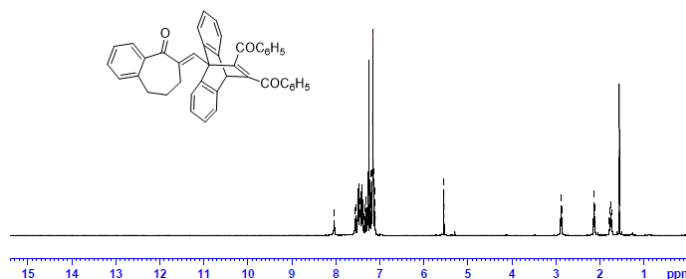


Fig 3.6: ^1H NMR spectrum of **14c**

The IR spectrum of **14d** showed the ester carbonyl stretching frequencies at 1657 cm^{-1} and 1677 cm^{-1} and the α,β -unsaturated carbonyl stretching frequency at 1641 cm^{-1} . In the ^1H NMR spectrum the bridgehead proton appeared as a singlet at δ 5.60 (1 H). The CH_2 protons adjacent to the oxygen of the chromanone moiety appeared as a singlet at δ 4.61 (2 H). The vinylic and aromatic protons appeared as multiplets in the range from δ 6.91-8.03(23 H). Several peaks were missing in the ^{13}C NMR

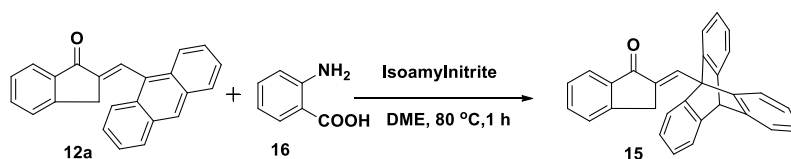
spectrum of this compound making structural analysis on the basis of NMR spectral data tenuous.

For **14e**, the ester carbonyl stretching frequencies were found at 1655 cm^{-1} and 1671 cm^{-1} and the α - β unsaturated carbonyl stretching frequency at 1643 cm^{-1} . The singlet at δ 5.56 (1 H) denoted the bridgehead proton. The CH_2 protons of the thiochromanone moiety was seen as a singlet at δ 4.15 (2 H). The vinylic and aromatic protons appeared as multiplets in the range from δ 7.07-8.54 (23 H). In the ^{13}C NMR spectrum carbonyl carbons corresponding to α , β -unsaturated and the ester carbonyl carbons appeared at δ 192.7, 192.3 and 177.1 and the signals from δ 121.6-143.5 denoted the aromatic and vinylic carbons. The two bridge head carbons appeared at δ values 52.9 and 51.8. Signal due to the aliphatic carbon in the thiochromanone moiety was observed at δ 26.8.

The IR absorption peaks of **14f** appeared at 1650, 1665 and 1640 cm^{-1} indicating the stretching frequency of the benzoyl carbonyl moiety and that of the α , β -unsaturated carbonyl group respectively. The bridgehead proton appears at δ 5.58 in the ^1H NMR spectrum. The aromatic protons and a vinylic proton appeared as multiplets from δ 7.14 to δ 7.77 (24 H). The doublet at δ 7.89 indicates the other vinylic proton with a coupling constant value of 16.5 Hz. In the ^{13}C NMR spectrum, the bridgehead tertiary and quaternary carbons appear at 53.21 and 58.90 respectively. The signal at δ 189.62, indicates the α , β -unsaturated carbonyl group at the bridgehead position, whereas the signals at δ 193.73 and at δ 195.57 represents the benzoyl carbonyl groups.

3.3.3. Synthesis of enone appended dibenzobarrelenes with *in situ* generated benzyne as dienophile

We have also synthesized one triptycene analogue^{24,25} of the enone appended dibenzobarrelenes. Diels-alder reaction of the corresponding anthracene compound **12a** with benzyne intermediate²⁶ which was generated *in situ* by reaction of anthranilic acid (**16**), with isoamyl nitrite in dimethoxyethane as solvent gave compound **15** in very low yield.



Scheme 3.7

The IR spectrum of **15** showed the peak due to carbonyl stretching at 1701cm^{-1} . In the ^1H NMR spectrum the bridgehead proton was found as a singlet at δ 5.38 (1 H) and the CH_2 protons of the indanone moiety was seen as a singlet at δ 3.54 (2 H) and the vinylic and aromatic protons appeared as multiplets in the range from δ 6.89-8.32 (17 H). In the ^{13}C NMR spectrum the carbonyl carbon appeared at δ 193.8 and the signals from δ 122.5-149.7 denoted the aromatic and vinylic carbons. The two bridge head carbons appeared at δ values 55.8 and 54.3. Signal due to the aliphatic carbon in the indanone moiety was seen at δ 33.3.

3.4. Experimental

3.4.1. General procedures

Details of general experimental procedures and analytical instruments are provided in the experimental section of Chapter 2 of this thesis.

3.4.2. Starting materials

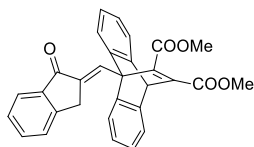
Dimethyl acetylenedicarboxylate (DMAD) was purchased from Sigma Aldrich and used as received. Dibenzoylacetylene (DBA) was synthesized as per known procedures (70%, mp 110-111°C).²⁷

3.4.3. General Procedure for the Synthesis of enone-appended dibenzobarrelenes 13a-h

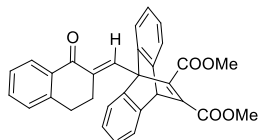
For the synthesis of dibenzobarrelenes **13a-h**, the corresponding anthracene compounds **12a-h** were dissolved in minimum quantity of dry xylene (5 mL) under inert atmosphere and excess DMAD (**2**) was added to it and stirred under reflux for 12 h. Solvent was removed under vacuum and the residue subjected to silica gel column chromatography to remove the unreacted dienophile. Elution with 85:15 hexane-ethyl acetate solvent mixture afforded the dibenzobarrelenes as off-white crystalline powder.

3.4.4. Spectral and analytical data for the dibenzobarrelenes 13a-h

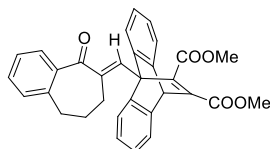
3.4.4.1. Compound 13a:



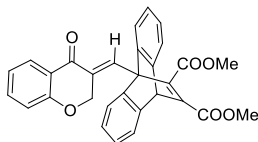
Yield 65%; mp 230 °C; IR (KBr) ν_{\max} : 1711, 1725 (C=O, ester), 1698 (C=O, ketone) cm^{-1} ; ^1H NMR (CDCl_3): δ 7.07-7.99 (13H, m, aromatic), 5.71 (1H, s, methine), 3.79 (3H, s, OCH_3), 3.75 (3H, s, OCH_3), 3.63 (2H, s); ^{13}C NMR (CDCl_3): δ 193.1, 167.0, 163.7, 155.4, 149.6, 144.7, 142.9, 142.8, 141.7, 137.4, 135.2, 129.5, 127.8, 126.2, 125.9, 125.0, 124.8, 124.4, 123.4, 58.1, 52.6, 52.4, 50.8; 33.1; MS (FAB, $[M^++1]$): Calcd for $\text{C}_{30}\text{H}_{22}\text{O}_5$: 462.14, Found: 463; Anal. Calcd for $\text{C}_{30}\text{H}_{22}\text{O}_5$: C: 77.91, H: 4.79, Found: C: 77.89, H: 4.71

3.4.4.2. Compound 13b:

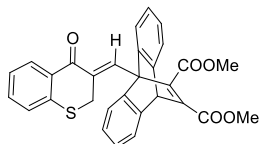
Yield 60%; mp 140 °C; IR (KBr) ν_{\max} : 1715, 1720 (C=O, ester), 1633 (C=O, ketone) cm^{-1} ; MS (FAB, $[\text{M}^++1]$): Calcd for $\text{C}_{31}\text{H}_{24}\text{O}_5$: 476.51, Found: 477; Anal. Calcd for $\text{C}_{31}\text{H}_{24}\text{O}_5$: C: 78.14, H: 5.08, Found: C: 78.05, H: 5.00

3.4.4.3. Compound 13c:

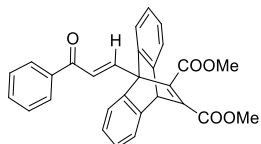
Yield 62%; mp 198 °C; IR (KBr) ν_{\max} : 1717, 1725 (C=O, ester), 1661 (C=O, ketone) cm^{-1} ; ^1H NMR (CDCl_3): δ 7.01-7.99 (13H, m, aromatic), 5.71 (1H, s, methine), 3.86 (3H, s, OCH_3), 3.73 (3H, s, OCH_3), 3.00 (2H, t), δ 2.21 (2H, t) δ 1.86 (2H, m); ^{13}C NMR (CDCl_3): δ 196.7, 167.1, 163.9, 144.5, 143.2, 142.9, 139.2, 139.1, 133.7, 132.4, 128.9, 128.5, 127.1, 126.0, 124.7, 124.2, 123.8, 58.2, 52.6, 52.5, 50.8, 31.6, 27.5, 24.9; MS (FAB, $[\text{M}^++1]$): Calcd for $\text{C}_{32}\text{H}_{26}\text{O}_5$: 490.17, Found: 491; Anal. Calcd for $\text{C}_{32}\text{H}_{26}\text{O}_5$: C: 78.35, H: 5.34, Found: C: 78.53, H: 5.25

3.4.4.4. Compound 13d:

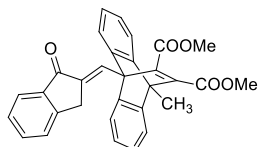
Yield 62%; mp 178 °C; IR (KBr) ν_{\max} : 1712, 1729 (C=O, ester), 1665 (C=O, ketone) cm^{-1} ; ^1H NMR (CDCl_3): δ 6.97-8.13 (13H, m, aromatic), 5.71 (1H, s, methine), 3.85 (3H, broad peak, OCH_3), 3.76 (3H, s, OCH_3), 4.68 (2H, broad peak,); MS (FAB, $[\text{M}^++1]$): Calcd for $\text{C}_{30}\text{H}_{22}\text{O}_6$: 478.14, Found: 479.11; Anal. Calcd for $\text{C}_{30}\text{H}_{22}\text{O}_6$: C: 75.30, H: 4.63, Found: C: 75.28, H: 4.55

3.4.4.5. Compound 13e:

Yield 67%; mp 268 °C; IR (KBr) ν_{\max} : 1712, 1729 (C=O, ester), 1665 (C=O, ketone) cm^{-1} ; ^1H NMR (CDCl_3): δ 4.21 (2H, s), 3.75 (3H, s, OCH_3), 3.50 (3H, s, OCH_3), 5.67 (1H, s, methine), 7.07-8.7 (13H, m, aromatic); ^{13}C NMR (CDCl_3): δ 179.4, 166.9, 164.2, 145.5, 136.9, 136.7, 131.2, 131.1, 130.4, 129.2, 127.7, 125.5, 125.1, 123.8, 123.3, 54.1, 52.5, 52.1, 51.1, 28.6; MS (FAB, $[\text{M}^++1]$): Calcd for $\text{C}_{30}\text{H}_{22}\text{O}_5\text{S}$: 494.11, Found: 495.12; Anal. Calcd for $\text{C}_{30}\text{H}_{22}\text{O}_5\text{S}$: C: 72.86, H: 4.48, Found: C: 73.19, H: 4.38

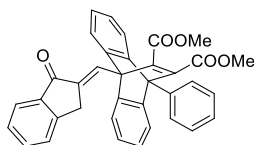
3.4.4.6. Compound 13f:

Yield 70%; mp 170 °C; IR (KBr) ν_{\max} : 1724, 1736 (C=O, ester), 1672 (C=O, ketone) cm^{-1} ; ^1H NMR (CDCl_3): δ 7.56 (1H, d, $J_{\text{AX}} = 19.5$ Hz, vinylic), 7.46 (1H, d, $J_{\text{AX}} = 17.7$ Hz, vinylic), 7.07-8.10 (13H, m, aromatic), 5.72 (1H, s, methine), 3.77 (3H, s, OCH_3), 3.71 (3H, s, OCH_3); ^{13}C NMR (CDCl_3): δ 189.4, 167.2, 163.5, 155.1, 144.8, 143.8, 142.1, 138.8, 137.3, 133.43, 132.51, 128.9, 128.8, 125.8, 125.2, 124.2, 122.4, 58.0, 52.5, 52.4, 50.4; MS (FAB, $[\text{M}^++1]$): Calcd for $\text{C}_{29}\text{H}_{22}\text{O}_5$: 450.14, Found: 451.21; Anal. Calcd for $\text{C}_{29}\text{H}_{22}\text{O}_5$: C: 77.32, H: 4.92, Found: C: 77.19, H: 5.08

3.4.4.7. Compound 13g:

Yield 56%; mp 248 °C; IR (KBr) ν_{\max} : 1700, 1723 (C=O, ester), 1648 (C=O, ketone) cm^{-1} ; ^1H NMR (CDCl_3): δ 6.94-8.11 (13H, m, aromatic), 3.66 (3H, s, OCH_3), 3.54 (3H, s, OCH_3), 2.18 (3H, s, CH_3); ^{13}C NMR (CDCl_3): δ 193.3, 166.1, 166.6, 152.0, 149.4, 148.5, 146.5, 143.7, 141.6, 137.6, 135.0, 130.8, 127.7, 126.2, 125.5, 125.0, 124.7, 122.7, 121.5, 55.7, 52.3, 52.2, 50.1, 32.4, 13.5; MS (FAB, $[\text{M}^++1]$): Calcd for $\text{C}_{31}\text{H}_{24}\text{O}_5$: 476.16, Found: 477.16; Anal. Calcd for $\text{C}_{31}\text{H}_{24}\text{O}_5$: C: 78.14, H: 5.08, Found: C: 78.10, H: 5.00

3.4.4.8. Compound 13h:



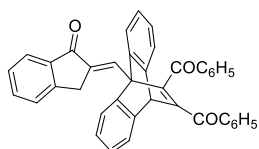
Yield 45%; mp 230 °C; IR (KBr) ν_{\max} : 1708, 1735 (C=O, ester), 1698 (C=O, ketone) cm^{-1} ; ^1H NMR (CDCl_3): δ 7.07-7.99 (18H, m, aromatic), 3.79 (3H, s, OCH₃), 3.75 (3H, s, OCH₃), 3.63 (2H, s); ^{13}C NMR (CDCl_3): δ 192.5, 167.2, 165.7, 156.4, 146.6, 143.7, 142.9, 142.8, 140.7, 137.9, 137.2, 129.8, 128.7, 126.7, 126.2, 125.6, 124.7, 124.3, 123.2, 58.1, 52.6, 52.4; 55.1, 33.2; MS (FAB, $[\text{M}^+ + 1]$): Calcd for $\text{C}_{36}\text{H}_{26}\text{O}_5$: 538.17, Found: 539.18; Anal. Calcd for $\text{C}_{36}\text{H}_{26}\text{O}_5$: C: 80.28, H: 4.87, Found: C: 80.25, H: 4.81

3.4.5. General Procedure for the Synthesis of enone–appended Dibenzobarrelenes 14a-f

For the synthesis of dibenzobarrelenes **14a-f** the corresponding anthracene compounds **12a-f** were dissolved in minimum quantity of dry xylene (5 mL) under inert atmosphere, excess DBA (**5**) was added to it and stirred under reflux for 12h. The solvent was removed under vacuum and the residue subjected to silica gel column chromatography to remove the unreacted dienophile. Elution with 85:15 hexane-ethyl acetate solvent mixture afforded the dibenzobarrelenes **14a-f**.

3.4.6. Spectral and analytical data for the dibenzobarrelenes 14a-f

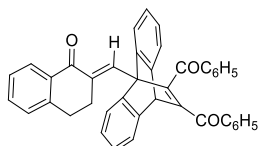
3.4.6.1. Compound 14a:



Yield 26%; mp 190 °C; IR (KBr) ν_{\max} : 1643, 1656, 1699 (C=O, ketone) cm^{-1} ; ^1H NMR (CDCl_3): δ 7.10-7.90 (23H, m, aromatic and vinylic), 5.58 (1H, s, methine), 3.52 (2H, s); ^{13}C NMR (CDCl_3): δ 194.5, 194.1, 192.9, 156.8, 153.3, 149.3, 144.6, 142.7, 142.0, 137.4, 137.2, 136.8, 134.9, 133.5, 133.2, 130.1,

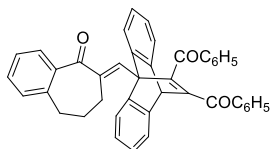
128.9, 128.8, 128.4, 127.6, 125.9, 125.2, 124.7, 124.5, 123.5, 58.4, 53.6, 32.9; MS (FAB, $[M^+ + 1]$): Calcd for $C_{40}H_{26}O_3$: 554.18, Found: 555; Anal. Calcd for $C_{40}H_{26}O_3$: C: 86.62, H: 4.73, Found: C: 86.59, H: 4.71

3.4.6.2. Compound 14b:



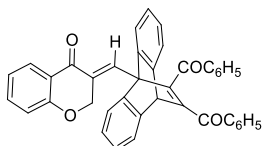
Yield 25%; mp 225 °C; IR (KBr) ν_{max} : 1623, 1649, 1681 (C=O, ketone) cm^{-1} ; MS (FAB, $[M^+ + 1]$): Calcd for $C_{41}H_{28}O_3$: 568.20, Found: 569.15; Anal. Calcd for $C_{41}H_{28}O_3$: C: 86.60, H: 4.96, Found: C: 86.58, H: 4.90

3.4.6.3. Compound 14c:



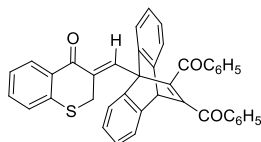
Yield 22%; mp 258 °C; IR (KBr) ν_{max} : 1643, 1655, 1671 (C=O, ketone) cm^{-1} , 1H NMR ($CDCl_3$): δ 7.10-8.03 (23H, m, aromatic and vinylic), 5.54 (1H, s, methine), δ 2.87 (2H, t), δ 2.12 (2H, t), δ 1.86 (2H, m); ^{13}C NMR ($CDCl_3$): δ 196.5, 194.1, 144.3, 144.2, 139.4, 138.9, 137.5, 134.4, 133.3, 133.2, 132.1, 129.0, 128.8, 128.4, 128.3, 127.0, 126.0, 124.9, 124.2, 123.7, 53.8, 31.5, 27.3, 24.8; MS (FAB, $[M^+ + 1]$): Calcd for $C_{42}H_{30}O_3$: 582.21, Found: 583.22; Anal. Calcd for $C_{42}H_{30}O_3$: C: 86.57, H: 5.19, Found: C: 86.53, H: 5.05

3.4.6.4. Compound 14d:



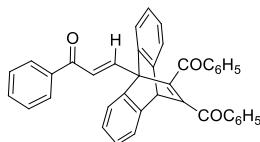
Yield 20%; mp 170 °C; IR (KBr) ν_{max} : 1641, 1657, 1677 (C=O, ketone) cm^{-1} ; 1H NMR ($CDCl_3$): δ 6.91-8.03 (23H, m, aromatic), 5.60 (1H, s, methine), 4.61 (2H, s,); ^{13}C NMR ($CDCl_3$): δ 181.5, 161.9, 144.3, 135.9, 132.3, 129.0, 128.8, 128.5, 128.3, 128.2, 126.2, 125.4, 124.5, 122.0, 118.1, 69.1, 53.5; MS (FAB, $[M^+ + 1]$): Calcd for $C_{40}H_{26}O_4$: 570.18, Found: 571.12; Anal. Calcd for $C_{40}H_{26}O_4$: C: 84.19, H: 4.59, Found: C: 84.17, H: 4.55

3.4.6.5. Compound 14e:



Yield 27%; mp 210 °C; IR (KBr) ν_{\max} : 1617, 1649, 1665 (C=O, ketone) cm^{-1} ; $^1\text{H NMR}$ (CDCl_3): δ 7.07-8.54 (23H, m, aromatic and vinylic), 5.56 (1H, s, methine), 4.15 (2H, s); $^{13}\text{C NMR}$ (CDCl_3): 192.7, 192.3, 177.1, 143.5, 135.0, 134.8, 134.8, 134.6, 131.3, 131.2, 129.3, 129.0, 127.11, 126.7, 126.4, 126.3., 125.5, 124.3, 123.7, 123.4, 121.9, 121.6, 52.9, 51.8, 26.8; MS (FAB, $[\text{M}^++1]$): Calcd for $\text{C}_{40}\text{H}_{26}\text{O}_3\text{S}$: 586.16, Found: 587.18; Anal. Calcd for $\text{C}_{40}\text{H}_{26}\text{O}_3\text{S}$: C: 81.89, H: 4.47, Found: C: 81.85, H: 4.38

3.4.6.6. Compound 14f

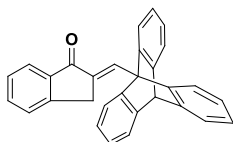


Yield 30%; mp 130 °C; IR (KBr) ν_{\max} : 1612, 1650, 1665 (C=O, ketone) cm^{-1} ; $^1\text{H NMR}$ (CDCl_3): δ 7.89 (1H, d, $J_{AX} = 16.5$ Hz, vinylic) 7.14-7.77 (24H, m, aromatic), 5.58 (1H, s, methine), 3.77 (3H, s, OCH_3), 3.71 (3H, s, OCH_3); $^{13}\text{C NMR}$ (CDCl_3): δ 195.7, 195.6, 189.6, 157.6, 154.5, 145.1, 144.8, 139.8, 137.3, 136.43, 132.51, 133.4, 133.2, 129.1, 128.8, 128.5, 128.3, 125.9, 125.3, 124.2, 122.8, 58.9, 53.5; MS (FAB, $[\text{M}^++1]$): Calcd for $\text{C}_{39}\text{H}_{26}\text{O}_3$: 542.18, Found: 543.20; Anal. Calcd for $\text{C}_{39}\text{H}_{26}\text{O}_3$: C: 86.32, H: 4.83, Found: C: 86.29, H: 4.78

3.4.7. General Procedure for the Synthesis of enone-appended Dibenzobarrelene 15.

In a three neck round bottom flask the anthracene compound **12a** (1.0 g, 3 mmol) dissolved in 10 mL of 1,2-dimethoxyethane was taken and refluxed for 1 h with stirring. During the first half an hour of the reaction anthranilic acid (0.428 g, 3 mmol) dissolved in 10 mL of 1,2-dimethoxyethane and isoamyl nitrite (**16**, 0.419 mL, 3mmol) dissolved in 10 mL of 1,2-dimethoxyethane were added drop wise simultaneously

using two separate dropping funnel. After being cooled to room temperature, the product was extracted using dichloromethane. The organic layer was washed with saturated solution of sodium bicarbonate to remove excess amount of anthranilic acid, dried over anhydrous sodium sulfate and concentrated. The residue obtained was purified by column chromatography using silica gel and hexane/ethyl acetate. Solvent was removed under reduced pressure, and the residue was washed several times with diethyl ether to give an off white crystalline solid.



Yield 25%; mp 292 °C; IR (KBr) ν_{\max} : 1701 cm^{-1} (C=O); ^1H NMR (CDCl_3): δ 6.89-8.32 (17H, m) 5.38 (1H, s), 3.54 (2H, s); ^{13}C NMR (CDCl_3): δ 193.8, 149.7, 145.8, 143.6, 142.5, 137.7, 135.1, 129.9, 127.7, 126.3, 125.5, 124.9, 124.8, 124.1, 122.5, 55.8, 54.3, 33.3; MS (FAB, $[\text{M}^++1]$): Calcd for $\text{C}_{30}\text{H}_{20}\text{O}$: 396.15, Found: 397; Anal. Calcd for $\text{C}_{30}\text{H}_{20}\text{O}$: C: 90.88, H: 5.08, Found: C: 90.85, H: 5.00

References

1. a) Cristol, S. J.; Lim, W. Y. *J. Org. Chem.* **1969**, *34*, 1. b) Cristol, S. J.; Bly, R. K. *J. Am. Chem. Soc.* **1960**, *82*, 6155. c) Cristol, S. J.; Hause, N. L. *J. Am. Chem. Soc.* **1952**, *74*, 2193.
2. Kloetzel, M.; *Organic Reactions* **1967**, *4*, 1.
3. Diels, O.; Alder, K. *Justus Liebigs Ann. Chem.* **1928**, *460*, 98.
4. Sauer, J. *Angew. Chem. Int. Ed.* **1966**, *5*, 211.
5. Holmes, H. L. *Organic Reactions.* **1948**, *4*, 60.
6. Alder, K.; Stein, G. *Angew. Chem.* **1937**, *50*, 510.
7. Sauer, J.; Wiest, H.; Mielert, A. *Chem. Ber.* **1964**, *97*, 3183.
8. Stockmann, H. *J. Org. Chem.* **1961**, *26*, 2025.
9. Diels, O.; Blom, J.; Koll, W. *Ann.* **1925**, *443*, 242.

10. Nicolaou, K. C.; Snyder, S. A.; Montagnon, T.; Vassilikogiannakis, G. *Angew. Chem. Int. Ed.* **2002**, *4*, 1668.
11. Jun-Li, C. *Chem. Rev.* **1993**, *93*, 2025.
12. Yates, P.; Eaton, P. *J. Am. Chem. Soc.* **1960**, *82*, 4436.
13. Raistrick, B.; Sapiro, R. H.; Newitt, D. M. *J. Chem. Soc.* **1939**, 1761.
14. Desimoni, G.; Taconi, G.; Barco, A.; Pollini, G. P. *Natural Products Synthesis Through Pericyclic Reactions*; ACS Monograph 180: American Chemical Society: Washington D. C; **1983**.
15. Atherton, J. C. C.; Jone, S. *Tetrahedron*, **2003**, *59*, 9039.
16. Becker, H.D. *Chem. Rev.* **1993**, *93*, 145.
17. Corey, E. J.; Shibata, S.; Bakshi, R. K. *J. Org. Chem.* **1988**, *53*, 2861.
18. Paddick, R. G.; Richards, K. E.; Wright, G. J. *Aust. J. Chem.* **1976**, *29*, 1005.
19. Ramaiah, D.; Sajimon, M. C.; Joseph, J.; George, M. V. *Chem. Soc. Rev.* **2005**, *34*, 48.
20. Pratapan, S.; Ashok, K.; Cyr, D. R.; Das, P. K.; George, M. V. *J. Org. Chem.* **1987**, *52*, 5512.
21. Pokkuluri, P. R.; Scheffer, J. R.; Trotter, J. *Acta Crystallogr., Sect. B: Cryst. Struct. Commun.*, **1993**, *B49*, 107.
22. Ciganek, E. *J. Org. Chem.* **1980**, *45*, 1497.
23. Mathew, E. M. *Ph.D Thesis*, CUSAT, **2013**.
24. Shashidher, R. B.; Vijaykumar, G. *Pharmaceutica Analytica Acta* **2011**, *2*, 137.
25. Mich, T. F.; Nienhouse, E. J.; Farino, T. E.; Tufariello, J. J. *J. Chem. Educ.* **1968**, *45*, 272.
26. Pavia, D L.; Lampman, G. M.; Kriz, G. S. *Introduction to Organic Laboratory Techniques*; Third Edition.
27. a) Lutz, R. E. *Organic Synthesis*, Horning, E. C., Ed.; Collect. Vol. 3; Wiley: New York, **1995**, 248. b) Lutz, R. E.; Smithy, W. R. *J. Org. Chem.* **1951**, *16*, 648.

Photochemical and photophysical studies on enone appended dibenzobarrelenes

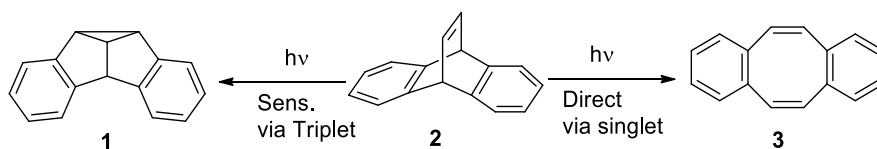
4.1. Abstract

This chapter deals with the photochemical and photophysical aspects of newly synthesized dibenzobarrelenes. Photochemistry of dibenzobarrelene has been the subject matter of investigation for the photochemist because of their mechanistic complexities. The electronic and steric effects of the substituents present have pronounced effect on their reaction pathways and product formation. Several attempts were made to control and direct their reaction pathways through appropriate substitution patterns. In the present work we have also made one such attempt by synthesizing several enone appended dibenzobarrelenes. The dibenzobarrelenes synthesized were subjected to photochemical irradiation in deaerated benzene to understand their photoreactivity in solution. We have also observed that several of the dibenzobarrelenes exhibited photochromism in the solid state. Attempts made to study the nature of the photochromism and our attempts to unravel the mechanism behind this are also depicted in this chapter. We carried out Laser flash photolysis studies for selected compounds to study the transient species involved in the photochemical reactions of these dibenzobarrelenes.

4.2. Introduction

Dibenzobarrelenes with different bridgehead substituents have been studied extensively by different research groups and a brief outlook into the photoreactivity of these compounds is given in Chapter 1. Dibenzobarrelene derivatives and related compounds exhibit competition between the di- π -methane photoisomerization products and dibenzocyclo-

octatetraene formation depending on the substituents present and reaction conditions.¹



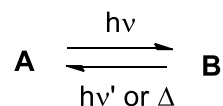
Scheme 4.1

In the present investigation, we examined the photochemistry of several dibenzobarrelenes with enone appendage with a view to improving product selectivity. Enones are efficient triplet quenchers,² so the triplet mediated di- π -methane rearrangement may be hindered. The presence of ester groups at the vinylic positions facilitates rapid intersystem crossing to triplet states under direct irradiation conditions and also stabilizes the radical intermediates formed during photoirradiation.³ As a synergetic effect of all these factors we expected some alternate reaction pathways for these compounds apart from dibenzosemibullvalene and cyclooctatetraene formation. During the course of our investigation, we accidentally stumbled upon remarkable photochromism exhibited by several of the enone appended dibenzobarrelenes synthesized by us. So we made a detailed investigation to establish the mechanism behind this photochromic behavior of dibenzobarrelenes which was not seen in the dibenzobarrelenes synthesized before by several research groups.⁴

4.2.1. Introduction to organic photochromic compounds

Photochromism is the light-induced reversible transformation of a chemical species between two isomers which shows difference in their

absorption spectra. Most photochromic compounds exist in two interconvertible forms of which at least one is sensitive to light.



Photochromism has now emerged as an active area of research because of their wide spread applications in photochromic lenses, photonic materials, optical memory switches, holography, DNA markers and also in sensors.⁵ The major families of organic compounds exhibiting photochromism are spiropyrans (**4**), fulgides (**5**), diarylethylenes (**6**), and azobenzenes (**7**) (Chart 4.1). All these compounds are either colorless or faintly colored and upon irradiation they change to colored forms. The reverse reaction, *i.e.* decoloration or bleaching process can take place both thermally and photochemically or only photochemically. Thermal irreversibility is the most essential property needed for their application in optoelectronic devices and molecular machines.

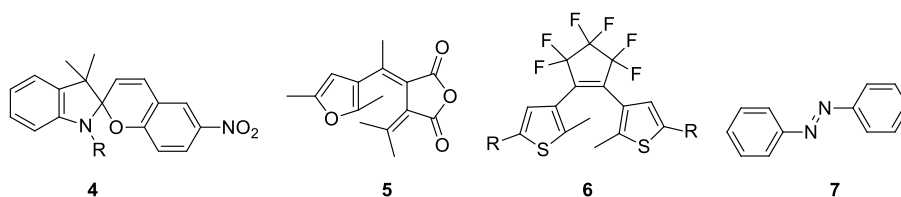


Chart 4.1

Among the large no of organic photochromic materials synthesized and studied, most of them showed this behavior in solution and only a few were found to be photochromic in solid state. Photochromic organic crystals are receiving much attention because it is easy for fabricating

devices using these materials. Fig. 4.1 shows the crystalline and solution state photochromic behavior of some diarylethene compounds.⁶

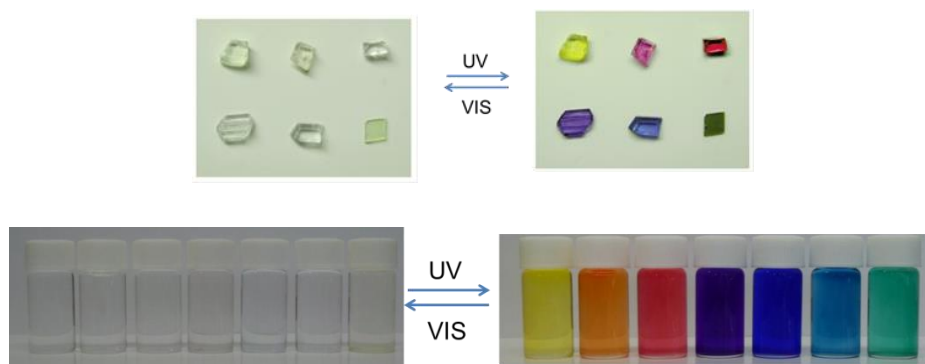


Fig. 4.1: Photochromism shown by some diarylethene derivatives in crystalline phase and in solution

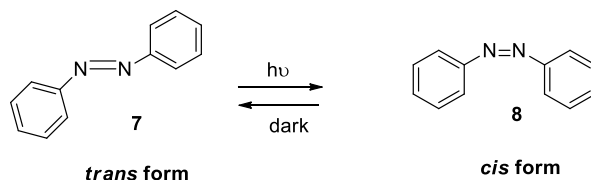
4.2.1.1. Mechanism of Photochromism

The mechanisms behind photochromism include (but not limited to):

- *cis-trans* isomerizations
- pericyclic reactions
- intramolecular hydrogen transfer

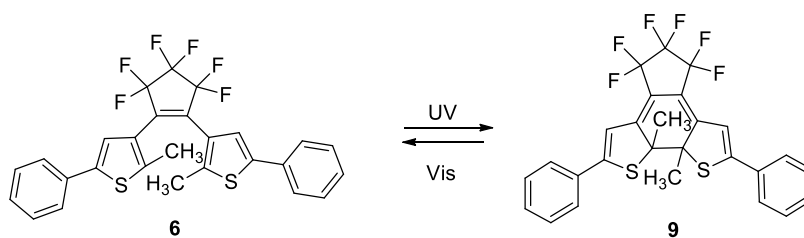
Photochromism of azobenzenes is attributed to their capability to undergo light induced *cis-trans* isomerization. The more stable *trans* form which is colorless upon UV-irradiation undergo isomerization to the colored *cis* form. The reverse reaction can take place either by irradiation with light or thermally. The thermal instability of these compounds is a major drawback for its use in optoelectronics. But synthetic modifications of this compound by introducing appropriate substituents on the benzene ring has led to the development of azobenzene containing

polymers and liquid crystals having potential applications as functional materials.⁷



Scheme 4.2

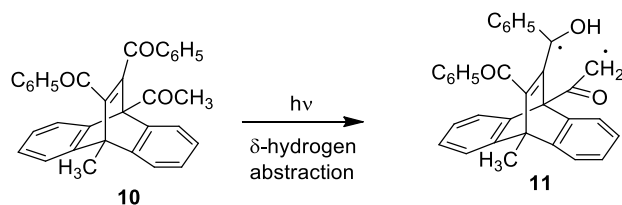
Electrocyclic ring opening and closing reactions are responsible for the photochromic behavior of spiropyrans, fulgides and bisthiénylenes.⁸ These compounds can exist in colorless ring opened form and colored ring closed forms upon alternate irradiation with UV and visible light. Scheme 4.3 shows the ring opening and closing reactions in diarylethenes which gives rise to photochromism. This is the basic mechanism responsible for the photochromism exhibited by different diarylethene derivatives in crystalline and solution state as shown in **Fig. 4.1**.



Scheme 4.3

Light induced intramolecular hydrogen abstraction resulting in the formation of long lived biradical intermediates was also reported as the reason for photochromism in organic compounds. A notable example is that of photochromism in 11,12-dibenzoyl-9-acetyl-10-methyl-

substituted dibenzobarrelene. The photochromic species involved are long lived triplet biradical intermediates formed as a result of a reversible δ -hydrogen abstraction by the benzoyl carbonyl group from the proximal acetyl group (Scheme 4.4).^{9,4}



Scheme 4.4

Scheffer and co-workers¹⁰ were the first to observe transient colors in the crystalline state photochemistry of a number of 9,10-ethenoanthracene derivatives bearing electron-withdrawing ester or carboxylic acid substituents on the bridging double bond. But they could not explain the exact reason behind photochromism satisfactorily. They noticed that these transient colorations were invariably associated with either 9-or 9,10-disubstitution. In the case of 9,10-dialkyl substituted triptycene-quinones they observed that these compounds on irradiation give rise to intensely colored norcaradiene derivatives in addition to the expected di- π -methane photorearrangement products. The color in these products has been attributed to charge-transfer interaction between the norcaradiene and quinone chromophores.

Tanaka and Toda have reported photochromism in biindenylidene compounds based on the formation of triplet biradicals in the crystalline state.¹¹ Li *et al.* have reported that some biindenylidenedione derivatives exhibiting crystalline state photochromism through the generation of

stable organic radicals.¹² In these compounds the X-ray studies reveal the possibilities of intramolecular and intermolecular hydrogen bonding which could stabilize these radicals leading to photochromism. In organic photochromic compounds where a triplet biradical species is responsible for photochromism we can see a co-existence of photomagnetism and photochromism which open up the possibilities for the development of new systems which possess optically generated magnetic properties and finds application as molecular magnets.¹³

A recent report on the photochromic reactivity of *N*-salicylidine derivatives in a polymer matrix¹⁴ shows the wide scope of research work that can be carried out in the field of organic photochromism. *N*-salicylidine aniline and its derivatives were found to display a photoinduced switching between fluorescence and photochromism depending on the substitution and the chemical environment. The mechanism operating here is the keto-enol tautomerism. When salicylidine derivatives were incorporated into a polymer matrix selective stabilization of the various keto and enol forms is possible depending on the host guest interactions and thereby photochromism can be induced or stabilized.

4.2.2. Laser Flash photolysis

Flash photolysis technique¹⁵ revolutionized the science of photochemistry since it provided an efficient tool to study extremely fast chemical reactions. Understanding the nature of physical processes of formation and decay of excited states has shed light on the chemical reactivity of these states and has lent models for predicting and

characterizing photochemical reaction mechanisms. The technique of flash photolysis was first employed by Norrish and Porter in 1949 to study the short lived transient species in microsecond timescale. The basis of flash photolysis is to irradiate the system with a very short intense pulse of light and then as soon as the pulse is over the changes in the system with time is monitored by some spectroscopic techniques. The photolysis pulse having high intensity produces a large number of photons which in turn increases the population of electronically excited states which can be monitored by absorption or emission spectroscopy. The monitoring device must have a time resolution fast enough to observe the transient state before it decays. The first generation pulsed sources were flash lamps that produced a wide range of wavelengths and pulses of 10^{-3} s. With the invention of laser, in 1960 and the development of pulsed lasers using Q-switching monochromatic and highly collimated light sources became available with pulse duration in the nanosecond timescale. During 1970s and 1980s the time scale of pulsed lasers decreased to the picosecond (10^{-12} s) and femtosecond (10^{-15} s) time scales. Thus during a short period, the time scale of photochemistry decreased from 10^{-3} s to 10^{-15} s. Fig. 4.2 shows the life time for the singlet and triplet transitions. For triplet it falls in the nano to micro second time scale and hence nano second laser flash photolysis is the appropriate technique for studying the triplet excited states. And for singlet excited states whose life time is in the femtosecond range need the femtosecond laser flash photolysis techniques.

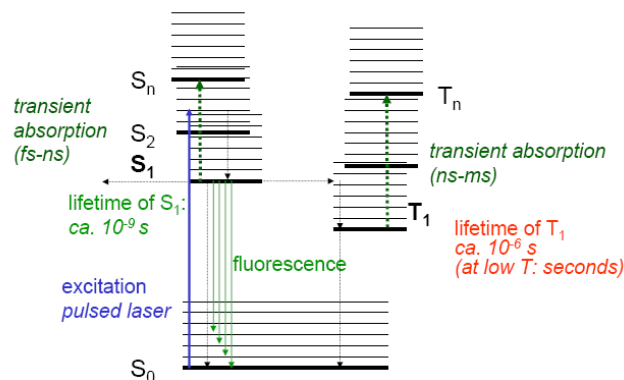


Fig. 4.2

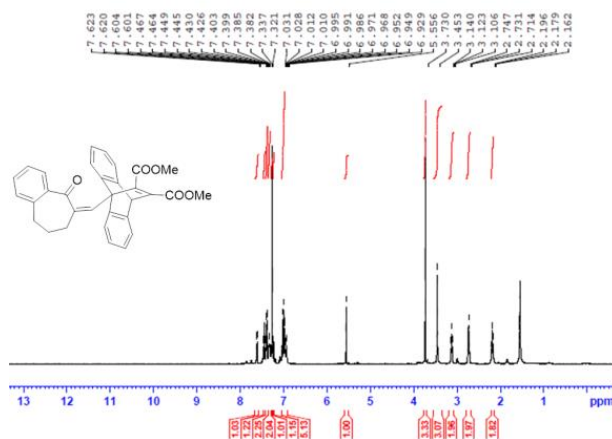
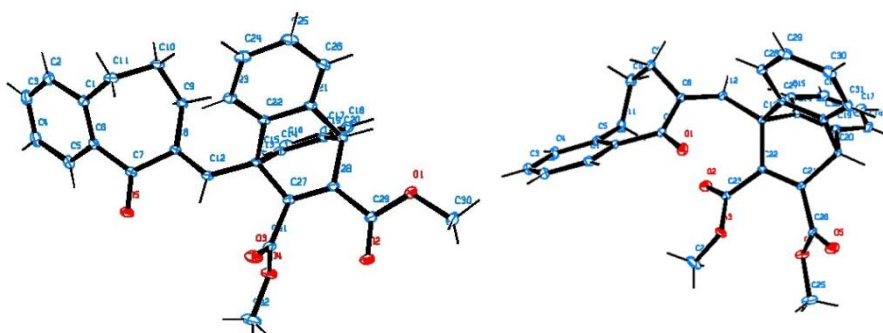
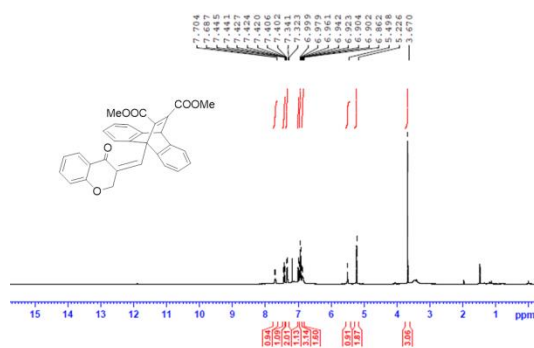
4.3. Results and discussion

In chapter 3, we reported the synthesis of several enone appended dibenzobarrelenes as shown in Chart 4.2. In order to have more understanding regarding their photochemical behavior they were subjected to steady state photolysis, laser flash photolysis and solid state photoirradiation.

4.3.1. Steady state irradiation of dibenzobarrelenes 12a-g & 13a-f.

Steady state irradiation of the compounds **12a-g** & **13a-f** was carried out in a Rayonet photochemical reactor employing 300 nm lamps in deaerated benzene. We choose the 300 nm region for the studies because this wavelength corresponds to the absorption tail of the compounds and hence we can minimize the absorption near surface. Benzene was the most suitable solvent for our compounds because of the solubility reasons and also due to its transparency in the 300 nm region. Benzene solution of the compounds purged with nitrogen gas were subjected to

position resulted in extensive decomposition. In the case of **12e**, the starting material was recovered along with some polymeric mass. For substrates where TLC analysis of photolysates indicated substantial generation of a new product upon irradiation, the new product could be isolated in pure form (single spot in TLC). Mass spectral analysis of the photoproduct revealed its identity as an isomer of the starting material suggesting possible photoisomerization of the starting materials. As mentioned in previous sections, photoisomerization possibilities for enone appended dibenzobarrelenes include: i) di- π -methane rearrangement leading to semibullvalenes, ii) pericyclic reactions leading to cyclooctatetraene and iii) *cis-trans* isomerization around the enone double bond. The major problem we faced during photochemical studies was that we could not identify photoproducts of **12a,b,d** on the basis of ^1H NMR data. The ^1H NMR spectra of these compounds exhibited broad characterless peaks reminiscent of polymeric mixtures (which, anyway, were also formed under irradiation conditions) casting serious concerns on their identity as isomeric products. Fortunately, we could generate diffraction quality crystals of the photoproducts and they were eventually identified as *Z*-isomers of **12a-d** (Chart 4.3) on the basis of SCXRD data. Icing on the cake was that, in the case **12c** we could get the SCXRD structures for both the starting *E* isomer and the photoproduct *Z* isomer. Our attempts to generate diffraction quality crystals of *E*-isomers of all other enone appended barrelenes remained futile.

Fig. 4.5: ^1H NMR spectrum of the *Z* isomer of compound 12cFig. 4.6: ORTEP diagrams of the *E* and *Z* forms of 12cFig. 4.7: ^1H NMR spectrum of the *Z* isomers of compound 12d

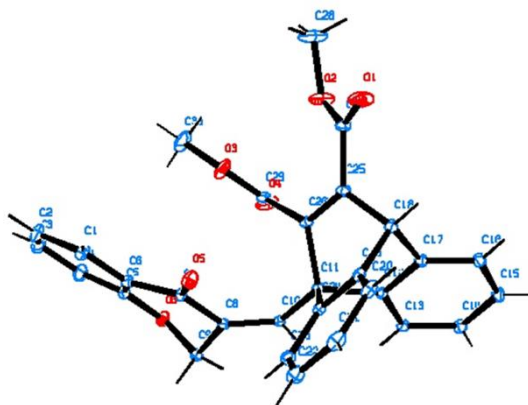


Fig. 4.8: ORTEP diagram of the Z-isomer of **12d**

A closer look at the structure of enone appended barrelenes revealed possible existence of different rotamers due to free rotation around the single bond connecting the dibenzobarrelene and enone components (Fig. 4.9). Co-existence and interconversion between different rotameric structures in the NMR timescale may be attributed for the broad and characterless peaks observed in the NMR spectra of these compounds.

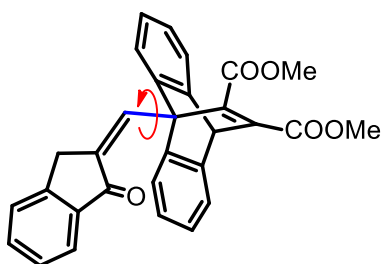


Fig. 4.9

In the case of compounds having the benzoyl substituents at the vinylic position we could not isolate any new photoproduct from the residual mixture after photoirradiation. They underwent extensive decomposition.

To account for the differences in the photochemical behavior of these compounds we have carried out more studies.

4.3.2. Photochromic properties of the dibenzobarrelenes in the solid state

We serendipitously observed that many of the dibenzobarrelenes synthesized showed photochromic behavior in the solid state. The photochromic behaviour was more relevant in the case of dibenzobarrelenes having carbomethoxy substituents at the vinylic position. These compounds, upon exposure to sunlight, developed a bluish green color that slowly vanished when kept in the dark. The coloration-decoloration sequence could be repeated several times without loss of material integrity. Even after ten cycles, no observable chemical change was observed with these compounds. However, in the case of compounds having benzoyl groups at the vinylic positions, though we could observe photochromic behavior for the compounds **13a,c,f**, they did not survive more than three cycles of coloration-decoloration sequence. At the end of three cycles, substantial decomposition of material was evident by TLC analysis. In the case of the compound **14** we could not observe photochromism. Based on these observations, we focused our investigation on photochromism to only compounds having carbomethoxy substituents at the vinylic (or 11,12-) positions.

Fig. 4.10-13 shows the photochromism exhibited by compounds **12a,c,e,f** synthesized by us. For these compounds, photochromic behavior was seen prominently in solid state while no noticeable color change was observed in dilute solutions in different solvents even after prolonged

exposure to sunlight. The UV-Vis absorption spectra of the compounds recorded before and after irradiation showed no difference (Fig. 4.14). In solution state there is no absorption beyond 400 nm. So we recorded the solid state UV-Vis diffuse reflectance spectra for these compounds before and after irradiation. In the case of compound **12c** which is quite sensitive to light we could clearly follow the photochromic behavior with the help of UV-DRS, here the compound reverted back to the colorless form only after hours in the dark. In the case of **12e** the compound reverted back in about 10 minutes, here also we could get the UV-DRS. For **12a,f** the color change was instantaneous: on exposure to light, the compound became colored but reverted back suddenly making precise DRS spectral measurements tedious.

An interesting feature of our investigation is the diversity in photochromism exhibited by compounds **12a-f**. While all compounds exhibited photochromism, timeframe for onset and fading of photochromism varied from sample to sample. For **12a,f** color change was instantaneous. In contrast, after short exposure to daylight, **12c** required hours for restoration to the original colorless form. Compound **12e** on the other hand reverted to the original colorless form in about 10 minutes. Upon prolonged exposure to daylight, crystals of **12d** obtained by recrystallization from acetonitrile exhibited slight change in color. From other solvents, **12d** separated as amorphous material that exhibited negligible photochromism. Though dependence of photochromism on crystalline nature of samples is a very interesting observation, we did not pursue it any further due to experimental constraints.

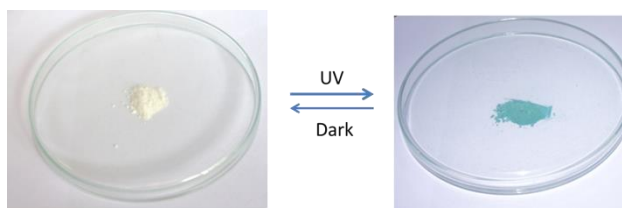


Fig. 4.10: Photochromism exhibited by compound 12a

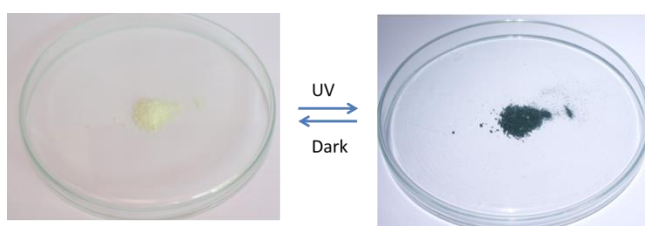


Fig. 4.11: Photochromism exhibited by compound 12c

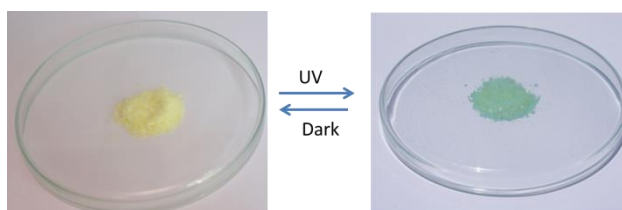


Fig. 4.12: Photochromism exhibited by compound 12f

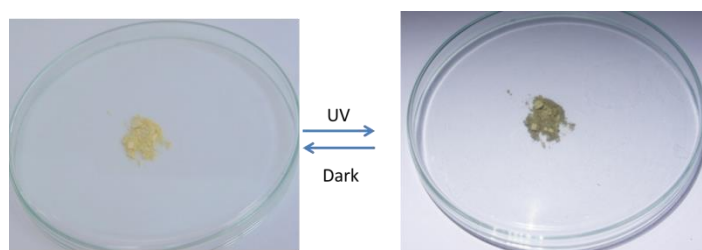


Fig. 4.13: Photochromism exhibited by compound 12e

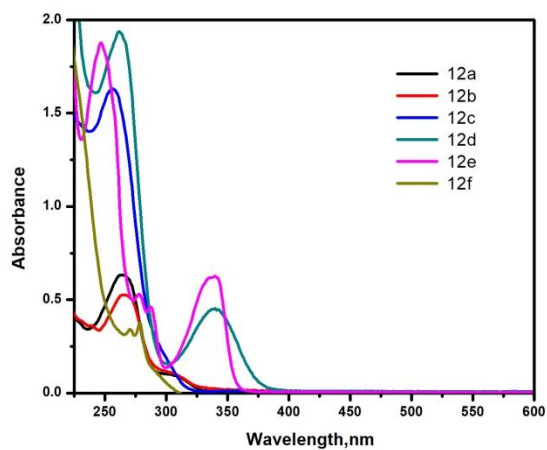


Fig. 4.14: UV-Vis absorption spectra of compounds **12a-f** in acetonitrile

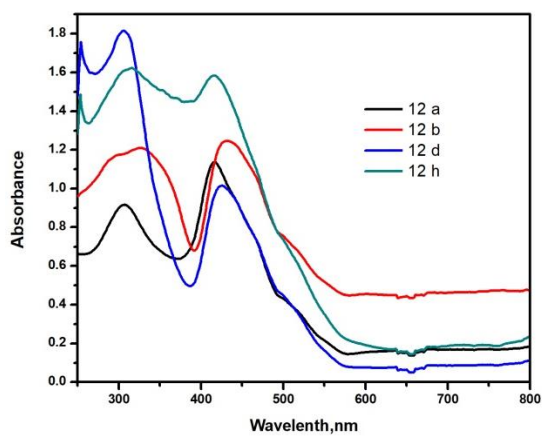


Fig. 4.15: UV-Vis diffuse reflectance spectra of **12a,b,d,h** before exposure to sunlight

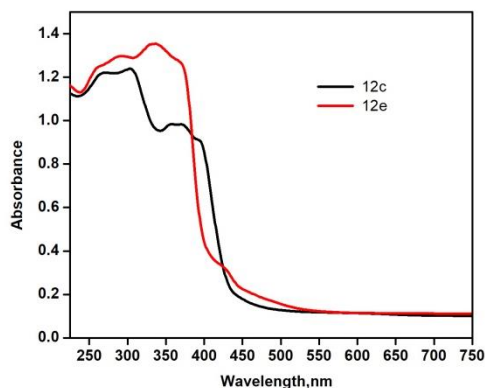


Fig. 4.16: UV-Vis diffuse reflectance spectral changes **12c,e** recorded before exposure to sunlight

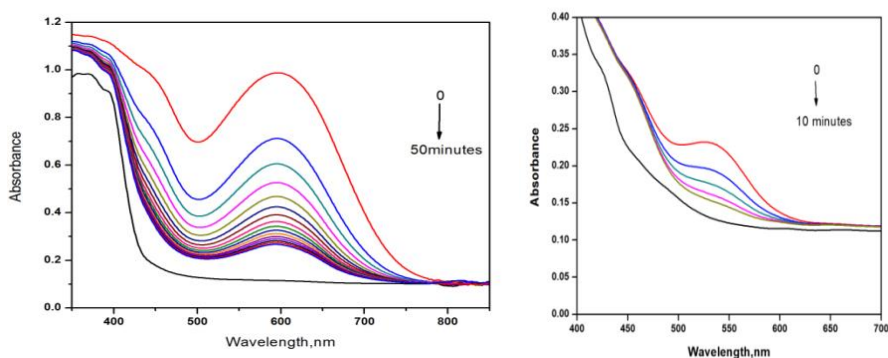
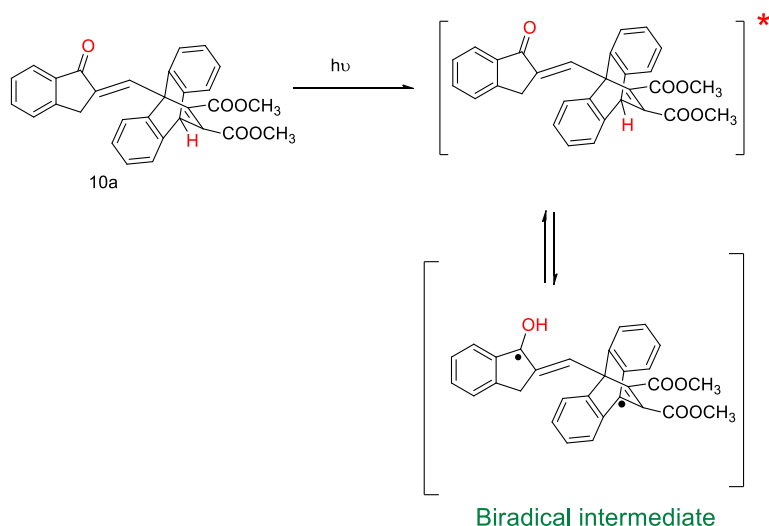


Fig. 4.17: UV-Vis diffuse reflectance spectral changes of **12c and 12e** recorded after exposure to sunlight

In order to account for the photochromic behavior of these compounds, we considered different possible mechanisms available in literature. The possibility for *cis-trans* isomerization behind this photochromic nature was ruled out because we could isolate the *Z*-isomers of the corresponding compounds. They were also colorless compounds exhibiting identical photochromic behavior with those of the corresponding *E*-isomer precursors. So the mechanism behind is not the

cis-trans isomerization. For these compounds the possibilities for electrocyclic ring opening and closing reactions as reason for photochromism is also not relevant. So we have proposed a plausible mechanism in which bridgehead hydrogen is abstracted by carbonyl group resulting in the formation of a diradical intermediate. As an evidence for this we observed that compound **12h** with a phenyl substituent at the bridgehead position is not photochromic. We have also tried methyl substitution at the bridgehead position (**12g**). But here also the compound showed photochromism but only to a small extent. So the mechanism we propose to explain the photochromism is shown in scheme 4.5.



Scheme 4.5

To authenticate the presence of triplet biradical intermediates we have first attempted EPR spectral studies for one of our compounds. Evidence for the presence of a paramagnetic biradical species was obtained from

the EPR-spectral studies. We recorded the EPR spectrum of **12c** which is the best photochromic material among the compounds synthesized by us. The EPR spectrum was recorded before and after exposure to sunlight (Fig. 4.18). The spectrum recorded after exposing the solid crystalline powder of the compound to sunlight for about 5 minutes showed a signal centered around 350 mT. Instead of a characteristic triplet EPR spectrum expected for the biradical species, we got a spectrum with a broad peak and a sharp peak. This broadening can be due to the dipolar coupling or due to spin relaxation process.^{16,17} Control experiments carried out on the compound before exposure to sunlight showed no EPR-active species on irradiation under analogous conditions.

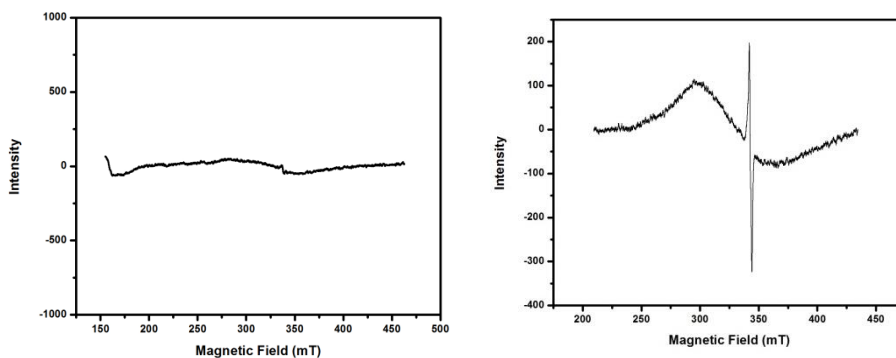


Fig. 4.18: ESR spectrum of compound **12c** recorded a) before exposure to sunlight b) after exposure to sunlight at room temperature in solid state

4.3.3. Laser flash photolysis studies

To get more information on transient intermediates formed, nanosecond laser flash photolysis was carried out. The third harmonic (355 nm) of a Q-switched Nd:YAG laser with 8 ns pulse width and 150 mJ pulse

energy was used to excite samples. Laser flash photolysis studies were conducted only for a few selected compounds shown in Chart 4.4.

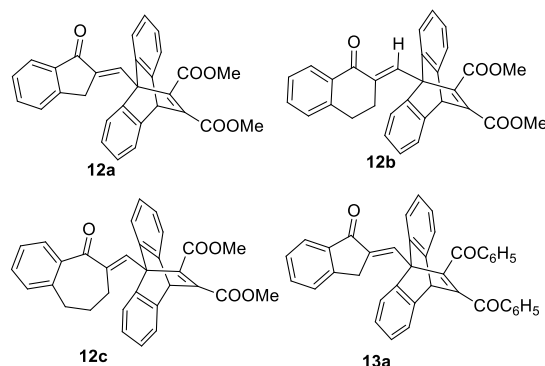


Chart 4.4

Among the compounds selected **12a** is photochromic, **12b** is not showing the photochromic behavior visibly, **12c** is the one which is having the best photochromic properties and for **13a** which is photochromic but the extent of photofatigue resistance is less, so in order to compare the nature of the transient species formed from each of these compounds and to find out its relation with the photochromism shown we have carried out the nanosecond laser flash photolysis for these compounds.

Laser flash photolysis experiments were carried out in degassed benzene solution. In the presence of air we were not getting the signals corresponding to the transients generated. This indicates that the species formed are triplets. Fig. 4.19 shows the transient absorption spectra and the decay curves for **12a**. The transient absorption spectra of **12a** showed two absorption maxima around 390 nm and 630 nm and the decay curves at these wavelengths showed that they were long-lived transients having lifetime in the range of milliseconds.

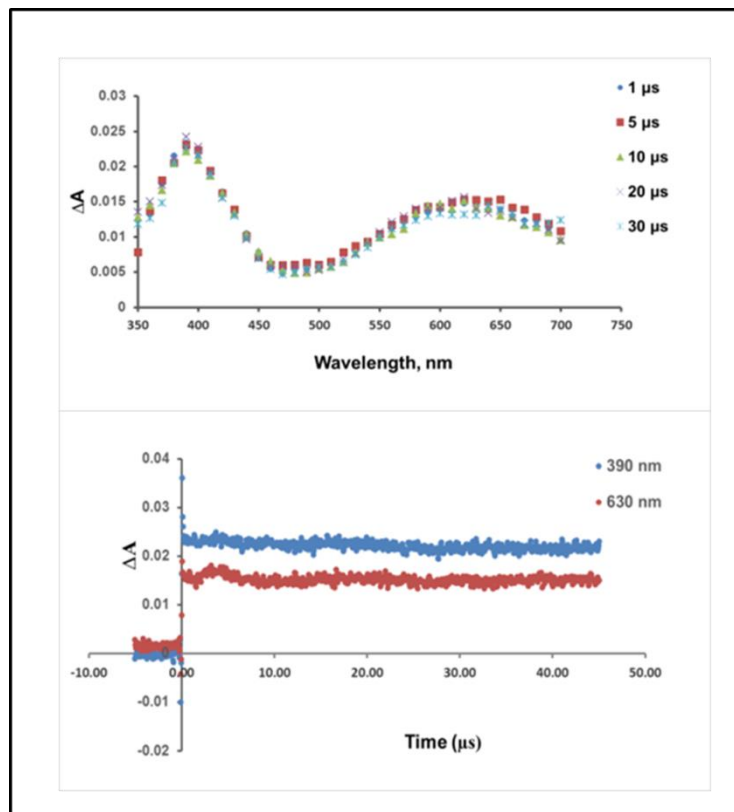


Fig. 4.19: Transient absorption spectra at the indicated times following 355 nm laser excitation and the decay curves at 390nm and 630nm for compound **12a**

Fig. 4.20 shows the transient absorption spectra and the decay curves for **12c**. In the transient spectra of **12c** also indicated the presence of two absorption maxima around 400 nm and 610 nm and the decay curves at these wavelengths shows that they were also long-lived transients having lifetime in the range of milliseconds.

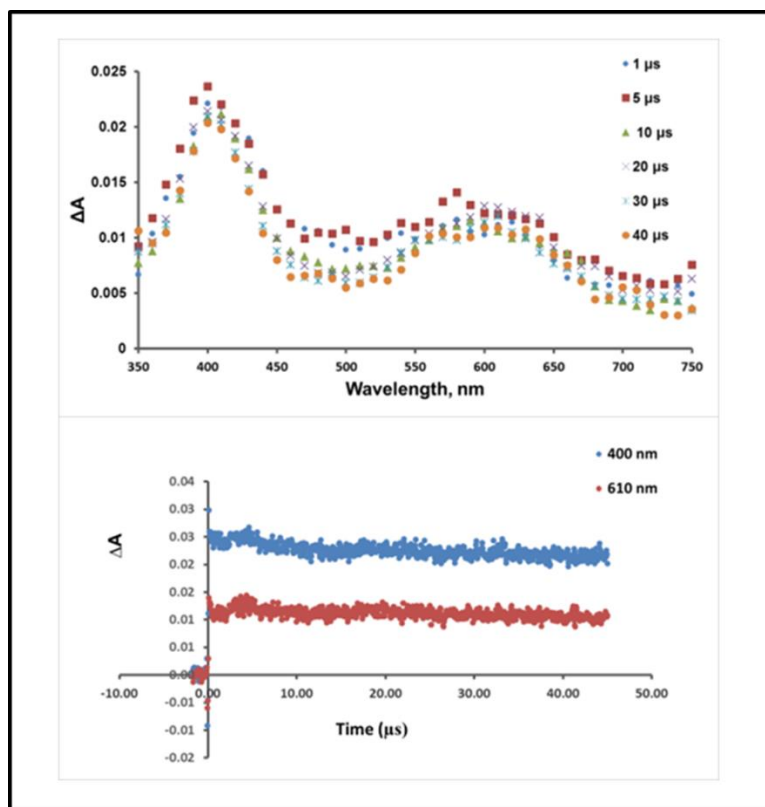


Fig. 4.20: Transient absorption spectra at the indicated times following 355 nm laser excitation and the decay curves at 400 nm and 610 nm for **12c**

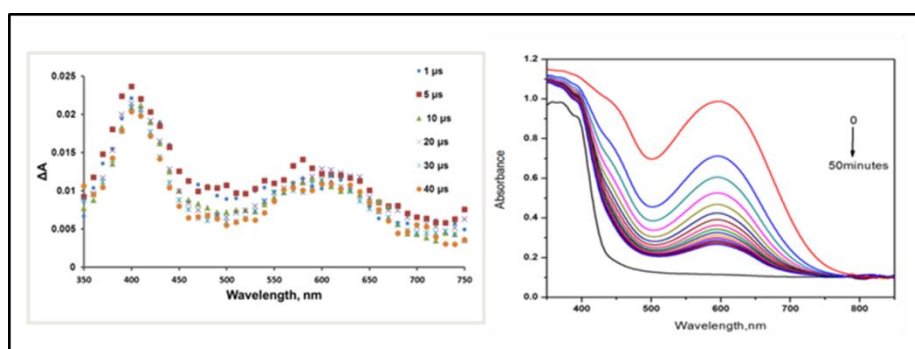


Fig. 4.21: Comparison of the transient spectra and the UV-DRS of **12c**

For compound **12c** from the UV-DRS we have seen that absorption peak with maxima around 600 nm is responsible for the photochromic behavior of this compound and on comparing this spectrum with the transient absorption spectra obtained we found that the transient species formed also has an absorption peak in this region and this gives a clear evidence that the formation of the transient species, probably a biradical, is responsible for the photochromism.

In the case of **12b** the transient absorption spectra shows absorption maxima at 430 nm and 630 nm but here we found that the peak at 430 nm is short-lived and decays with a life time of about 1 μ s and the one at 630 nm is having long lifetime in the range of milliseconds. This compound was not photochromic visibly. In the case of **13a** also the transient absorption spectra showed two absorption maxima around 390 nm and 630 nm and the one at the 390 nm region was short-lived with lifetime of about 0.5 μ s. This compound was photochromic but the fatigue resistance was less.

Laser flash photolysis studies on several 11,12-dibenzoyldibenzo barrelenes are reported by George *et al.*¹⁸ Transient absorption curves they obtained were having absorption maxima in the region below 550 nm and this corresponds to the triplet biradical formation from the dibenzobarrelene moiety and no absorption peak in the 600 nm region was found in their studies except for the photochromic barrelene reported by them.⁴ So the new transient absorption peak in our compounds around 600 nm is most likely due to a transient species formed in the irradiation of these compounds. The presence of the enone component has a

significant role in its formation. We attribute it to the biradical intermediates formed as result of hydrogen abstraction by the carbonyl oxygen (Scheme 4.5).

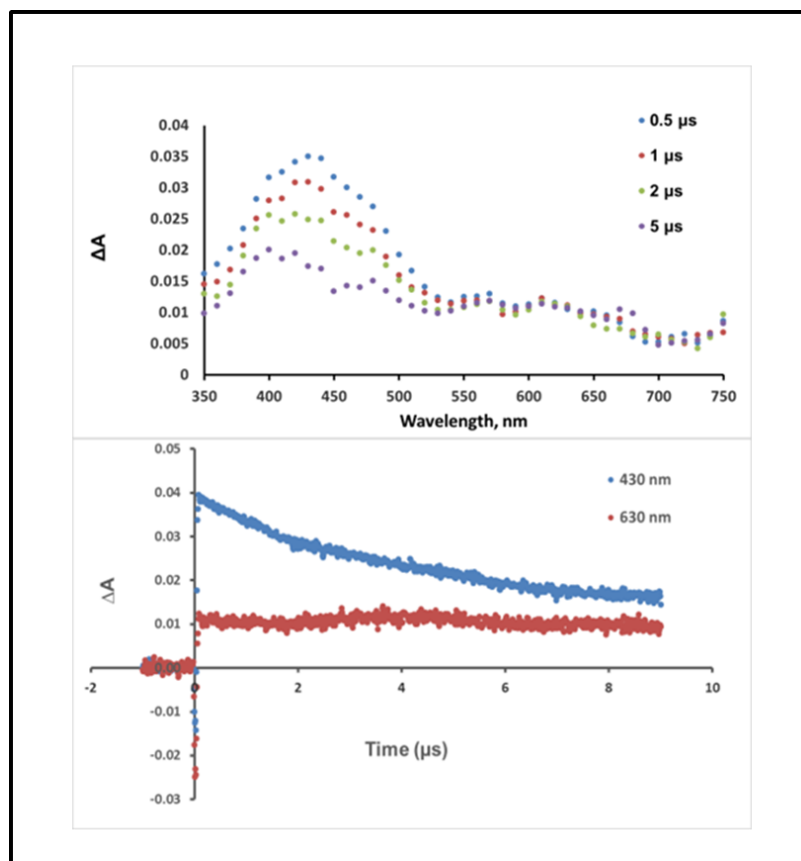


Fig. 4.22: Transient absorption spectra at the indicated times following 355 nm laser excitation and the decay curves at 430 nm and 630 nm for **12b**

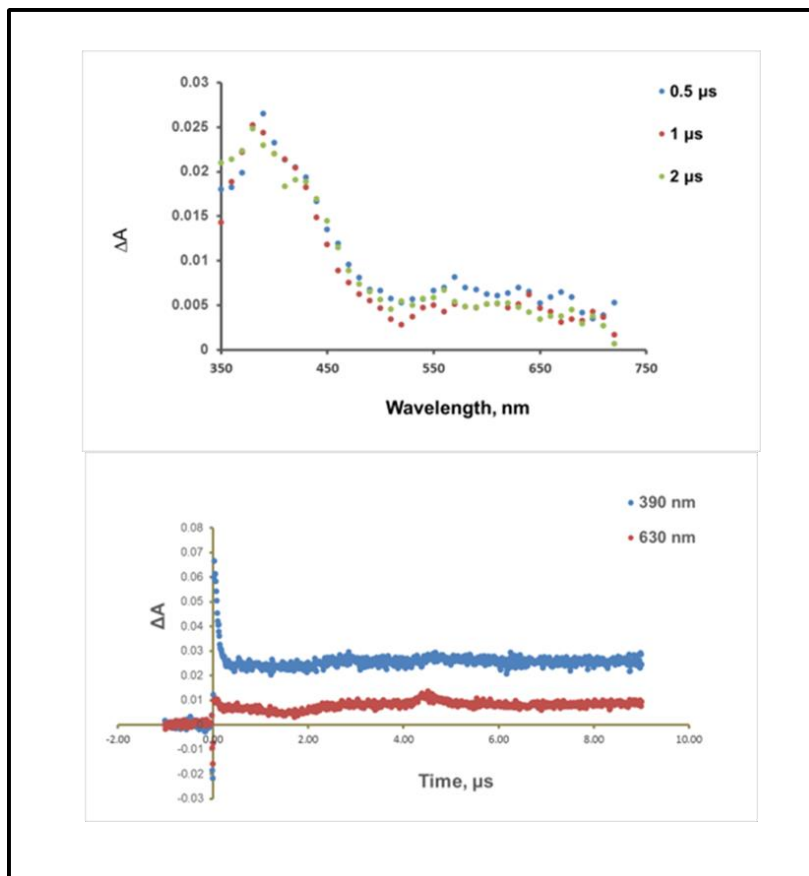


Fig. 4.23: Transient absorption spectra at the indicated times following 355 nm laser excitation and the decay curves at 390 nm and 630 nm for **13a**

4.3.4. Comparison of the photochromic behavior in different compounds

When we compare the photochromic behavior of the compounds shown in Chart 4.5, we observed that even though the enone component is same for all these compounds there is considerable variation in their response to light exposure. Though both **12a** and **13a** are photochromic, **13a** is more prone to photodecomposition. For **12h** we could not observe

photochromism. This observation supported the possibilities for the formation of biradical formation as a result of bridgehead hydrogen abstraction by the carbonyl oxygen. In the case of **14** which is the triptycene analog of the synthesized dibenzobarrelenes, inspite of the presence of bridgehead hydrogen we could not observe the photochromism. It appears that the carbomethoxy or the benzoyl substituent present at the vinylic position also plays a role in stabilizing the radical sites formed.

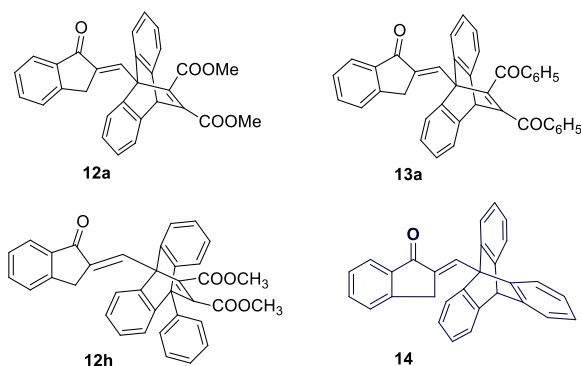


Chart 4.5

On comparison of the photochromism in compounds with different enone components the geometry of the compounds has also a crucial role. This can be explained with the help of the crystal structures obtained for the *Z* isomers of the dibenzobarrelenes with the carbomethoxy substituents at the vinylic positions. Here when we compare the different structures in **12a**, **12c** and **12d** the carbonyl oxygen and the bridgehead hydrogen are in the same plane but in **12b** they are not. The photochromic nature of these compounds are also closely related to the geometry of the

compounds, only in those where the carbonyl oxygen and the bridge head hydrogen are in the same plane photochromism was observed. In the case of **12b** they were not in the same plane. So we propose that the hydrogen abstraction process is easier when the carbonyl oxygen and the bridgehead hydrogen are in the same plane leading to efficient photochromism.

4.3.5. Solvent Polarity dependence studies

We have carried out solvent polarity dependence studies on the representative compounds to assign the orbital configuration to the electronic transitions responsible for an absorption band in the absorption spectra of the respective compounds. The electronic transitions expected for our compounds are $\pi-\pi^*$ and $n-\pi^*$ transitions. The absorption spectra for the dibenzobarrelenes synthesized are shown in Fig. 4.24. From this figure we observe that the absorption band in the region around 260 nm is more prominent and the absorption in the 300 nm region is weak.

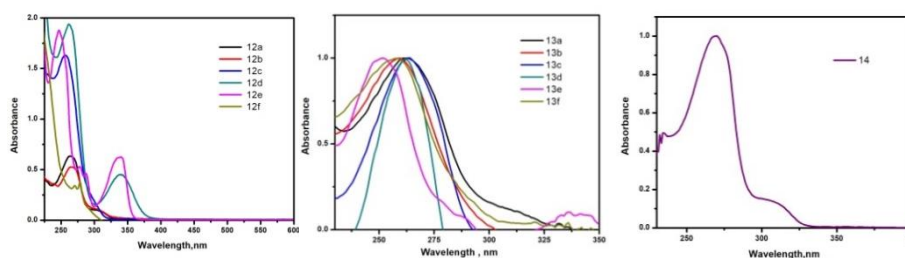


Fig. 4.24: UV-Vis absorption spectra of the dibenzobarrelenes

Solvent polarity dependence studies were carried out by taking one representative compound, each from the three class of compounds we have synthesized as shown in chart 4.6.

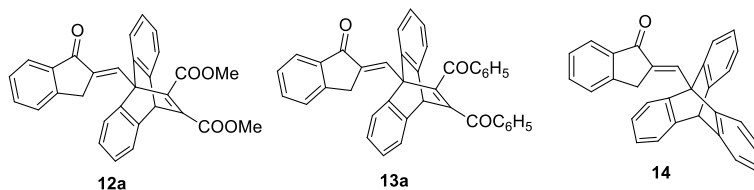
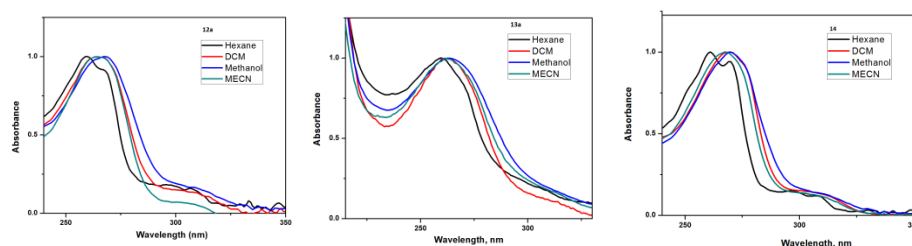
**Chart 4.6**

Fig. 4.25 show the absorption spectra for compounds **12a** and **13a** and **14** in different solvents. We can see in all the three compounds the peak around 260 nm shifts to a longer wavelength region as the polarity of the solvent increases and the peak at 300 nm shifts to shorter wavelength with increase in polarity. From this observations we may interpret that the absorption peak around 260 nm is due to π - π^* transitions and in the 300 nm region is due to n - π^* transitions.

**Fig. 4.25:** UV-Vis absorption spectra of **12a**, **13a** and **14** in different solvents

From the comparison of the absorption spectra of the compounds **12a**, **13a** and **14** as shown in Fig. 4.26 we observe that even though these three compounds differ in their substitution pattern at the vinylic positions of the dibenzobarrelene moiety they are not showing much difference in the absorption spectra.

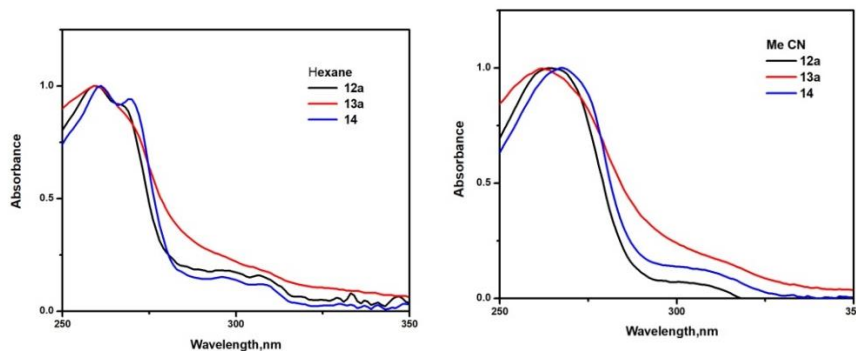


Fig. 4.26: Comparison of the absorption spectra of compounds **12a**, **13a** and **14** in non-polar and polar solvents

4.4. Experimental

4.4.1 Materials and method

All reactions were carried out using oven dried glasswares. All experiments were done with distilled and dried solvents by using standard protocols. All starting materials were purchased from either *Sigma-Aldrich* or *Spectrochem Chemicals* and were used without further purification. Separation and purification of compounds were done by column chromatography using silica gel. The products obtained were further recrystallized from suitable solvents. Melting points are uncorrected and were determined on a Neolab melting point apparatus. Infra-red spectra were recorded using *Jasco 4100* and *ABB Bomem (MB Series) FT-IR* spectrometers. The ^1H and ^{13}C NMR spectra were recorded at 400 MHz *Bruker Avance III* FT-NMR spectrometer with tetramethylsilane (TMS) as internal standard. Chemical shifts (δ) are reported in parts per million (ppm) downfield of TMS. Elemental analysis was performed using an Elementar systeme (Vario EL III). Molecular mass

was determined by direct injection to a Waters 3100 mass detector with an electron spray ionization unit. All Photochemical reactions were carried out in a Rayonet photochemical Reactor (RPR) using 300 nm lamps in deaerated benzene. ESR spectrum was recorded in solid state at room temperature with a JEOL JES-FA200 ESR Spectrometer. Absorption spectra were recorded using Evolution 201 UV-Visible spectrophotometer UV-DRS recorded in a Varian Carry 5000 UV-Vis-NIR spectrophotometer. Single crystal X-ray diffraction analysis carried out on a Bruker AXS Kappa Apex II CCD X-ray diffractometer.

4.4.1.1. Nanosecond Laser Flash Photolysis

Transient absorption experiments were carried out using nanosecond laser flash photolysis (Applied photophysics, UK) and the instrument set up is shown in Figure 4.27. The third harmonic (355 nm) of a Q-switched Nd:YAG laser (Quanta-Ray, LAB 150, Spectra Physics, USA) with 8 ns pulse width and 150 mJ pulse energy was used to excite the samples. Dichroic mirrors were used to separate the third harmonic laser from the second harmonic and the fundamental output of the Nd:YAG laser. The monitoring source was a 150 W pulsed xenon lamp, which was focused on the sample at 90° to the incident laser beam. The beam emerging through the sample was focused on to a Czerny-Turner monochromator using a pair of lenses. The detection was carried out using a Hamamatsu R-928 photomultiplier tube. The transient signals were captured with an Agilent infinity digital storage oscilloscope and the data were transferred to the computer for further analysis.

The output from the system is change in voltage versus time at a given wavelength. The voltage given by the PMT is directly proportional to the incident light intensity. The change in absorbance at time t after the laser pulse was calculated using the expression (4.1).

$$\Delta A_t = \log \left[\frac{I_0}{I_0 - \Delta I} \right] \quad (4.1)$$

where ΔA_t = absorbance change at time 't'

I_0 = signal voltage before flash

ΔI = difference between the signal voltage before flash and the signal voltage at time t after flash

A plot of $\ln(\Delta A)$ versus time gives a straight line for the first-order decay process, and rate constant for the decay was calculated from the slope of the plot. Time-resolved transient spectra were recorded by plotting change in absorbance at a given time 't' obtained at different monitoring wavelength. The energy of the laser was measured using a thermocouple power head which is connected to the power meter (Moletron, USA). For laser flash photolysis studies, samples were purged with either argon or N_2O gas for 45 minutes prior to the laser irradiation. All the experiments were conducted at room temperature.

4.4.2. General Procedure for the photochemical reaction of enone–appended dibenzobarrelenes

A degassed solution of the dibenzobarrelenes (< 1 mmol) in 100 mL dry benzene was irradiated for 90 minutes in a Rayonet Photochemical reactor using 300 nm lamps. The reaction was monitored by TLC. After removal of the solvent under vacuum the residual solid was subjected to

silica gel column chromatography and eluted with hexane-ethyl acetate solvent mixture to get the product.

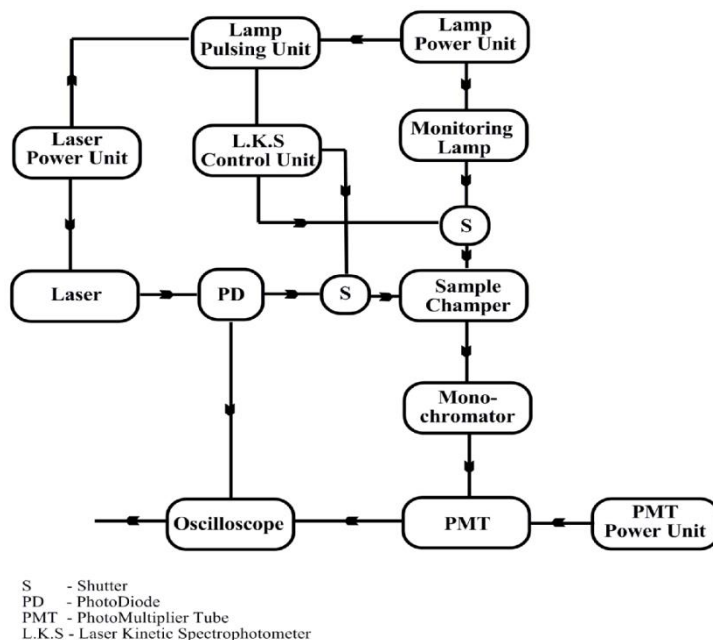
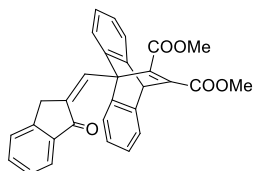


Fig. 4.27: Schematic representation of nanosecond laser flash photolysis setup.

For the compounds **12a-g** upon photoirradiation we got a new product or the unchanged starting material, but for compounds **13a-f** we could not isolate a new product as they were undergoing decomposition and resulted in the formation of a polymeric residue. In case where new products were obtained high quality crystals for SCXRD analysis was obtained by further recrystallization from acetonitrile.

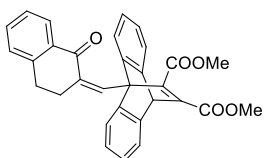
4.4.3. Spectral and analytical data of the photoproducts obtained.

4.4.3.1. Compound 12a1:



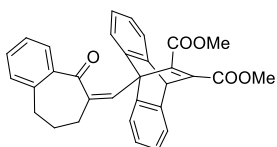
Yield 35%; mp 206 °C; IR(KBr) ν_{\max} : 1710, 1727 (C=O, ester), 1633 (C=O, ketone) cm^{-1} ; MS (FAB, $[M^+ + 1]$): Calcd for $\text{C}_{30}\text{H}_{22}\text{O}_5$: 462.14, Found: 463; Anal. Calcd for $\text{C}_{30}\text{H}_{22}\text{O}_5$: C: 77.91, H: 4.79, Found: C: 77.89, H: 4.71

4.4.3.2. Compound 12b1:



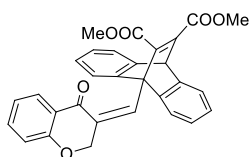
Yield 32%; mp 228 °C; IR(KBr) ν_{\max} : 1703, 1721 (C=O, ester), 1671 (C=O, ketone) cm^{-1} ; MS (FAB, $[M^+ + 1]$): Calcd for $\text{C}_{31}\text{H}_{24}\text{O}_5$: 476.51, Found: 477; Anal. Calcd for $\text{C}_{31}\text{H}_{24}\text{O}_5$: C: 78.14, H: 5.08, Found: C: 78.05, H: 5.00

4.4.3.3. Compound 12c1:

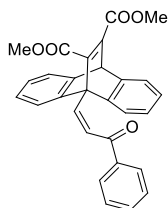


Yield 36%; mp 230 °C; IR(KBr) ν_{\max} : 1710, 1732 (C=O, ester), 1662 (C=O, ketone) cm^{-1} ; MS (FAB, $[M^+ + 1]$): Calcd for $\text{C}_{32}\text{H}_{26}\text{O}_5$: 490.17, Found: 491; Anal. Calcd for $\text{C}_{32}\text{H}_{26}\text{O}_5$: C: 78.35, H: 5.34, Found: C: 78.53, H: 5.25

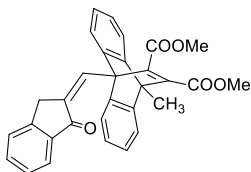
4.4.3.4. Compound 12d1:



Yield 39%; mp 207 °C; IR(KBr) ν_{\max} : 1710, 1730 (C=O, ester), 1663 (C=O, ketone) cm^{-1} ; MS (FAB, $[M^+ + 1]$): Calcd for $\text{C}_{30}\text{H}_{22}\text{O}_6$: 478.14, Found: 479; Anal. Calcd for $\text{C}_{30}\text{H}_{22}\text{O}_6$: C: 75.30, H: 4.63, Found: C: 75.25, H: 4.58.

4.4.3.5. Compound 12f1:

Yield 38%; mp 202 °C; IR(KBr) ν_{\max} : 1712, 1733 (C=O, ester), 1667 (C=O, ketone) cm^{-1} ; MS (FAB, $[M^+ + 1]$): Calcd for $\text{C}_{29}\text{H}_{22}\text{O}_5$: 450.14, Found: 451.21; Anal. Calcd for $\text{C}_{29}\text{H}_{22}\text{O}_5$: C:77.32, H: 4.92 Found: C: 77.19, H: 5.08

4.4.3.6. Compound 12g1:

Yield 30%; mp 198 °C; IR(KBr) ν_{\max} : 1706, 1733 (C=O, ester), 1631 (C=O, ketone) cm^{-1} ; MS (FAB, $[M^+ + 1]$): Calcd for $\text{C}_{31}\text{H}_{24}\text{O}_5$: 476.16, Found: 477; Anal Calcd for $\text{C}_{31}\text{H}_{24}\text{O}_5$: C: 78.14, H: 5.08, Found: C: 78.04, H: 5.02

References

1. a) Ciganek, E. *J. Am. Chem. Soc.* **1966**, *88*, 2882, b) Rabideau, P.W.; Hamilton, J. B.; Friedman, L. *J. Am. Chem. Soc.* **1968**, *90*, 4465.
2. a) Herz, W.; Iyer, V. S.; Nair, M. G.; Saltiel, J. *J. Am. Chem. Soc.* **1977**, *99*, 2708 b) Bhattacharya, K.; Ramaiah, D.; Das, P. K.; George, M. V. *J. Phys. Chem.* **1986**, *90*, 5984.
3. Chen, J.; Scheffer, J. R.; Trotter, J. *Tetrahedron* **1992**, *48*, 3251.
4. For an exception, see Sajimon, M. C.; Ramaiah, D.; Suresh, C. H.; Adam, W.; Lewis, F. D.; George, M. V. *J. Am. Chem. Soc.* **2007**, *129*, 9439.
5. a) Brown, G. H. *Photochromism*; Wiley-Interscience: New York, **1971**. b) Kelly, J. M.; McArdle, C. B.; Maunder, M. J. *Photochemistry and Polymeric Systems*; RSC: Cambridge, **1993**. c) Irie, M. *Photoreactive Materials for Ultrahigh-density Optical Memory*; Elsevier: Amsterdam, **1993**. d) Irie, M.; Yokoyama, Y.; Seki, T. *New Frontiers in Photochromism*; Springer: Tokyo, **2013**. e) Crano, J. C.; Guglielmetti, R. J. *Organic Photochromic and Thermochromic Compounds*; Plenum Press: New York and London, **1998**. f) Bouas-Laurent, H.; Du`rr, H. *Pure Appl. Chem.* **2001**, *73*, 639. g) Du`rr, H.; Bouas-Laurent, H. *Photochromism: Molecules and Systems*; Elsevier: Amsterdam, **2003**.
6. Irie, M.; Fukaminato, T.; Matsuda, K.; Kobatake, S. *Chem. Rev.* **2014**, *114*, 12174.

7. a) Yokoyama, Y. *Chem. Rev.* **2000**, *100*, 1717. b) Berkovic, G.; Krongauz, V.; Weiss, V. *Chem. Rev.* **2000**, *100*, 1741.
8. Irie, M. *Chem. Rev.* **2000**, *100*, 1685.
9. Sajimon, M. C.; Ramaiah, D.; Muneer, M.; Rath, N. P.; George, M. V. *J. Photochem. Photobiol. A.* **2000**, *136*, 209.
10. Borecka, B.; Gamlin, J. N.; Gudmundsdottir, A. D.; Olovsson, G.; Scheffer, J. R.; Trotter, J. *Tetrahedron Lett.* **1996**, *37*, 2121.
11. a) Tanaka, K.; Toda, F. *J. Chem. Soc., Perkin Trans. 1* **2000**, 873. b) Tanaka, K.; Yamamoto, Y.; Ohba, S. *Chem. Commun.* **2003**, 1866.
12. Li, X.; Han, J.; Pang, M.; Cheng, K.; He, Z.; Meng, J. *J. Mol. Struct.* **2008**, *874*, 28.
13. a) Rajca, A. *Chem. Rev.* **1994**, *94*, 871. b) Rajca, A.; Wongsriratanakul, J.; Rajca, S.; *Science* **2001**, *294*, 1503. c) Kaupp, G. *J. Mol. Struct.* **2006**, *786*, 140. d) Wienk, M. M.; Janssen, R. A. J.; Mejer, E. *Synth. Met.* **1995**, *71*, 1833.
14. Avadanei, M.; Tigoianu, R.; Serpa, C.; Pina, J.; Cozan, V. *J. Photochem. Photobiol. A.* **2017**, *332*, 475.
15. Turro, N. J.; Ramamurthy, V.; Scaiano, J. C. *Modern Molecular Photochemistry of organic molecules*, University Science Books, Sausalito, CA, **2010**.
16. Forbes, M. D. E.; Ruberu, S. R. *J. Phys. Chem.* **1993**, *97*, 13223.
17. Scaiano, J. C. *Acc. Chem. Res.* **1982**, *15*, 252.
18. a) Kumar, C. V.; Murty, B. A. R. C.; Lahiri, S.; Chackachery, E.; Scaiano, J. C.; George, M. V. *J. Org. Chem.* **1984**, *49*, 4923. b) Prathapan, S.; Ashok, K.; Cyr, D. R.; Das, P. K.; George, M. V. *J. Org. Chem.* **1987**, *52*, 5512. c) Prathapan, S.; Ashok, K.; Gopidas, K. R.; Nath, R. P.; Das, P. K.; George, M. V. *J. Org. Chem.* **1990**, *55*, 1304.

Variable temperature NMR studies and frontier orbital analysis using DFT for selected compounds

5.1. Abstract

This chapter deals with various studies we have carried out on newly synthesized dibenzobarrelenes, which provides additional information on their structure and reactivity. In order to explain their anomalous NMR spectra, we performed variable temperature studies on a representative sample. Frontier orbital analysis using DFT was carried out on a few selected compounds to account for the difference in reactivity of dibenzobarrelenes holding carbomethoxy vs benzoyl substituents at the 11, 12-positions. The redox properties of dibenzobarrelenes were studied using cyclic voltammetry.

5.2. Introduction

From the photochemical and photophysical studies carried out on enone appended dibenzobarrelenes synthesized by us, we observed significant differences in their reactivity and properties. Their unusual NMR spectra suggested dynamic conformational changes resulting in unresolved NMR signals. In order to amass useful information on their chemical and physical properties, we carried additional studies with these compounds. Variable-temperature NMR (VT NMR) studies were carried out to explain the NMR spectrum of the compounds, frontier orbital analysis using DFT for predicting their reactivity and cyclic voltammetry to

analyze the redox properties. Results obtained from preliminary VT NMR experiments, cyclic voltammetry and the frontier orbital analysis using DFT are discussed in this chapter.

5.2.1. Variable Temperature NMR—basics and applications

VT NMR finds application in elucidation of rotational barriers in molecular rotor systems, ortho-disubstituted biaryls and other hindered heterocyclic systems.¹ In the present work we have employed this technique to confirm the presence of rotational isomers for the synthesized dibenzobarrelenes.

From the basic principles of NMR spectroscopy, we know that the resonant frequency of a nucleus depends on its specific magnetic environment and if there is any change happening to this environment within the NMR time scale we get only an averaged spectrum. At high temperatures this chemical exchange process will be rapid and the signals will be broadened and at low temperature where the exchange processes are slowed down we get well resolved signals and in between these two extremes the NMR spectrum gives a rich variety of chemical exchange line shapes.^{2,3} In Fig. 5.1 NMR spectral pattern for a system of two chemical shift distinct but interchangeable protons at different temperatures is presented. At low temperature, the two protons appear at different chemical shift positions as two sharp singlets. With increasing temperature, exchange rate also increases and this is reflected in broadening of the signal and eventual coalescence at their mean chemical shift position. Temperature at which the two signals merge to form a

broad peak is termed the coalescence temperature (T_c) that is different for different compounds.

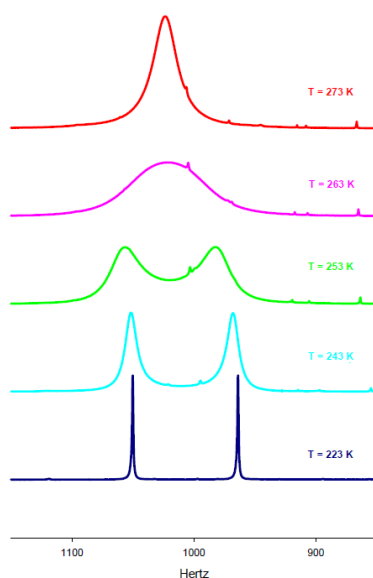


Fig. 5.1: Schematic representation showing the dynamic behavior of protons at different temperatures.

From the line shape analysis of the VT NMR spectrum we could calculate the activation parameters such as ΔG , ΔH and ΔS . The easiest method of determining activation energy parameters is through the determination of temperature at which the NMR resonances of two exchanging species coalesce. The coalescence temperature (T_c) is then used in conjunction with the maximum peak separation in the low-temperature (i.e. slow-exchange) limit ($\Delta\nu$ in Hz).⁴ The rate constants, k_c for a dynamic process at the coalescence temperature (T_c) can be calculated using the Gutowsky-Holm equation^{5,6} (5.1) and ΔG^\ddagger at T_c is determined by the Eyring equation.⁷ (5.2)

$$k_c = \pi \Delta\nu / \sqrt{2} \quad (5.1)$$

$$\Delta G_c^\ddagger = RT_c (23.760 + \ln (T_c/k_c)) \quad (5.2)$$

where $R = 1.9872$ for calories/mol,

$R = 8.3144$ for Joules/mol

5.3. Results and Discussion

5.3.1. Variable temperature NMR studies (VTNMR)

When we examined the room temperature NMR spectra of the *E* and *Z*-isomers of enone appended dibenzobarrelenes we observed that some of them exhibited broad, characterless peaks. This indicates possibility of dynamic processes taking place in these compounds within the NMR time scale. In order to reveal this we carried out the VT NMR studies on a representative sample. Compound **1** and its photoproduct **1a** (Chart 5.1) were selected for the studies. Incidentally **1** and **1a** constitute a diastereomeric pair of *E* and *Z*-isomers respectively. Fig 5.2 shows the ^1H NMR spectra for compounds **1** and **1a** at room temperature. From the spectrum we find that for **1** which is the *E* isomer the spectrum is fully resolved and all the characteristic peaks are present in the spectrum. But this is not the case with the *Z*-isomer **1a**. Several peaks are broadened in the aromatic as well as aliphatic regions, some are missing and intensity turns topsy-turvy.

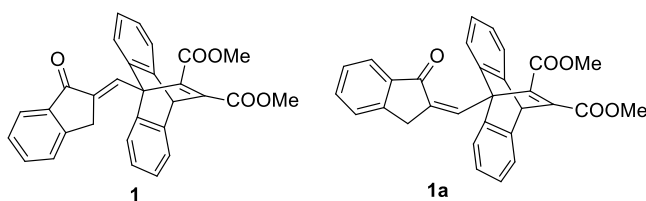


Chart 5.1

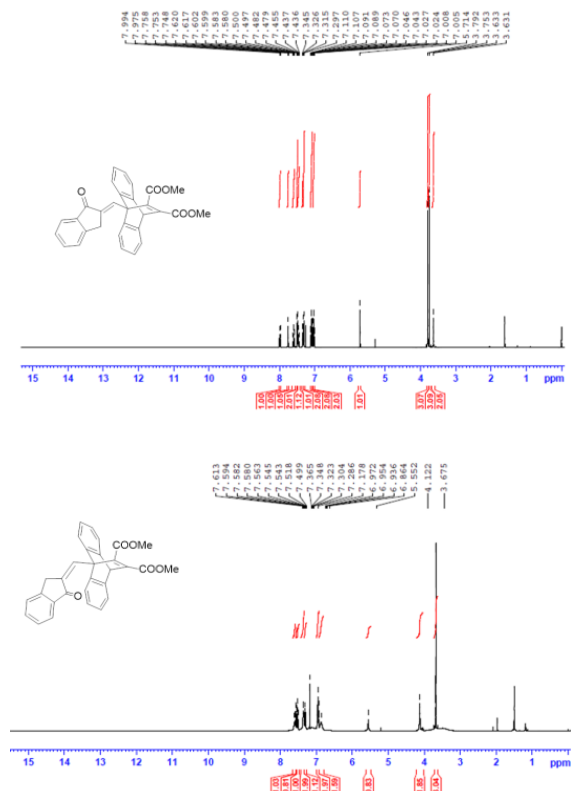


Fig. 5.2: Comparison of the 400 MHz ¹H NMR spectra for **1** and **1a** in CDCl₃ at 298 K

In the ¹H NMR spectrum of **1a**, peaks corresponding to the two OCH₃ groups appear as a single peak at δ 3.68 (3H) whereas for the *E*-isomer **1**, as expected, two distinct singlets at δ 3.79 (3H) and δ 3.75 (3H) are discernible. For **1a**, coalescence accompanied by loss of precise proton count is observed for aromatic protons as well. We employed variable temperature NMR experiments on **1a** over a temperature range of 248–318 K in CDCl₃ solvent to unravel the mystery behind curious NMR peak positions, peak shape and distortion in peak intensity. Fig 5.3 shows the VT NMR spectral traces for **1a**. Change in spectral pattern with

temperature clearly and convincingly depicts dynamic behavior of this compound.

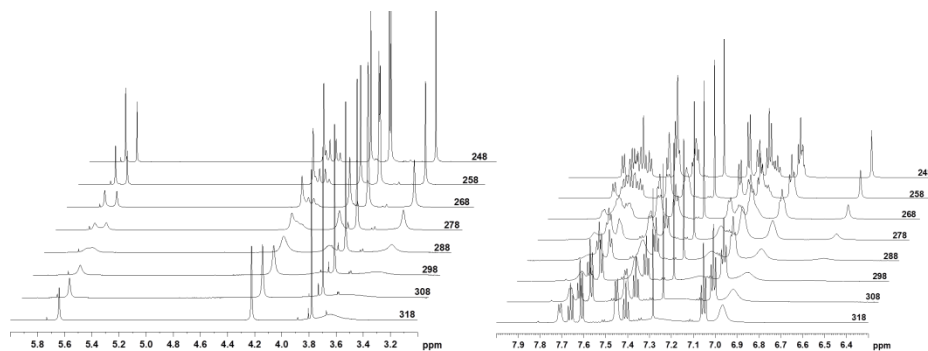


Fig. 5.3: Variable temperature ^1H NMR spectrum of **1a** showing dynamic proton exchange behavior

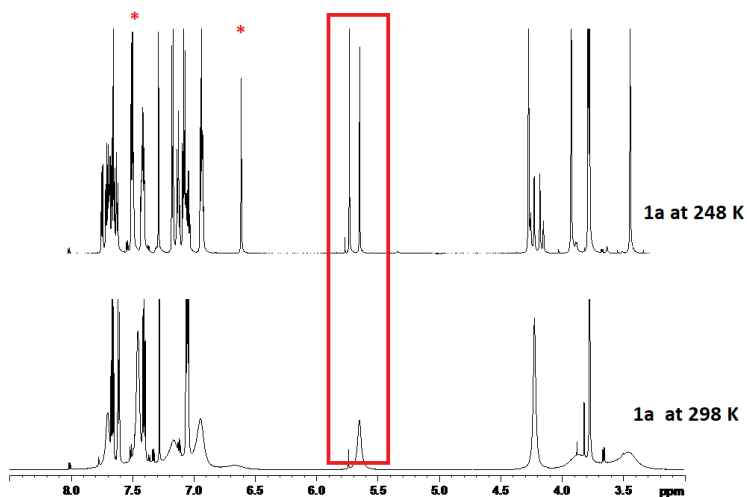
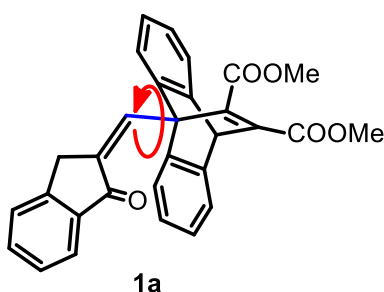


Fig. 5.4: Comparison of the ^1H NMR spectra at 248K and 298 K of **1a**

Fig 5.4 shows the 700 MHz ^1H NMR spectra of **1a** at 248 K and 298K when we make a close examination of the two spectra we can see that at 248 K the compound exist as an equilibrium mixture of two different conformers. We choose the signal appearing around δ 5.7 and δ 6.9 in

spectra recorded at 298 K and 248 K attributable to the bridgehead proton and vinylic proton respectively to corroborate our arguments on the existence of different rotamers. In the spectrum recorded at 298 K, broad singlets corresponding to bridgehead and vinylic protons are observed at these positions. However, in the spectrum recorded at 248 K, the signals resolved to sharp singlets of nearly equal intensity with bridgehead protons appearing as two separate peaks around 5.7 and the vinylic proton appears as two rather widely separated sharp singlets around δ 6.6 and 7.6. Similar trend is discernable for other signals appearing in these two spectra. We postulate that at 298 K, free rotation around the marked bond in **1a** is a distinct possibility leading to the coexistence of several rotamers causing peak coalescence and broadening. On the other hand, at 248 K, barrier for free rotation may not be surmountable and two rotamers coexist as two distinct, non-interchangeable entities. Structure of **1a** and two of its possible rotamers formed as a result of rotation about the single bond connecting the enone and the dibenzobarrelene components are presented in Fig 5.5.



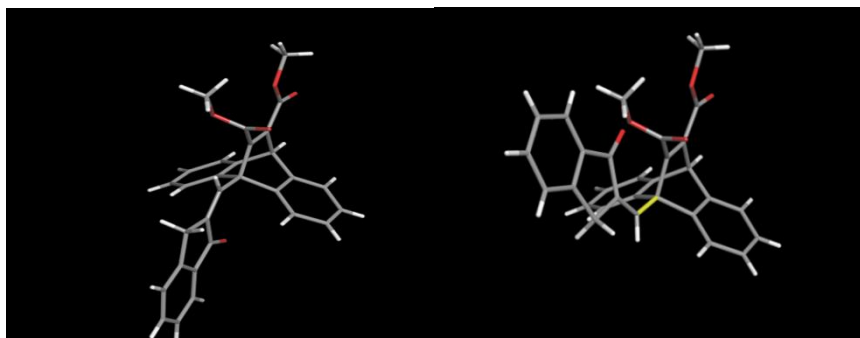


Fig 5.5: Different rotamers for compound **1a**

In Fig 5.5 we have shown only two of the many possible rotameric structures for the compound **1a**. Considerable difference in the chemical environment for different protons of **1a** is evident in the two structures presented in Fig 5.5. Wide separation in the positions for the vinylic proton in two different rotamers corroborates this observation. Based on these observations, we conclude that distortion of NMR signals due to coexistence of interchangeable rotamers is a distinct possibility for **1a** and related compounds.

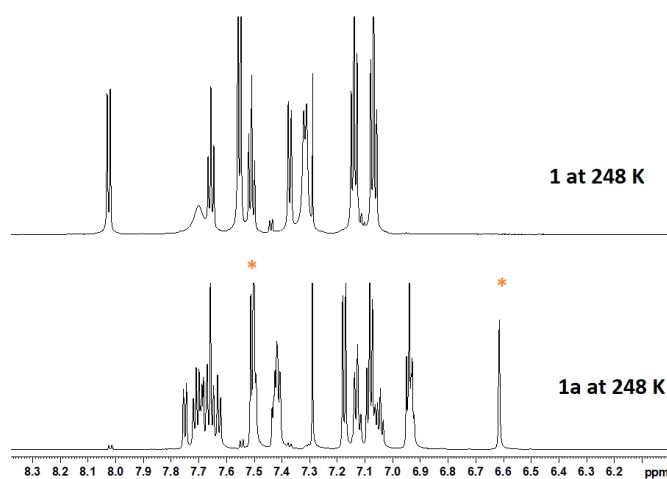


Fig. 5.6: Comparison of the ^1H NMR spectra of **1** and **1a** at 248 K

Due to the unresolved nature of their NMR spectra, we could not assign the stereochemistry of **1** and **1a** on the basis of spectral data alone. However, as mentioned in Chapter 4, we could collect single crystal X-ray diffraction data for one enone appended dibenzobarrelene and its photoproduct. SCXRD data clearly indicated *E*-geometry for the starting material and *Z*-geometry for the corresponding photoproduct. Well resolved NMR spectra of **1** and **1a** also supported *E* and *Z* geometry for these two isomers. It is generally observed that in *Z*-isomers, vinylic protons appear upfield with respect to that in the corresponding *E*-isomers. In the present case, at 248 K, vinylic protons in the two rotamers of **1a** appear at δ 6.7 and 7.5 while the vinylic proton in **1** appears as a broad peak above δ 7.7. Yet another curious observation on rotational isomerism of **1** and **1a** is worth mentioning here. For **1a**, free rotation is restricted at 248 K leading to sharp signals (Fig 5.6) whereas, in the case of **1**, interconversion of rotamers is evident at 248 K by slight distortion of signals. However, at 298 K, NMR spectrum of **1** is well resolved and no signal broadening is apparent at this temperature. It appears that fast and free rotation around the bond connecting enone and dibenzobarrelenes components is possible at this temperature (Fig. 5.7).

In the case of the *Z*-isomer **1a**, ^1H NMR spectrum (700 MHz) recorded at 248 K clearly indicated the presence of two rotamers in nearly 1:1 (53:47 to be more precise) ratio. We estimated rate of rotation kc at 288 K and free energy barrier ΔG_c^\ddagger from VTNMR data using standard methods.^{5,6,7} For **1a** the rate constant kc at $T_c = 288$ K (from Fig 5.3) was calculated as 186.50 s^{-1} and the free energy ΔG_c^\ddagger was calculated using Equation 5.2

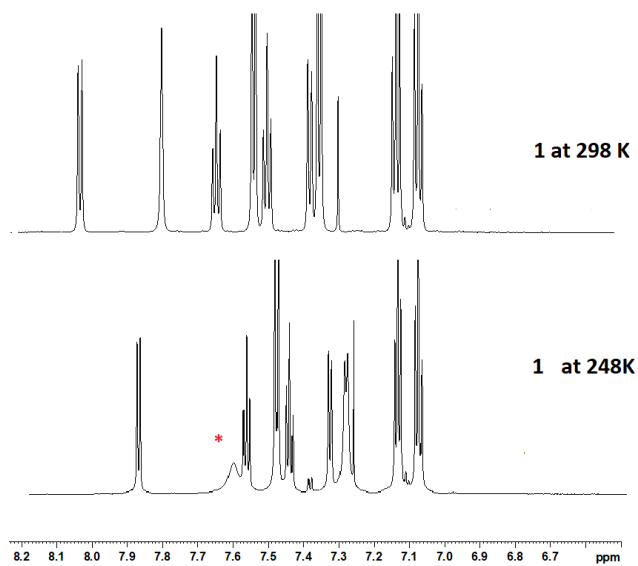


Fig. 5.7: Comparison of the ¹H NMR spectra of **1** at 248 K and 298 K

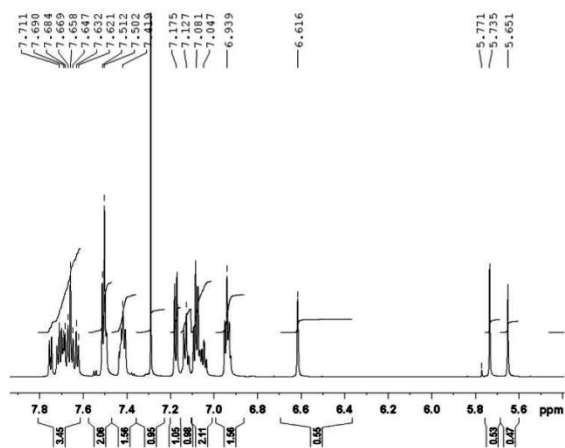


Fig 5.8: 700 MHz ¹H NMR spectra of **1a** at 248 K

$$\Delta G_c^\ddagger = RT_c (23.760 + \ln (T_c/k_c)) \quad (5.2)$$

For **1a**, ΔG_c^\ddagger was estimated as 13.76 kcal/mol.

In continuation we collected variable temperature ^{13}C NMR spectra for **1a**. ^{13}C NMR spectra of **1a** recorded at 248 K and 298 K are given in Fig. 5.9. As with the ^1H NMR spectrum of **1a** recorded at 298 K, ^{13}C NMR spectrum is also poorly resolved to an extent where it has zilch analytical relevance. However, spectrum recorded at 248 K provides strong evidence for the coexistence of two rotamers. Appearance two signals around δ 190 corresponding to α,β -unsaturated carbonyl groups is a telling evidence for the co-existence of two rotamers.

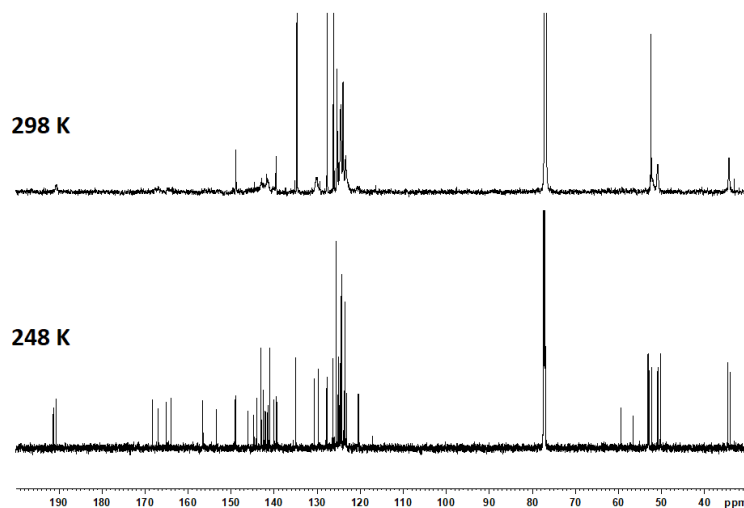


Fig 5.9: Comparison of 700 MHz ^{13}C NMR spectra of **1a** at 248 K and 298 K

Thus from the VT NMR studies carried out on **1a** we could confirm the presence of the existence of different rotamers in dynamic equilibrium at

298 K and as distinct isomers at 248 K. Rotation barrier for **1a** was estimated as 13 kcal/mol.

5.3.2. Cyclic voltammetric studies

In order to study the redox properties of the synthesized dibenzobarrelenes we have carried out the cyclic voltammetry for selected compounds. A three electrode system with platinum disc electrode as the working electrode, platinum wire as counter electrode and Ag/AgCl as reference electrode was used. The potential of the reference electrode under vacuum level was calibrated using Ferrocene/Ferrocenium redox system and was found to be 4.8 eV. From the cyclic voltammogram of Ferrocene/Ferrocenium E_{foc} is calculated as 0.46 V which is the average of the observed anodic potential and cathodic potential. HOMO-LUMO energy levels and band gaps were calculated from the cyclic voltammetric measurements. The energy of the HOMO levels was calculated using the equation 5.3.

$$E_{\text{HOMO}} = -e(E_{1/2\text{OX}} - E_{\text{foc}}) - 4.80 \text{ eV} \quad (5.3)$$

$$E_{1/2} \text{ values were estimated as } \frac{1}{2} (E_{\text{pa}} + E_{\text{pc}})$$

Furthermore, energy of the LUMO levels were calculated using the corresponding HOMO energy and the optical band gap $E_{\text{g}}^{\text{opt}}$. The optical band $E_{\text{g}}^{\text{opt}}$ corresponds to the energy of the long wavelength edge of the absorption band.⁸ The optical band gap values were approximated from the onset of the low energy side of the absorption spectra (λ_{onset} , solution) to the baseline according to the equation $(E_{\text{g}}^{\text{opt}}) = 1240/\lambda_{\text{onset}}$. Then E_{LUMO} is obtained from Equation 5.4.

$$E_{\text{LUMO}} = E_{\text{HOMO}} + E_{\text{g}}^{\text{opt}} \text{ (eV)} \quad (5.4)$$

Cyclic voltammetric experiments were performed for the compounds listed in Chart 5.2 and the voltammograms obtained are shown in Fig 5.10. From the analysis of the CV curves we can see that in all cases, one electron oxidation is taking place. CV curves show an anodic peak and a cathodic peak during a full cycle. This shows that the dibenzobarrelenes synthesized can undergo reversible oxidation. Data obtained from the cyclic voltammetric studies are tabulated in Table 5.1

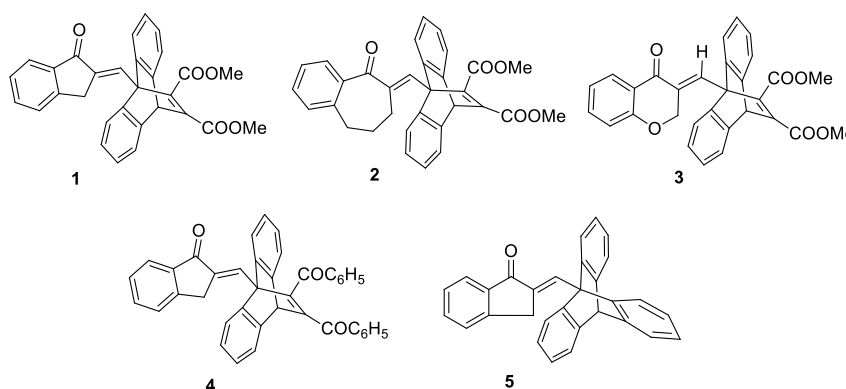


Chart 5.2

Compound	$E_{1/2 \text{ OX}}$ (eV) ^a	E_{HOMO} (eV) ^b	$E_{\text{g}}^{\text{opt}}$ (eV) ^c	E_{LUMO} (eV) ^d
1	0.992	-5.676	3.769	-1.907
2	1.041	-5.724	3.887	-1.838
3	1.101	-5.785	3.263	-2.521
4	1.020	-5.704	3.768	-1.935
5	1.044	-5.727	4.189	-1.537

^a Oxidation potential relative to Ag/AgCl electrode, ^b Calculated HOMO from the onset Oxidation potentials of the compounds, ^c Optical band gap calculated using the equation $1240/\lambda$, where λ is the edge wavelength obtained from absorption spectra, ^d Estimated LUMO using empirical equations

Table 5.1: Electrochemical data of the compounds

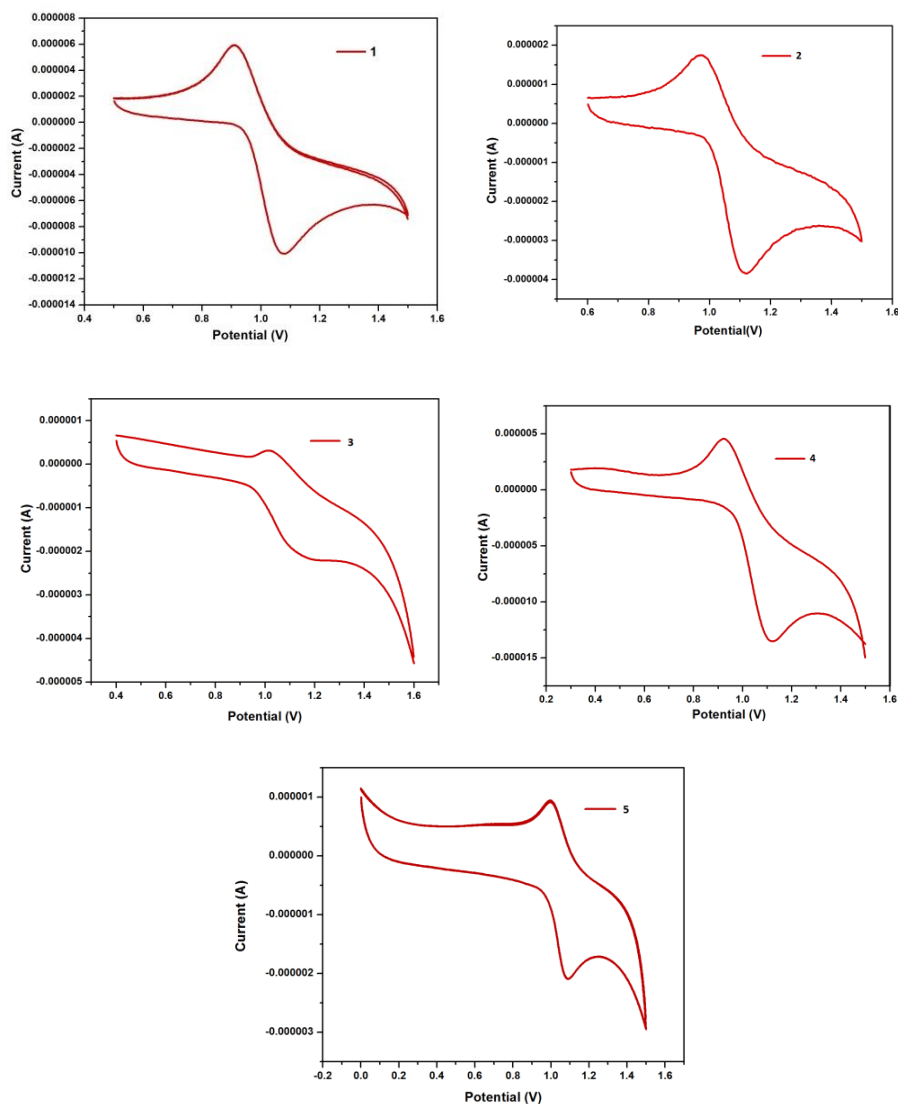


Fig 5.10: CV curves for the compounds measured in acetonitrile in the presence of $n\text{-Bu}_4\text{NPF}_6$ at a scan rate of 100 mVs^{-1} .

5.3.3. Frontier orbital analysis using DFT

Theoretical calculations of the HOMO-LUMO band gap and the electronic structures of the frontier orbitals were obtained from DFT using Gaussian 09 software with basis sets (B3LYP/6-31G).⁹ The

minimum energy structures for the molecules were obtained by geometry optimization followed by frequency calculation. Frontier Molecular orbitals (FMOs) can be used to get information regarding the excited state properties of the molecules.¹⁰ We selected compounds **1,3,4** and **5** for DFT calculations.

Photochemical and photophysical studies carried out on the synthesized dibenzobarrelenes revealed the difference in their reactivity. Upon irradiation, dibenzobarrelenes with the carbomethoxy groups at the vinylic position underwent *E-Z* isomerization readily and for those with benzoyl substituents underwent extensive decomposition to give an intractable product mixture. To account for this difference in reactivity we carried out DFT studies. The molecular orbital amplitude plots obtained for HOMO and LUMO for the compounds studied and their optimized geometries are shown in Fig 5.11. From the energy eigen values for HOMO and LUMO we have also calculated their band gap values that are tabulated in Table 5.2. The band gap calculated using DFT and the optical band gap values calculated are in good agreement.

Thus the difference in reactivity of the compounds with carbomethoxy and benzoyl groups at 11,12-positions, can be explained with the help of Frontier orbitals obtained from DFT calculations. Based on this we could establish that in case of dibenzobarrelenes with ester moiety LUMO is concentrated on the enone moiety and thus *cis-trans* isomerization around this bond is important here. On the other hand, for dibenzobarrelene holding benzoyl groups at 11, 12-positions, LUMO is spread over the entire molecule enabling multiple reaction pathways.

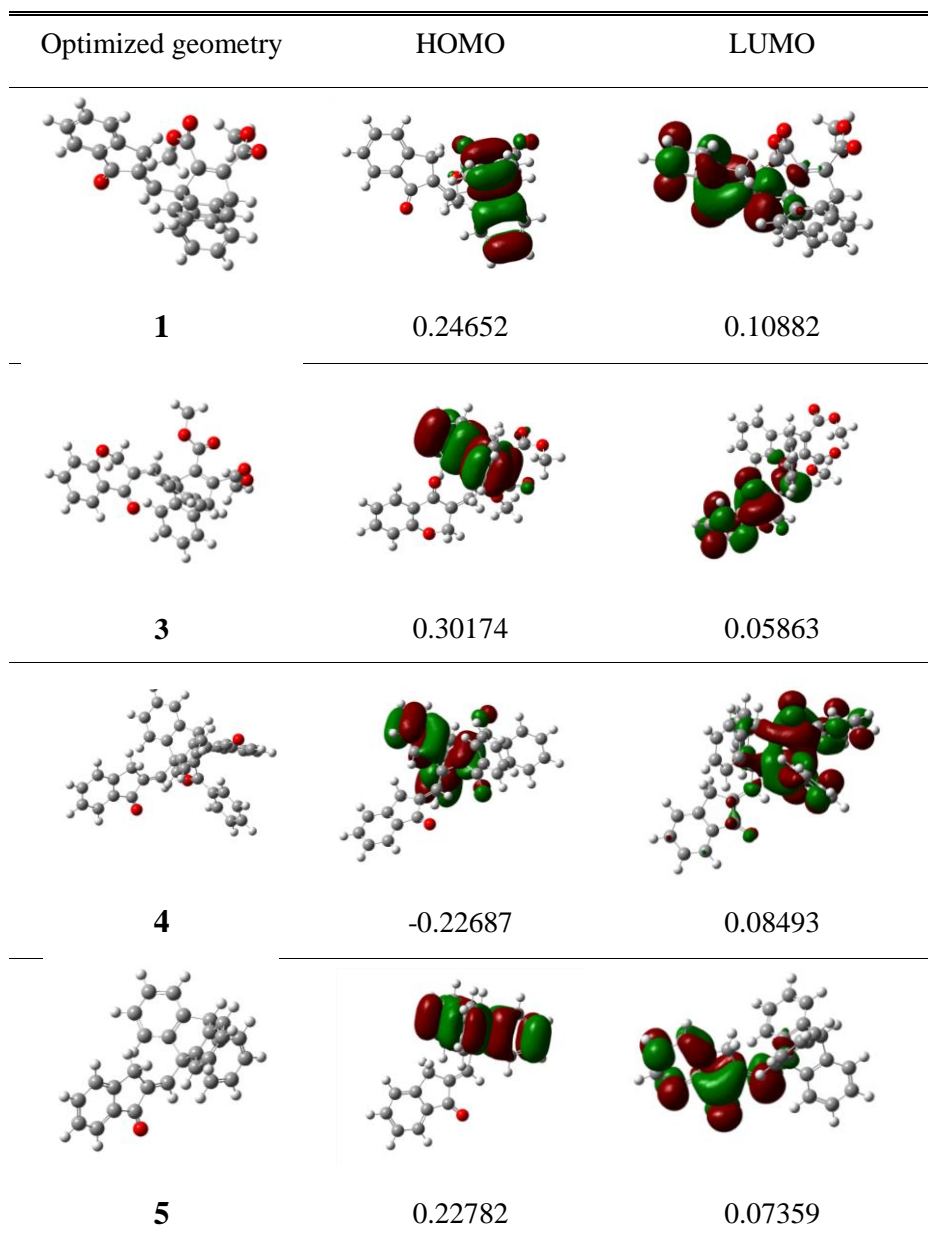


Fig. 5.11: Frontier molecular orbitals (HOMO& LUMO) and optimized geometry of compounds obtained from DFT calculations

Compound	E_{HOMO} (eV) ^c	E_{LUMO} (eV) ^c	ΔE (eV)	$E_{\text{g}}^{\text{opt}}$ (eV)
1	-6.708	-2.961	3.747	3.769
3	-6.405	-2.567	3.838	3.263
4	-6.275	-2.615	3.659	3.768
5	-6.199	-2.002	4.196	4.189

Table 5.2: Comparison of band gap calculated using DFT with optical band gap

5.4. Experimental

Variable temperature NMR spectra were recorded at 700 MHz on a *Bruker Avance III* FT-NMR spectrometer over a temperature range from 248 to 318 K in CDCl_3 . Cyclic voltammograms were recorded with a Bas 50W Voltammetric analyser. The compounds were dissolved in acetonitrile containing 0.1 M tetra-*n*-butylammonium hexafluorophosphate as supporting electrolyte. Computational calculations were done using Density Functional Theory (DFT) with B3LYP/6-31G hybrid function.

References

1. a) Mazzanti, A.; Chiarucci, M.; Bentley, K. W.; Wolf, C. *J. Org. Chem.* **2014**, *79*, 3725. b) Szatmari, I.; Heydenreich, M.; Koch, A.; Fulop, F.; Kleinpeter, E. *Tetrahedron.* **2013**, *69*, 7455. c) Alfonso, I.; Burguete, M. I.; Galindo, F.; Luis, S. V.; Vigara, L. *J. Org. Chem.* **2007**, *72*, 7947.
2. Jackman, L. M.; Cotton, F. A. *Dynamic Nuclear Magnetic Resonance Spectroscopy*; Academic Press: New York, **1975**.
3. Sandstrom, J. *Dynamic NMR Spectroscopy*; Academic Press: London, **1982**.
4. Gutowsky, H. S.; Holm, C. H. *J. Chem. Phys.* **1956**, *25*, 1228.

5. Pinto, B. M.; Grindley, T. B.; Szarek, W. A. *Magn. Reson. Chem.* **1986**, *24*, 323.
6. Garratt, P. J.; Thom, S. N.; Wrigglesworth, R. *Tetrahedron* **1994**, *50*, 12211.
7. Dabbagh, H. A.; Modarresi-Alam, A. R.; Tadjarodi, A.; Taeb, A. *Tetrahedron*. **2002**, *58*, 2621.
8. Djurovich, P. I.; Mayo, E. I.; Forrest, S. R.; Thompson, M. E. *Org. Electron.* **2009**, *10*, 515.
9. Gaussian 09, Revision D.01, M. J. Frisch *et al.* *Gaussian, Inc.*, Wallingford CT, **2013**.
10. Andres, L. S.; Merchan, M. *Comp. Theor. Chem.* **2005**, *729*, 99.

Summary and Conclusion

In the thesis entitled “Investigations on the photochemistry and photophysics of a few enone appended dibenzobarrelenes” we report the synthesis and studies of a few dibenzobarrelene derivatives tailored to exhibit photochemical and photophysical properties different from that of dibenzobarrelenes so far studied by several research groups. To this end, we synthesized several dibenzobarrelenes having enone appendages by utilizing Diels-Alder reaction of the corresponding anthracene precursors with suitable dienophiles like DMAD, DBA and *in situ* generated benzyne intermediate. The classical phototransformation reactions of dibenzobarrelenes involve formation of dibenzosemibullvalene through triplet mediated pathway and dibenzocyclooctatetraene through singlet mediated pathway. In principle, judicious incorporation of substituents onto barrelene chromophores can shut both singlet and triplet mediated product formation. With this idea in mind, in the present work we decorated dibenzobarrelenes with substituents such as carbomethoxy and benzoyl groups to promote intersystem crossing and an enone appendage that can potentially act as efficient intramolecular triplet quencher. As a combined effect of these substituents, we expected the photochemistry of dibenzobarrelenes to be diverted to hitherto unknown pathways.

Steady state irradiation of these compounds were carried out in benzene solution and we have observed that for compounds having carbomethoxy substituents *E-Z* isomerization was the major reaction pathway. In the case of compounds with benzoyl substituents we could not find any

isolable products as they were undergoing extensive decomposition. During our studies with these compounds we serendipitously observed that many of the dibenzobarrelenes synthesized by us were showing photochromic properties in the solid state. We could follow the photochromic behaviour of a few compounds with the help of UV-DRS. In order to understand the mechanism involved in this photochemical behaviour of these compounds we carried out further studies like EPR and Laser Flash photolysis. EPR studies indicated generation of free radical upon exposure of these dibenzobarrelenes to sunlight. From Laser flash photolysis experiments also we could identify the formation of a transient species having absorption in the region around 600 nm which can be attributed to the colour forming species during the exposure of these compounds to sunlight. So the mechanism we have proposed for the photochromic behaviour of these compounds involves a reversible bridgehead hydrogen abstraction by carbonyl group resulting in the formation of a diradical intermediate. As an evidence for this we observed that the dibenzobarrelenes with a phenyl substituent at the bridgehead position is not photochromic.

Another important observation we have made for these compounds is the presence of rotamers. We have identified the possibilities for rotamers in these compounds from the NMR spectra of the synthesized dibenzobarrelenes which showed unresolved NMR signals which suggested the presence of dynamic conformational changes. To gain further information, we carried out variable temperature NMR studies for a selected sample. The results obtained substantiated the presence of rotamers in that compound. At low temperature, both ^1H and ^{13}C NMR

spectra showed the presence of two distinct conformers existing as an equilibrium mixture and as the temperature rises, the signals begin to broaden and above the coalescence temperature we could observe only an averaged spectrum.

The difference in reactivity of the compounds with carbomethoxy and benzoyl groups at 11,12-positions were explained on the basis of the Frontier Orbital Analysis using Density Functional Theory. In case of dibenzobarrelenes with carbomethoxy substituents LUMO is concentrated on the enone moiety and thus the reaction is only a *cis-trans* isomerization. In the dibenzobarrelene with benzoyl group at 11,12-positions, LUMO is spread over the entire molecule enabling multiple reaction pathways.

We have succeeded in diverting the reaction of the dibenzobarrelene from generally observed reaction pathways. The photochromic nature of these compounds which is due to the presence of triplet biradical species opens up the possibilities for carrying out more studies leading to the development of organic molecular magnets which is now an active area of research. The photochromic properties of these compounds can also be utilized for developing photonic devices and for that more studies regarding the thermal stability, fatigue resistance etc. have to be done.

List of publications

1. Synthesis of Photochromic Dibenzobarrelenes, **Saumya T. S.**, Aswathi C. S., Nishad K. M., Prathapan S. and Unnikrishnan P. A., International Conference on Materials for Millennium (MatCon 2016), Department of Applied Chemistry, Cochin University of Science And Technology, Kerala, India. **ISBN:978-93-80095-738**
2. Synthesis of Anthracene - Barrelene dyads with cycloalkanone spacer. **Saumya T. S.**, Prathapan S. and Unnikrishnan P. A., International Conference on "New Trends in Applied Chemistry" (NTAC-2017), Post Graduate and Research Department of Chemistry, Sacred Heart College, Thevara, Cochin, Kerala, India. **ISBN:978-81-930558-2-3**

Poster presentations

1. Conformational effects on the geometry of bisanthracenes, **Saumya T. S.**, and Gisha George, *Current Trends in Chemistry* (CTriC 2013), Department of Applied Chemistry, Cochin University of Science And Technology, Kerala, India
2. Site selective Diels-Alder reaction of 9-(2-furylmethoxymethyl) anthracene, **Saumya T. S.**, Nishad K. M., Prathapan S and Unnikrishnan P. A., *Current Trends in chemistry* (CTriC 2014), Department of Applied Chemistry, Cochin university of science and Technology, Kerala, India
3. Synthesis of Photochromic Dibenzobarrelenes, **Saumya T. S.**, Aswathi C. S., Nishad K. M., Prathapan S. and Unnikrishnan P A., International Conference on Materials For Millennium (MatCon 2016), Department of Applied Chemistry, Cochin University of Science And Technology, Kerala, India
4. Synthesis of Anthracene -Barrelene dyads with cycloalkanone spacers. **Saumya T. S.**, Prathapan S. and Unnikrishnan P. A., International Conference on "New Trends in Applied Chemistry" (NTAC-2017), Post Graduate and Research Department of Chemistry, Sacred Heart College, Thevara, Cochin, Kerala, India
5. Photochemical cis-trans isomerization in enone-appended dibenzobarrelenes, **Saumya T. S.**, Prathapan S and Unnikrishnan P. A., *Current Trends in Chemistry* (CTriC 2017), Department of Applied Chemistry, Cochin university of science and Technology, Kerala, India